THE ROLE OF RHOA/ROCK SIGNALING IN THE DEVELOPMENT OF DIABETIC CARDIOMYOPATHY

by

Vongai Nyamandi

B.Sc., Lee University, 2009

M.Sc., University of Calgary, 2012

A THESIS SUBMITTED IN PARTIAL FULFILLMENT OF

THE REQUIREMENTS FOR THE DEGREE OF

DOCTOR OF PHILOSOPHY

in

THE FACULTY OF GRADUATE AND POSTDOCTORAL STUDIES

(Pharmaceutical Sciences)

THE UNIVERSITY OF BRITISH COLUMBIA

(Vancouver)

December 2017

Abstract

Diabetic patients have an increased risk of heart failure and sudden death, attributed in part to the development of diabetic cardiomyopathy, defined as ventricular dysfunction independent of hypertension and coronary artery disease. The mechanisms contributing to diabetic cardiomyopathy are not completely understood, but over-activation of the RhoA/ROCK pathway has been identified as a contributor. This research further investigated the roles of cardiomyocyte RhoA and of ROCK2 in the development of diabetic cardiomyopathy.

In study one, the effects of heterozygous deletion of ROCK2 ($ROCK2^{+/-}$) on cardiac function in a CD1 mouse model of type 1 diabetes induced by streptozotocin (STZ) were analyzed, since homozygous ROCK2 deletion is embryonically lethal. Thirteen weeks after diabetes induction, global cardiac function was unchanged in diabetic compared to non-diabetic mice. However, cardiomyocytes isolated from wild-type diabetic mice exhibited arrhythmic Ca^{2+} transients associated with increased ryanodine receptor 2 and CAMKII phosphorylation. These observations were attenuated in $ROCK2^{+/-}$ animals, suggesting that inhibition of ROCK2 may protect against arrhythmogenesis in the diabetic heart.

The purpose of study two was to compare the development and progression of cardiac dysfunction in C57BL/6 mice, the strain of mice used in the final study, made diabetic or insulin resistant by dietary intervention and/or STZ treatment. Mice made diabetic with STZ showed the earliest and most severe signs of cardiac dysfunction compared to other models investigated, establishing this as an appropriate model.

Given that RhoA is expressed in many different cell types in the heart, the purpose of study three was to analyze the role of cardiomyocyte RhoA in the development of diabetic cardiomyopathy, using mice with inducible cardiac-specific knockdown of RhoA ($RhoA^{-/-}$).

Hearts from diabetic RhoA$^{-/-}$ mice were protected against the development of contractile dysfunction. This was associated with prevention of cardiomyocyte fibrosis, hypertrophy and apoptosis, and with normalization of signaling through the TGF-β pathway, including Smad2 and 3 phosphorylation, and Smad7 expression.

Overall, the results demonstrate that deletion of ROCK2 and of cardiomyocyte RhoA protect the diabetic heart. Inhibition of this pathway may be an important therapeutic avenue to decrease the risk of heart failure and sudden death in diabetes.

Lay Summary

Research has established that diabetics have an increased incidence of heart failure compared to non-diabetics. The form of heart failure that we studied is called diabetic cardiomyopathy. We found that mice are more likely to develop heart failure when fed a diet high in fat and sugar compared to those fed a diet high in fat alone. In addition, since our previous studies implicated over-activation of the RhoA-rho kinase (ROCK) signaling pathway in diabetic cardiomyopathy, we investigated cardiac function in type 1 diabetic mice with lowered levels of RhoA or ROCK2 in their hearts. Diabetic mice lacking ROCK2 were protected from developing irregular heart-beats, while those lacking RhoA did not develop diabetic cardiomyopathy, unlike diabetic mice expressing functional ROCK2 or RhoA, respectively. This research has the potential to assist in the development of new treatment strategies for diabetic cardiomyopathy through inhibiting RhoA or ROCK2, or by dietary modifications.

Preface

The work outlined in this thesis was carried out by Vongai Nyamandi under the guidance and supervision of Dr. Kathleen MacLeod in the Faculty of Pharmaceutical Sciences, University of British Columbia. Where otherwise noted, Dr. Kathleen MacLeod and Vongai Nyamandi were responsible for designing the experiments. The thesis was edited by Dr. Kathleen MacLeod.

The work described in chapter 2 is included in a manuscript in preparation, Hesham Soliman*, Vongai Nyamandi*, Marysol Garcia-Patino, Ping-Cheng Zhang, Eric Lin, Zheng Ping Jia, Glen F Tibbits, Leif Hove-Madsen and Kathleen M. MacLeod. ROCK2 promotes ryanodine receptor phosphorylation and arrhythmic calcium release in diabetic cardiomyocytes. *These authors contributed equally to the work described in the manuscript. Vongai Nyamandi, Dr. Hesham Soliman and Dr. Kathleen Macleod designed the experiments. Vongai Nyamandi was responsible for breeding the CD1 mice, treating the animals to become diabetic, echocardiography measurements, western blot analysis, isolation of cardiomyocytes for the Ca^{2+} studies and statistical analysis in whole hearts. Dr. Hesham Soliman assisted with treatment and imaging of the isolated cardiomyocytes. Dr. Leif Hove-Madsen analyzed the data for the Ca^{2+} studies. Drs. Zhang and Lin, members of Dr. Glen Tibbit's laboratory, assisted with imaging studies. The $ROCK2^{+/-}$ mice used in these experiments were generously donated to Dr. MacLeod's laboratory by Dr. Zheng Ping Jia from the University of Toronto.

A version of chapter 3 has been submitted for publication. Vongai Nyamandi, Marysol Garcia-Patino, Julia Noguera Varela, Kathleen M. MacLeod. Comparison of the development and progression of cardiac dysfunction in mouse models of metabolic stress. *Submitted 2017*. Vongai Nyamandi was responsible for conducting all experiments, data analysis and writing the manuscript. Marysol Garcia-Patino and Julia Noguera Varela assisted with sample collection of

the glucose and insulin tolerance tests and tissue collection after euthanasia. Dr. Kathleen MacLeod edited the manuscript.

The experiments described in chapter 4 were carried out by Vongai Nyamandi under the guidance of Dr. Kathleen MacLeod. Vongai Nyamandi conducted all the experiments and data analysis.

The data in chapter 5 are included in a manuscript in preparation for submission for publication. Vongai Nyamandi, Marysol Garcia-Patino, Jeffery Molkentin, Kathleen M. MacLeod. Deletion of RhoA in cardiomyocytes protects the heart from contractile dysfunction and associated fibrosis in a mouse model of type 1 diabetes. *Expected submission 2017/18*. Vongai Nyamandi conducted all the experiments and data analysis and drafted the manuscript. Dr. Kathleen MacLeod edited the manuscript. The cardiac specific RhoA-floxed and RhoA-cre mice used in these experiments were generously donated by Dr. Jeffery Molkentin of the University of Cincinnati.

All animal experiments were approved by the University of British Columbia as follows:

1. For breeding the CD1 mice – Animal Care Committee Certificate A13-0283
2. For breeding the RhoA-floxed and RhoA-cre mice - Animal Care Committee Certificate A13-0132
3. For studies on diabetic cardiomyopathy in CD1, C57Bl/6 and RhoA mice - Animal Care Committee Certificate A14-0001

Vongai Nyamandi was supported by a Doctoral Student Research Award from Diabetes Canada (formerly The Canadian Diabetes Association), 2014-2017.

Table of Contents

List of Tables

List of Figures

List of Abbreviations

°C	Degrees celsius
A1C	Glycated hemoglobin
ACC	Acetyl-CoA carboxylase
AET	Aortic ejection time
AGEs	Advanced glycosylation end products
AMPK	5' adenosine monophosphate-activated protein kinase
ANOVA	Analysis of variance
ATI	Angiotensin II type I
ATP	Adenosine triphosphate
AUC	Area under the curve
BMP	Bone morphogenetic protein
bpm	Beats per minute
C3	Clostridium botulinum C3 transferase exotoxin
CH	Chow
CAMKII	Ca2+/calmodulin-dependent protein kinase II
DAG	Diacylglycerol
E/A	Ratio of early (E) to late (A) ventricular filling velocities
EAT	Duration time of the E and A waves
ECM	Extracellular matrix
EDT	E wave deceleration time
ERK1/2	Extracellular signal–regulated kinases 1/2

ET	Ejection time
ETC	Electron transport chain
FA	Fatty acid
FADH2	Flavine adenine dinucleotide
FAO	Fatty acid oxidation
FAPs	Fibro/adipogenic progenitor cells
FFA	Free fatty acids
GAPDH	Glyceraldehyde 3-phosphate dehydrogenase
GAPs	GTPase activating proteins
GDIs	Guanine nucleotide dissociation inhibitors
GEFs	Guanine nucleotide exchange factors
GLUT	Glucose transporter
gp130	Glycoprotein 130
GPx	Glutathione peroxidase
GTP	Guanosine triphosphate
GTT	Glucose tolerance test
HF	High fat
HFHS	High fat high sucrose
HLA	Human leucocyte antigen
I/R	Ischemia reperfusion
IL-6	Interleukin-6
iNOS	inducible nitric oxide synthase

ITT	Insulin tolerance test
IVCT	Isovolumic contraction time
IVRT	Isovolumic relaxation time
JAK/STAT	janus kinase-signal transducer and activator of transcription
JNK	C-jun N-terminal kinase
LAP	Latency-associated peptide
LBD	Ligand binding domain
LVAW; d	Left ventricular anterior wall (diastole)
LVAW; s	Left ventricular anterior wall (systole)
LVID; d	Left ventricular internal diameter (diastole)
LVID; s	Left ventricular internal diameter (systole)
LVPW; d	Left ventricular posterior wall (diastole)
LVPW; s	Left ventricular posterior wall (systole)
LV Vol; d	Left ventricular volume (diastole)
LV Vol; s	Left ventricular volume (systole)
LBD	Ligand binding domain
MKK4	Mitogen-activated protein kinase kinase 4
MLC	Myosin light chain
MPI	Myocardial performance index
mPTP	Mitochondrial permeability transition pore
MRTF	Myocardin response transcription factor
MV	Mitral valve

MYPT-1	Myosin phosphatase target subunit 1
NADH	Nicotinamide adenine dinucleotide
NADPH	Nicotinamide adenine dinucleotide phosphate
NOX4	NADPH oxidase 4
O-GlcNAC	O-Linked β-N-acetylglucosamine
PI3K	Phosphoinositide 3-kinase
PKC	Protein kinase C
PKCβ2	Protein kinase C β2
PLB	Phospholamban
PP2A	Protein phosphatase 2A
PPARα	Peroxisome proliferator-activate receptor α
RAGE	Advanced glycation end product receptors
ROCK	Rho-associated coiled-coil-containing protein kinase
ROS	Reactive oxygen species
RYR2	Ryanodine receptor 2
S6K	p70 S6 kinase
SDS-PAGE	Sodium dodecyl sulphate-polyacrylamide gel electrophoresis
SERCA	Sarco/endoplasmic reticulum calcium ATPase 2
Smad	Small mothers against decapentaplegic
SOD	Superoxide dismutase
SR	Sarcoplasm reticulum
SRF	Serum response factor

STZ	Streptozotocin
T1D	Type 1 diabetes
T2D	Type 2 diabetes
TAC	Transverse aortic constriction
TCA	Tricarboxylic acid
TG	Triglyceride
TGF-β	Transforming growth factor beta
TNF-α	Tumor necrosis factor α
TGFβRI	Transforming growth factor beta receptor I
TGFβRII	Transforming growth factor beta receptor II
WT	Wild-type mice
XDH	Xanthine dehydrogenase
XO	Xanthine oxidase
XOR	Xanthine oxidoreductase
Y27632	(1R,4r)-4-((R)-1-aminoethyl)-N-(pyridin-4-yl)cyclohexanecarboxamide
μ	Micro
μM	Micromolar

Acknowledgements

My journey the past few years has been filled with challenges, laughter and at times tears, but I would not trade that for anything. To all my mentors, family and friends, thank you for all the support and making this experience memorable.

I would like to extend my sincerest gratitude to my supervisor, Dr. Kathleen MacLeod, for her constant support and mentorship. I am humbled by her passion, dedication, scholarly integrity and ability to translate her knowledge in order to assist me throughout this journey. Her guidance and profound knowledge have been a pillar to my success in this program.

I am grateful to my Research Committee members: Dr. John McNeill, Dr. Michael Allard, Dr. Sanjoy Ghosh and Dr. Larry Lynd, for providing me with the guidance to complete my research and dissertation.

I would like to thank both current and former Macleod lab members: Marysol Garcia-Patino, Julia Noguera Varela, Dr. Hesham Soliman, Dr. Guorong Lin, Girish Bankar and Yanzhi Jia, for their knowledge and lending me a helping hand when I needed one.

Thanks to the "The Cool Kids" who provided me with some much-needed breaks away from the lab and for being there for every birthday and important life event. I am fortunate to have such exceptional friends.

Above all, I would like to thank my family for their love and support: My mother, for the unconditional love and being a constant pillar in my life; my sister, for her selflessness and dedication; my brother, for reminding me the importance of working hard and being patient; my husband, for the love and care he has shown me and being by my side at all times; and, my son, for teaching me the art of perseverance.

To my family

Chapter 1: Introduction

1.1 Overview of diabetes

Diabetes mellitus (or diabetes) is characterized by multiple metabolic disorders including perturbations in glucose metabolism, dyslipidemia and hormonal imbalance [1]. These lead to both micro- and macrovascular complications with debilitating long-term effects including diabetic cardiomyopathy [2], retinopathy [3], neuropathy [4] and nephropathy [5]. The pathways that contribute to these complications are interconnected and complex in nature, resulting in gaps in knowledge in the best approaches to tackle them. Mechanisms that have been shown to contribute to the development of these complications include an increase in reactive oxygen species (ROS) production [6], the generation of glycation end products [7], inflammation [8], apoptosis, fibrosis [9], hypertrophy [10], impaired cardiac Ca^{2+} handling [11], increased diacylglycerol production and protein kinase C activation [12], and increased hexosamine pathway activity [13], among others.

1.1.1 History

The World Health Organization estimates that the incidence of diabetes, which is defined as exhibiting a fasting blood glucose level equal to or greater than 7 mmol/L, has increased from 4.7% in 1980 to 8.5% in 2014 in adults aged 18 years or over despite advancements in modern medicine [14]. The history of diabetes dates back to the early 1500's BC, where physicians identified diabetes as a disease characterized by excessive urination, loss of body mass and dehydration. Ancient Hindu writings show that diabetes was diagnosed by the use of black ants, which fed on the sweet urine of patients. Numerous remedies were postulated and attempted to no avail [15]. In 1869, Paul Langerhans identified cells in the pancreas, but it was not until 1889

that Oskar Minkowski and Joseph von Mehring identified that the absence of the pancreas contributed to the development of diabetes [16]. Research at the University of Toronto by John James Rickard MacLeod in collaboration with Frederick Grant Banting, Charles Herbert Best and James B. Collip resulted in the identification of insulin, for which MacLeod and Banting were awarded a Nobel prize in 1923 [15].

Despite the discovery and use of insulin and human insulin analogues, not all diabetics needed it in order to control their blood glucose levels. The further introduction of diabetes self-management protocols as well as other drugs proved that the treatment of diabetes is complex, multifaceted and dependent on the type of diabetes that a patient has. As such, in order to proceed with the generation of new approaches to treating diabetes, it is important to understand both the different classes of diabetes and their characteristics.

1.1.2 Classification

Even though all classes of diabetes are characterized by hyperglycemia, diabetes is classified according to the mechanism that contributes to the hyperglycemia presented by the patient. As such, diabetes is classified into:

1. Type 1 diabetes (T1D),
2. Type 2 diabetes (T2D),
3. Gestational diabetes, and,
4. Diabetes due to other causes

1.1.2.1 Type 1 diabetes

Only about 5-10% of diabetic patients have T1D, which is characterized by pancreatic β-cell destruction that usually leads to complete insulin deficiency. The damage to the β-cells may be due to an autoimmune response (Type 1A diabetes) or may be idiopathic in nature (Type 1B

diabetes) [17]. The autoimmune induction of diabetes is caused by the destruction of pancreatic β cells by activated CD4+ and CD8+ cells and macrophages that infiltrate the pancreas. This may be caused by environmental factors having an effect on a genetic predisposition [1]. For example, observational studies have shown a significant association between pancreatic enterovirus infection resulting in an autoimmune response and the development of T1D [18]. Lonrot et al [19] showed that respiratory infections in young children are associated with the onset of T1D. In detail, 3-month-old children were followed until they were 4 years of age and for each case of respiratory infection recorded, the incidence of pancreatic autoimmunity increased by 5.6% per year. Furthermore, other studies have shown that abnormalities in the gene for the human leucocyte antigen (HLA), the proteins of which enable the body to determine the differences between normal and foreign cells, is also associated with the development of T1D. Defects in the HLA proteins result in an autoimmune response [1]. In fact, Mustonen et al [20] recently showed that children with an HLA gene defect are susceptible to infections prior to the development of T1D.

Idiopathic T1D or type 1B diabetes, which is common in Asians and Africans, does not involve an autoimmune response and the mechanisms contributing to its onset are not completely understood. Hanafusa and Imagawa [21] recently reported the presence of a subtype of type 1B diabetes known as fulminant T1D, which is characterized by the development of common cold or gastrointestinal symptoms, followed by the rapid onset of hyperglycemia (an average of 4 days later) and other symptoms associated with T1D including ketoacidosis which, if left untreated, may result in the death of the patient within 24 hours [21].

1.1.2.2 Type 2 diabetes

T2D is the most common form of diabetes and accounts for 90-95% of all diabetic patients. The onset and progression of T2D occurs over many years, and often patients are diagnosed years later, by which time deleterious complications have established. This form of diabetes is characterized by hyperglycemia due to the development of insulin resistance and reduced insulin secretion [22]. Risk factors for T2D include obesity, hypertension and dyslipidemia [23], and patients with T2D have increased risk of cardiovascular disease compared to non-diabetics [24].

Numerous studies have been undertaken in order to determine the exact mechanisms that contribute to the pathogenesis of T2D, but due to the heterogeneous nature of the disorder and the multiple interconnections between the suggested mechanisms, there is no one mechanism that is all encompassing. Reports show that obesity is a major cause of T2D and is accompanied by increases in circulating free fatty acids (FFA) which result in the development of peripheral insulin resistance and hyperglycemia [25]. Specifically, FFA mediate insulin resistance and hyperglycemia by inhibiting peripheral insulin stimulated glucose uptake [26] and increasing hepatic glucose output [27]. Randle et al [28] suggested that FFA inhibit pyruvate dehydrogenase which leads to increases in citrate concentrations and subsequent decreases in hexokinase activity resulting in decreased glucose uptake. Yu et al [26] further showed that increases in FFA are associated with a decrease in insulin stimulated glucose uptake through reduced insulin signaling, in particular, decreased insulin receptor substrate-1 tyrosine phosphorylation and phosphatidylinositol 3-kinase activity. In association with this is the induction of a state of chronic, low-grade inflammation, thereby linking metabolism to inflammation (reviewed in [29]). Tumor necrosis factor α (TNF-α) has been identified as one of the cytokines that infiltrate

adipose tissue in order to induce inflammation as well as insulin resistance [30]. When combined with the pro-inflammatory cytokines IL-1β and IFN-γ, TNF-α has also been shown to induce islet dysfunction in humans by increasing the expression of IL-12 and its receptor, which in turn have been shown to inhibit glucose-stimulated insulin secretion [31]. Both the metabolic disturbances and low-grade inflammation associated with T2D are interlinked with the development of oxidative stress, fibrosis, hypertrophy and apoptosis, which have all been associated with the pathophysiology of T2D. These mechanisms are relevant to the scope of the studies discussed herein and will be discussed in detail in section 1.2.

1.1.2.3 Gestational diabetes

Gestational diabetes is defined as "any degree of glucose intolerance with onset or first recognition during pregnancy" [17]. Diabetes in pregnancy increases the risk of mothers developing diabetes in the future [32], and leads to increased risk of both preeclampsia [33] and preterm labor [34]. In addition, women diagnosed with gestational diabetes give birth to infants with higher mean birth weight and that are large for gestational age [35]. Infants that are large for gestational age are in turn at an increased risk of developing obesity, diabetes and insulin resistance later in life. Unfortunately, female offspring of women with gestational diabetes also have increased chances of developing gestational diabetes [36]. It is proposed that gestational diabetes results from both the development of insulin resistance, which most likely begins before pregnancy, as well as pancreatic β-cell dysfunction [37, 38]. Similar to the pathogenesis of T1D, recent studies have shown an association between variants in the HLA class II alleles and antigens with gestational diabetes [39], suggesting that HLA may play a role in the development of gestational diabetes.

1.1.2.4 Diabetes due to other causes

Various other specific types of diabetes include diabetes due to defects in the pancreatic β cells, genetic defects in insulin action, diseases that affect the function of the pancreas (e.g. pancreatitis and cystic fibrosis), drug- or chemical- induced diabetes, diabetes due to infections (e.g. congenital rubella and cytomegalovirus) as well as genetic syndromes that are associated with diabetes (e.g. Down's syndrome, Turner's syndrome and Prader-Willi syndrome) [17].

Though there are various causes and hence classifications of diabetes, for the purposes of this study, only type 1 and 2 diabetes were assessed. This was due in part to the fact that both types affect the highest number of diabetic patients and result in the most significant contribution to the development of heart disease, which was the main consequence of concern.

1.1.3 Diagnosis of types 1 and 2 diabetes

Based on previous studies, the Canadian guidelines for the diagnosis of diabetes include a fasting (8 hours) plasma glucose level of ≥7.0 mmol/L or a 2-hour plasma glucose ≥11.1 mmol/L as measured by an oral glucose tolerance test using 75g of glucose. These values have also been closely linked with the development of diabetic retinopathy [40-42]. Random plasma glucose levels, regardless of the fasting state of the patient, can also be measured and diabetes is diagnosed at random plasma blood glucose levels of ≥11.1 mmol/L. In addition to elevated blood glucose, diabetes leads to increased levels of glycated hemoglobin (A_{1C}) which have also been correlated with the development of retinopathy [40] as well as being a significant predictor for the development of cardiovascular diseases [43, 44]. A_{1C} is a glycation end-product resulting from glucose entering the red blood cell and non-enzymatically binding to the β-chain N-

terminal valines and ε-amino groups of lysyl groups of hemoglobin. Since red blood cells have a half-life of 2-3 months, measuring the amount of glucose bound- or glycated hemoglobin gives a reflection of how much blood glucose has been circulating in the blood for the past 2-3 months [45]. Diabetes is diagnosed at an A_{1C} that is equal to or greater than 6.5% of total hemoglobin. However, it is important to note that patients diagnosed with diabetes using blood glucose measurements may not have elevated $A_{1C.}$ The opposite is also true, elevated A_{1C} levels are not always correlated to elevated blood glucose levels [46]. The choice of which test to use is at the discretion of the physician as there are advantages and disadvantages for using each test [47] and combinations of tests may be used in order to ascertain the presence of disease and treat accordingly.

1.2 Cardiac disease as a consequence of diabetes

1.2.1 Overview

As previously mentioned, both T1D and T2D are associated with the development of diabetic retinopathy [48, 49] and neuropathy [50], cardiovascular disease and an overall decline in quality of life [51]. Obese patients are often diagnosed with insulin resistance, glucose intolerance, pre-diabetes and T2D and with 51% of the population expected to be obese by year 2030, the need to curtail its progression and eventual consequences, including T2D, is imminent [52].

Cardiovascular complications are contributory factors to mortality and morbidity in both obese and diabetic patients. The Framingham study showed that diabetes has the same impact on the incidence of coronary heart disease and stroke in men and women. However, diabetic women have a 5-fold and diabetic men a 2-fold greater likelihood of developing heart failure compared to age-matched controls [53]. Of interest is diabetic cardiomyopathy, which is defined as

“diabetes-associated changes in the structure and function of the myocardium that are not directly attributable to other confounding factors such as coronary artery disease and hypertension” [54]. Diabetic cardiomyopathy is characterized by diastolic dysfunction (during cardiac relaxation) and/or systolic dysfunction (during cardiac contraction) that eventually leads to heart failure [55].

Earlier studies suggested that diastolic dysfunction precedes systolic dysfunction in diabetes, however, Ernande et al [56] found patients with systolic dysfunction in the absence of detectable diastolic dysfunction. In addition, more recent studies have identified diabetic and obese individuals with heart failure but preserved ejection fraction, a measure of systolic function [57, 58]. Heart failure with preserved ejection fraction is characterized by diastolic dysfunction, which is associated with cardiac fibrosis as well as stiffness [59]. Together these suggest that in diabetic cardiomyopathy, systolic dysfunction may not necessarily follow diastolic dysfunction. Diastolic dysfunction in diabetic patients is characterized by a decrease in early diastolic filling and an increase in atrial filling as well as increases in both the isovolumetric relaxation time and the deceleration time [60]. Systolic dysfunction is characterized by a decrease in left ventricular ejection fraction [61]. The factors contributing to impaired cardiac function under diabetic conditions include impaired calcium homeostasis, a reduction in ATP production, reduced coronary flow reserve and cardiac extracellular matrix (ECM) remodeling [62]. The underlying mechanisms contributing to these changes include, pertinent to this study, cardiac metabolic dysregulation, oxidative stress, fibrosis and hypertrophy.

1.2.2 Metabolic dysregulation

In the normal heart, oxidative phosphorylation accounts for the majority of ATP synthesis (>95%) even when workload is increased by 3- to 5- fold. In contrast, glycolysis and, to a lesser extent, the citric acid cycle generate ~5% of cardiac ATP [63, 64]. The primary source for cardiac ATP generation is through fatty acid (FA) metabolism (70-90%) and the remaining 10-30% is generated through glucose oxidation, lactate metabolism and the metabolism of ketone bodies [64].

It is well established that disturbances in cardiac metabolism are associated with the development of cardiac dysfunction. Back in 1977, Regan et al [65] identified lipid deposits in left ventricular biopsies from patients with T2D. These were also associated with accumulation of both cholesterol and cardiac triglycerides. Cardiac lipotoxicity has been closely linked with the development of diastolic dysfunction but not systolic dysfunction in T2D [66]. Using a working heart model, Belke et al [67] showed that in a diabetic db/db mouse model fatty acid oxidation was increased by two-fold, glycolysis was decreased by 52% and glucose oxidation was also reduced compared to non-diabetic control animals. Increases in cardiac fatty acid oxidation (FAO) are also associated with increases in both fatty acid uptake and cardiac lipid accumulation in the form of various lipid metabolites including diacylglycerol (DAG), long chain acyl CoAs, triacylglycerides (TAG) and ceramides [68, 69]. Lipid accumulation is also associated with cardiac dysfunction as substantiated by a reduction in cardiac output, left ventricular developed pressure and cardiac power, and an increase in left ventricular end diastolic pressure [67]. In addition, cardiac triglyceride accumulation has also been detected in rodent STZ induced T1D models and this is associated with impairment in both cardiac diastolic and systolic function [70]. The accumulation in cardiac lipids is attributed to the inability of the

cell to balance energy oxidation and energy availability (metabolic flexibility). Specifically, in the heart, lipid availability outpaces lipid oxidation as the cell loses its ability to switch between energy substrates due to its reliance on insulin, thereby leading to decreased glucose oxidation, lipotoxicity and eventually cardiac dysfunction [71].

Insulin resistance, a hallmark of T2D, is associated with a decrease in glucose uptake. It is postulated that the decrease in glucose uptake and oxidation is due to a reduction in cytoplasmic glucose transporter 4 (GLUT 4) protein expression and translocation to the cell membrane. GLUT1 and GLUT4 are the most abundant glucose transporters in the heart. GLUT1 is ubiquitous, located on the plasma membrane and is responsible for basal glucose uptake. On the other hand GLUT4 is only found in insulin sensitive tissues (heart, adipose tissue, skeletal muscle) and, under basal conditions, is located in transport vesicles in the cytoplasm and is translocated to the cell membrane upon stimulation by insulin [72]. The latter involves insulin binding to the cardiac insulin receptor resulting in tyrosine auto-phosphorylation of the β subunits of the receptor and subsequent recruitment and activation of phosphatidyl-inositol-3 kinase (PI3K), phosphoinositide-dependent kinase 1, Akt/protein kinase B, and protein kinase C-λ and ζ [73]. The absence of insulin, as seen in T1D, or the inability of insulin to bind to its receptor, as seen with insulin resistance, contributes to impaired GLUT 4 recruitment to the cell surface membrane.

In T2D there is decreased insulin-activated Akt signaling and failure of the GLUT4 transporter to translocate to the cell membrane [74]. In fact, it has been shown that db/db mice that overexpress human GLUT4 do not develop cardiac contractile dysfunction and both glucose and palmitate metabolism are similar to that of control animals [67]. In addition, rats treated with streptozotocin (STZ) in order to induce T1D exhibit reduced cardiac GLUT4 protein expression

[75]. These data suggest that insulin plays a pivotal role in the regulation of cardiac metabolism through regulation of the Akt/GLUT4 pathway and subsequently glucose uptake and cardiac function in both T1D and T2D.

With respect to the observed cardiac dysfunction associated with lipotoxicity, several mechanisms involving alterations in fatty acid uptake, triglyceride (TG) synthesis and TG breakdown have been postulated but the mechanisms are not completely understood. For example, Yagyu et al [76] suggest that cardiac lipoprotein lipase (LPL), an enzyme that hydrolyzes circulating TG to free fatty acids, contributes to increased cardiomyocyte fatty acid uptake. Due to the impaired glucose uptake observed in the diabetic heart, LPL activity is increased with both acute [77] and chronic [78] T1D in order to meet the FA acid requirement of the cardiomyocyte. However, other studies have shown no change [79] or decreases [80] in LPL activity under diabetic conditions. These differences could be attributed to differences in dosage and duration of STZ treatment (reviewed in [81]).

Mice overexpressing cardiac peroxisome proliferator-activated receptor α (PPARα), a nuclear factor that regulates genes involved in FA uptake and oxidation, show increased levels of FA uptake and oxidation, triglyceride accumulation and decreased glucose uptake and oxidation which is accompanied by cardiac hypertrophy and systolic dysfunction similar to observations made in diabetic mice [82]. In a T2D model utilizing low dose STZ and high fat feeding, diabetic mice with cardiac specific deletion of PPARα are in fact protected from the development of hypertrophy and cardiac dysfunction whereas diabetic mice overexpressing PPARα exhibit severe lipotoxicity and cardiac dysfunction. Removal of the high fat diet from diabetic mice overexpressing PPARα ameliorates the observed cardiac TG accumulation [83]. This suggests

that PPARα may play a significant role in lipotoxicity associated with diabetes as well as the accompanying cardiac dysfunction.

The fatty acid transporter CD36 has also been implicated as a possible contributor to cardiac lipid accumulation and dysfunction. CD36 is the main long chain fatty acid transporter into the heart, skeletal muscle and adipose tissue, accounting for about 70% of FA uptake in cardiomyocytes [84]. Under basal conditions, 50% of the cellular CD36 pool is stored in compartments that are rapidly translocated to the cell membrane for FA uptake in response to various stimuli including insulin [85] and contraction [86]. In high-fat fed rats, CD36 translocation to the plasma membrane is increased and this is accompanied by cardiac systolic dysfunction [87]. In hearts of T1D rodents, CD36 protein expression and sarcolemmal translocation are increased [88] and in T2D hearts CD36 mRNA expression is increased and this is accompanied by diastolic dysfunction [89], suggesting that in diabetic mice, alterations in fatty acid uptake by CD36 may contribute to cardiac dysfunction.

1.2.3 Oxidative stress

At physiological levels, ROS are important secondary messengers regulating a variety of cellular activities including hypoxia, autophagy and immunity [90]. They are regulated by anti-oxidants including superoxide dismutase, glutathione peroxidase and catalase [91]. However, under diabetic conditions, an imbalance between ROS production and regulation occurs whereby ROS are increased and the cell's antioxidant capacity is diminished thereby leading to oxidative stress which ultimately facilitates cardiovascular complications associated with diabetes [92]. In cardiomyocytes, sources of ROS include the mitochondrial electron transport chain (ETC), nicotinamide adenine dinucleotide phosphate (NADPH) oxidases and xanthine oxidase.

Under normal conditions, cytoplasmic glucose oxidation via glycolysis results in the production of nicotinamide adenine dinucleotide (NADH) and pyruvate. NADH can subsequently convert pyruvate to lactic acid, a substrate for hepatic gluconeogenesis, or enter the mitochondrial ETC for the generation of ATP. Pyruvate may also enter the mitochondrial tricarboxylic acid (TCA) cycle to produce both NADH and flavine adenine dinucleotide ($FADH_2$), both of which are reducing equivalents for the ETC [93].

The ETC comprises of 5 enzyme complexes (Complex I, II, III, IV, V), cytochrome c and ubiquinone. NADH donates electrons to complex I (NADH:ubiquinone oxidoreductase) whereas $FADH_2$ donates electrons to complex II (succinate:ubiquinone oxidoreductase). Complex II may also receive electrons from glycerol 3-phosphate dehydrogenase, an enzyme that catalyzes the conversion of dihydroxyacetone phosphate to sn-glycerol 3-phosphate, thereby providing a link between glucose and lipid metabolism. Both complexes I and II then transfer the electrons to ubiquinone which subsequently donates them to ubisemiquinone and then complex III (ubiquinol:cytochrome c oxidoreductase) [93]. Ubesemiquinone has been identified as a superoxide generator [94]. Electrons from complex III are then transferred to cytochrome c, then complex IV (cytochrome c oxidase) and finally to oxygen to produce water. The transfer of electrons through complexes I, III and IV results in a proton gradient that drives complex V (ATP synthase) and ATP synthesis [93]. An increase in the proton gradient, as seen with hyperglycemia, inhibits electron transfer at complex III resulting in accumulation of superoxide [95]. Superoxide generated by NADH dehydrogenase at complex I and ubisemiquinone on complex III through the partial reduction of O_2 to $O_2^{-}\bullet$ instead of water are released into the intermembrane space and subsequently the cellular cytoplasm [93, 96, 97].

Even though the mitochondrial ETC is the major source of ROS in cardiomyocytes, there are other cellular processes that can result in ROS production. The NADPH oxidases (Nox) catalyze the conversion of O_2 to $O_2^-\bullet$ using NADPH as the electron donor thereby serving as a source for ROS. There are seven members of the NOX family of enzymes, Nox 1-5 and dual oxidase 1-2, and NOX4 is the most abundant in the cardiomyocyte mitochondria [98]. *In vitro* studies have associated hyperglycemia with increased NADPH oxidase activity and Nox4 protein expression. In addition, in T1D rats, Nox4 activity is increased in the left ventricle [99].

Xanthine oxidoreductase (XOR), an enzyme catalyzing the oxidation of hypoxanthine and xanthine to uric acid using O_2 results in the production of $O_2^-\bullet$ and H_2O_2 as by-products and has also been identified as a source of ROS in cardiomyocytes. XOR exists as a dimer of which each monomer has a molybdoterin cofactor, two Fe-S units and an FAD domain. It is expressed in the dehydrogenase form, XDH, but when inflammation occurs the reductase switches to an oxidase form (XO) by oxidation of the cysteine 535 and 992 residues or by proteolytic conversion. XDH reduces NAD^+ to NADH when xanthine is converted to uric acid whereas XO reduces oxygen to $O_2^-\bullet$ and H_2O_2 (reviewed in [100]). Levels of XO have been found to be increased in plasma of both type 1 [101] and type 2 [102] diabetic patients and treatment with the XO inhibitor allopurinol results in a decrease in plasma XO [101]. In T1D mice, serum XO activity is elevated and this is associated with increased myocardial ROS production and both systolic and diastolic dysfunction. Treatment of these animals with allopurinol attenuates the cardiac dysfunction, increased XO activity and cardiac ROS production [103].

Increases in ROS are associated with various cellular changes that contribute to cardiac dysfunction associated with diabetes. Oxidative stress has been linked to myocardial cell death through initiating mitochondrial damage. It is postulated that increases in ROS result in increases

in mitochondrial Ca^{2+} which in turn activates the opening of the mitochondrial permeability transition pore (mPTP), a transmembrane protein which when open allows the efflux of solutes across the membrane. This causes further depolarization of the mitochondria and results in a reduction in ATP generating capacity, efflux of cytochrome c and eventual cell death [104]. Further studies suggest that low ATP synthesis due to an increase in mPTP sensitivity associated with T2D induced oxidative stress may result in increased sarco/endoplasmic reticulum calcium ATPase 2 (SERCA2) activity which may contribute to the observed diastolic dysfunction [105]. SERCA2 is a transmembrane protein located in the cardiomyomyocyte sarcoplasmic reticulum (SR) and transfers cytosolic Ca^{2+} into the lumen of the SR thereby playing a significant role in cardiac contractility [106].

Oxidative stress also increases the expression of advanced glycation end product receptors (RAGE). Hyperglycemia results in an increase in advanced glycation end products (AGE) which activate RAGE to increase fibrosis [107] and activate nuclear factor κB (NFκB) signaling [108] and also promotes crosslinking of AGEs with SERCA2 [109], thereby promoting myocardial stiffness and impairing cardiac function.

1.2.4 Fibrosis and hypertrophy

The common structural features associated with diabetic cardiomyopathy are cardiomyocyte hypertrophy and fibrosis [110]. Cardiac fibrosis is characterized by the accumulation of ECM proteins in the myocardium, often resulting in diastolic and/or systolic dysfunction. Under normal cellular conditions, fibroblasts are inactive but can be activated to myofibroblasts in response to growth factors, cytokines and mechanical changes in order to maintain the ECM homeostasis [111]. Subsequently, fibroblasts also further secrete cytokines and growth factors which affect myocytes [112]. Hyperglycemia, a hallmark of diabetes, triggers

oxidative stress and inflammatory responses resulting in cardiomyocyte injury and apoptosis. Consequently, this results in activation of cardiac remodeling including collagen deposition and eventually cardiac stiffening and altered cardiac function [62].

The primary effector of hyperglycemia induced cardiac fibrosis is transforming growth factor beta (TGF-β). Increased production of reactive oxygen species results in increased levels of TGF-β gene expression, which are implicated in both cardiac hypertrophy and collagen deposition [113]. There are 3 isoforms of TGF-β protein, TGF-β1, β2 and β3, which play a pivotal role in cardiac remodeling in mammals. Of all the isoforms, TGF-β1 is the most abundant and ubiquitous while the other isoforms are found in limited cell types. TGF-β is abundant in the heart and is regulated through its ability to exist in a latent or an active form. The latent form of TGF-β is the most abundant and cannot bind to the TGF-β receptor [114].

Each isoform of TGF-β is encoded by a different gene and undergoes proteolytic cleavage between amino acids 278 and 279 by the enzyme furin prior to secretion. This results in two products: The N-terminal region known as the latency-associated peptide (LAP) and the C-terminal region known as the mature TGF-β. These two products form dimers that, due to the LAP region, are inactive. Various factors have been shown to be able to either remove LAP from the mature TGF-β or induce a conformational change in LAP, therefore, making TGF-β active by allowing access to the receptor binding site on mature TGF-β. *In vitro* studies have assisted in showing that low pH, ROS, proteases, glycoproteins and urea are capable of activating TGF-β. TGF-β1 is the isoform most susceptible to activation (reviewed in [115]). Upon activation TGF-β binds to the TGF-β receptor II (TGFβRII) on the cell membrane, which subsequently heterodimerises with and activates TGFβRI. The TGF-β signal cascade then follows either a canonical pathway involving the Small mothers against decapentaplegic (Smad), also known as

the Smad-dependent pathway, or non-canonical pathways known as the Smad-independent pathways (Figure 1).

In the Smad-independent signaling pathway, TGF-β activates multiple downstream effectors that have different outcomes. For example, TGF-β can activate the mitogen-activated protein kinase kinase 4 (MKK4), which in turn, phosphorylates and hence activates the c-jun N-terminal kinase (JNK) [116]. Phosphorylated JNK activates c-Jun [117]. Studies in human BAHgpt cells, which are derived from fibrosarcoma HT1080, show that c-Jun increases the synthesis of fibronectin, a protein involved in cytoskeletal organization, cell adhesion and migration. Tissue fibrosis is associated with a marked increase in fibronectin [118].

Activation of TGFβRI can also result in the activation of RAS and subsequent activation of c-Raf, MEK and Erk which has been shown to play a role in fibrosis [119]. Studies show that Erk can facilitate the phosphorylation of both Smad2 and Smad3 at sites that prevent their translocation to the nucleus, thus decreasing fibrosis [120]. *In vitro* studies show that protein phosphatase 2A (PP2A), which plays a role in dephosphorylating substrates, can also be activated through TGF-β signaling, resulting in inhibition of p70 S6 kinase (S6K), a serine/threonine kinase which phosphorylates the S6 ribosomal protein thereby activating protein synthesis. Inhibition of S6K results in cell-cycle G1 arrest [121]. PP2A activity has previously been shown to be increased in T1D rat hearts and as early as 1 week after onset of diabetes and this was associated with cardiac dysfunction, thereby providing a link between diabetes and cardiac dysfunction through the Smad-independent pathway [122].

In the Smad-dependent pathway, a signal cascade that travels through Smad proteins is initiated and propagated to the nucleus. There are different classes of Smads, that is, (1) the receptor regulated Smads or R-Smad (Smad1, 2, 3, 5 and 8), (2) the common mediator Smad or

co-Smad (Smad4) and (3) the antagonistic or inhibitory Smads or I-Smads (Smad6 and 7). In vertebrates, Smad2 and Smad3 are substrates of TβRI, Smad1, 5 and 8 are substrates for the bone morphogenetic protein (BMP) type I receptor kinases, Smad4 is the common signaling protein, Smad7 inhibits Smad2/3 activation and Smad6 inhibits BMP signaling. Smad2 and Smad3 are activated via phosphorylation by TβRI kinase and are translocated from the receptor and form a complex with Smad4. The Smad2/3/4 complex then moves to the nucleus where it is involved in activation or suppression of specific genes [123]. Upon entering the nucleus, the Smad2/3/4 complex binds to the Smad binding elements located on the regulatory regions of genes encoding ECM proteins. Genes that are activated by the TGFβ/Smad pathway include those for Col1A1 and COL1A2 which encode for collagen type 1, COL3A1 which encodes for collagen type 3 and Col6A1 and Col6A3 which encode for collagen type VI [124].

Upon activation of TGFβ signaling, Smad7 mRNA expression is increased. Smad7 is involved in regulating TGFβ signaling in a well-established negative feedback loop [125, 126]. While Smads 2, 3 and 4 are ubiquitously found in all cell types, expression of Smad7 is dependent on extracellular signals [123]. Smad7 stably interacts with activated TβRI and competes with R-Smads at the receptor thereby hindering their activation and subsequent translocation to the nucleus [125, 126]. Overexpression of Smad7 in adult rat fibroblasts is associated with decreased collagen I and III expression, while scar tissue in post-myocardial infarct rat hearts has decreased levels of Smad7, suggesting that reduced levels of Smad7 contribute to fibrosis [127]. There is limited information on the role of Smad7 in diabetic heart disease. To date, one study using a rat model of STZ-induced T1D has been able to show that after 12 weeks of diabetes, cardiac dysfunction is induced and both TGFβ1 and Smad3 protein and mRNA expression levels are upregulated whereas Smad7 protein and mRNA expression

levels are reduced. However, the exact mechanism contributing to those observations is not known [128].

Studies in transgenic mice have shown that over-expression of TGFβ also induces cardiac hypertrophy [129]. However, efforts to determine the exact mechanism contributing to this observation have been impeded by the complexity of the TGFβ signaling pathways [130]. With respect to diabetes, T2D patients are 1.5 times more likely to develop left ventricular hypertrophy, independent of other covariants such as ethnicity, compared to non-diabetics [10]. Whether this is associated with an increase in cardiac TGFβ activity in humans is unknown, as studies of TGFβ signaling in relation to diabetic cardiac hypertrophy have been done in cell culture or in small animal models [130].

Cardiac hypertrophy may also be induced through activation of IL-6. Co-culture of murine cardiac myocytes with cardiac fibroblasts in the presence of interleukin-6 (IL-6) results in cardiomyocyte hypertrophy [131]. However, culturing myocytes or fibroblasts alone does not result in a significant increase in IL-6 [132]. This finding suggests a cross-talk between myocytes and fibroblasts in order to initiate hypertrophy. IL-6 is significantly increased in both T1D [133] and T2D [134] and contributes to left ventricular dysfunction in diabetic cardiomyopathy [133]. It is postulated that IL-6 initiates hypertrophy through the janus kinase-signal transducer and activator of transcription (JAK/STAT) pathway and other subsequent pathways including the extracellular signal-regulated kinase 1/2 (ERK1/2) and PI3Kinase/Akt pathways [135]. In addition, angiotensin II, which is increased under diabetic conditions, binds to angiotensin II type I (AT1) receptors of fibroblasts and activates increases in IL-6 in fibroblasts [136]. AT1 receptors are minimal on cardiomyocytes and angiotensin II binds preferentially to fibroblasts [137]. IL-6 subsequently phosphorylates glycoprotein 130 (gp130) and consequently the Janus-

family tyrosine kinases (JAK)-signal transducer and activator of transcription-3 (STAT3) pathway, resulting in hypertrophy [136].

1.3 Mouse models of obesity and diabetic cardiac dysfunction

For the purposes of the studies described herein, mouse models were used to investigate the development of cardiac dysfunction associated with diabetes and obesity. The use of mice is preferable as they are both cost effective and can be genetically manipulated. With respect to diabetic cardiomyopathy, previous studies have shown that mouse models of obesity and diabetes exhibit some similarities to human cardiac diabetic dysfunction including diastolic and systolic dysfunction, hypertrophy, lipotoxicity and altered mitochondrial function [81, 138]. We employed the STZ-treated mouse as a model for T1D, high-fat fed STZ-treated mice as a model for T2D, and mice fed a high fat diet as models for obesity. These models are discussed in more detail below.

1.3.1 Steptozotocin-induced type 1 diabetic mouse model

STZ has been used for many years to induce a form of poorly controlled type 1 diabetes in animal models. Indicated for the treatment of pancreatic β cell carcinoma, STZ is a glucosamine-nitrosurea (1-methyl-1-nitrosurea linked to the 2 carbon of d-glucose) compound that can induce both hyperglycemia and hypoinsulinemia depending on the dosage used [139]. The glucose moiety of STZ allows the compound to selectively enter the pancreatic β cell through its ability to bind to the glucose transporter 2 (GLUT2) receptor due to the structural similarity of the compound to glucose. The nitrosurea group is believed to be responsible for the

cytotoxic effects of the drug due to its alkylating capabilities which are believed to occur at high doses of the drug [140].

Wilson et al [141] postulated that STZ exerts its cytotoxic effects by initially increasing the intracellular concentration of carbonium ions which are by-products of the decomposition of the nitrosurea moiety. Consequently, the carbonium ions alkylate DNA and, in an attempt to repair this DNA alteration, the poly ADP-ribose system is triggered resulting in depletion of NAD+ through its catabolism by poly ADP ribose synthetase. NAD+ is vital in energy production and its depletion results in eventual pancreatic β cell necrosis [141]. Other studies have postulated that STZ acts as a diabetogenic agent through altering the ROS scavenging capabilities of the cell. This is supported by the observation that treatment with STZ results in decreases in the free radical scavengers superoxide dismutase [142] and reduced glutathione [143] and increases intracellular free radicals thereby resulting in oxidative stress, which then leads to cell death [144]. The effects of STZ on oxidative stress are supported by the observation that treatment of animals with superoxide dismutase 50 min prior to injection with STZ partially inhibits the associated depletion in insulin [144].

Both single high dose and multiple low dose (over several days) injections are used to develop T1D mouse models. However, the Diabetic Complications Consortium (DiaComp) recommends using multiple low dose treatments as single high dose injections may result in toxic effects outside of the pancreas. The recommended treatment is 50mg/kg STZ for 5 consecutive days [145].

Mice treated with low dose STZ for 5 days exhibit hyperglycemia within 7 to 10 days after the first injection and this is accompanied by increased serum triglycerides [146] and serum fatty acids [147]. Insulin levels decrease gradually as the disease progresses [148]. Yu et al [149]

showed that STZ-treated hyperglycemic C57Bl/6 female mice exhibit both systolic dysfunction, as shown by reductions in both left ventricular ejection fraction and cardiac output, and diastolic dysfunction, as reflected by an increase in the ratio of the early (E) to late (A) ventricular filling velocities (E/A ratio), measured by both magnetic resonance imaging and echocardiography 4 weeks after STZ treatment. Male C57Bl/6 mice show both diastolic and systolic dysfunction 12 weeks after STZ treatment [150]. In contrast, in CD1 mice, female mice exhibit diastolic dysfunction at 8 weeks and systolic function at 12 weeks after STZ treatment. However, in the same study, treatment of male CD1 only showed diastolic dysfunction 12 weeks after treatment and systolic dysfunction became more apparent after 16 weeks of diabetes [151]. These data suggest that in addition to the mouse strain, sex also plays a significant role in determining the effects of STZ treatment on cardiac function.

STZ offers advantages for the induction of T1D including the following: it is rapidly eliminated after treatment thereby limiting systemic toxicity, STZ-induced diabetes is reversible using insulin, and the pancreatic ß cell damage caused by STZ can be reversed using phytochemicals and natural plant products [152]. However, several limitations to the use of STZ exist, including (1) strain, gender and diet influence the sensitivity of animals to STZ; (2) there is no set protocol for STZ preparation, including the pH of the buffer STZ is dissolved in and the time period in which the prepared solution should be used before it degrades; (3) variations exist in the methods of its administration, i.e. intraperitoneal or intravenous, resulting in varying extents of diabetes induction; (4) there are variable reports on the time at which persistent diabetes starts; and, (5) there are limited data on the mortality rate associated with STZ treatment (reviewd in [153]).

1.3.2 High-fat and low-dose streptozotocin type 2 diabetic mouse model

In T2D patients, both insulin resistance and hyperglycemia occur following the onset of obesity [154]. As such, some mouse models for T2D try to mimic this by feeding mice a high fat diet in order to initiate obesity and insulin resistance, followed by treatment with low dose STZ in order to partially ablate pancreatic insulin production, thereby inducing hyperglycemia. Mice are maintained on a high fat diet for the duration of the study [155]. In this model, mice not only exhibit signs of obesity, glucose intolerance, insulin resistance and cardiac dysfunction but also impaired cardiac mitochondrial respiratory function [156].

1.3.3 Diet-induced obese mouse model

In order to study the effects of diet on the induction of obesity and diabetes, experimental models involving feeding mice either a diet high in fat or a diet high in both fat and sugar, particularly sucrose, have been implemented. Previous studies have shown that diet is more effective in inducing obesity in C57Bl/6 mice compared to other strains, including C3H/He and BALB/c mice [157]. Similar to observations made in humans, high-fat fed C57Bl/6 mice are obese and develop insulin resistance and hyperglycemia compared to their chow-fed counterparts (reviewed in [158]). However, the effects of high fat feeding on cardiac function have not been consistent in different studies. For instance, Park et al [74] showed that high fat feeding (55% Kcal fat, 20 weeks) results in cardiac dysfunction in C57Bl/6 mice. In contrast, Brainard et al [159] were unable to detect cardiac dysfunction following high fat feeding (60% Kcal fat, 6 months) in the same strain of mice.

A “Western” diet, which has been defined as a diet high in both fat and sugar, not only increases cardiac cholesterol and fatty acid content in mice but also induces mild cardiac

hypertrophy after 12 weeks of feeding [160]. Mice fed a Western diet have been shown to have decreased left ventricular ejection fraction and increased isovolumic relaxation time as measured by echocardiography, thereby showing both systolic and diastolic dysfunction, respectively [161]. Similarly, mice fed the same diet for 16 weeks [162] or extended periods of as long as 6 months [163] exhibit cardiac dysfunction.

Though there is flexibility in the dietary compositions and feeding duration used to induce obesity in mice, it is worth noting that multiple studies have found different outcomes pertaining to their effect on blood glucose and cardiac function and this makes the results following chronic feeding unpredictable. These discrepancies are discussed later in chapter 3 as we sought to determine which composition would best result in the induction of dietary-induced cardiac dysfunction.

1.4 The RhoA/ROCK pathway

1.4.1 Overview

Multiple mechanisms have been postulated to contribute to the pathogenesis of diabetic cardiomyopathy. Of importance is the contribution of the RhoA/Rho-associated coiled-coil-containing protein kinase (ROCK) signaling pathway (Figure 2). RhoA is a member of the Ras superfamily and is inactive when GDP-bound and active when GTP-bound. Guanine nucleotide exchange factors (GEFs) regulate the activation of RhoA by enabling the exchange of GDP for GTP, whereas GTPase activating proteins (GAPs) promote its inactivation by hydrolyzing GTP to GDP [164]. In order to maintain the inactive state, guanine nucleotide dissociation inhibitors (GDIs) bind to the RhoA/GDP complex and promote its relocation from the cell membrane to the cytoplasm. Activated RhoA binds and stimulates various effectors, the best known of which

is ROCK. There are two isoforms of ROCK: ROCK 1 and ROCK 2 [165]. These exhibit an overall 65% homology in their amino acid sequence, and 92% homology in the kinase domain [165] and are expressed in multiple tissues including smooth muscle and heart [166].

The RhoA/ROCK pathway mediates multiple cellular activities including smooth muscle contraction [165], regulation of the cytoskeleton, and cell adhesion [167]. Targets of ROCK include myosin light chain (MLC) and myosin phosphatase target subunit 1 (MYPT-1) [166].

1.4.2 RhoA and ROCK as targets in cardiac disease

The role of RhoA in cardiac function has been documented through studies involving its downstream targets, primarily through overactivation of ROCK. However, other targets of RhoA are also now being explored. Cardiac overexpression of RhoA results in atrial enlargement, ventricular dilatation and eventual heart failure [168]. Studies by Lauriol et al [169] have shown that RhoA mediates both cardioprotective and cardio-deleterious mechanisms in a model of transverse aortic constriction (TAC). Specifically, in a model of TAC, which induces cardiac pressure overload and eventual heart failure, mice with cardiomyocyte deletion of RhoA (Esr cre-RhoA$^{fl/fl}$) show similar levels of hypertrophy as wild-type mice 2 weeks after TAC. However, after 8 weeks of TAC, cre-RhoA$^{fl/fl}$ mice had larger hearts and ventricular dimensions compared to wild type mice. Together, these observations suggest that RhoA plays an important role in compensatory hypertrophy to prevent cardiac dilation. Interestingly, in the same study, after 8 weeks of TAC, cre-RhoA$^{fl/fl}$ mice showed lower levels of fibrosis and apoptosis compared to control animals subjected to the same treatment. RhoA was suggested to contribute to fibrosis through activating pro-fibrotic gene regulators such as myocardin response transcription factor (MRTF) and serum response factor (SRF) [169].

In a model of ischemia-reperfusion (I/R) injury, Xiang et al [170] show that cardiac specific knockdown of RhoA is in fact deleterious, as shown by the inability of RhoA knockout mice to withstand injury. It was suggested that RhoA plays a role in cardioprotection through its ability to phosphorylate and activate protein kinase D, a pro-survival enzyme [170]. These studies show that RhoA has a role in cardiac diseases, but its contribution varies by disease state.

ROCK has been found to also play a role in I/R injury, where ROCK activation by RhoA is increased [171-173]. Treatment of isolated rat hearts with the non-specific ROCK inhibitors Y27632 and fasudil before, during and after coronary occlusion results in a smaller infarct size through activation of the pro-survival reperfusion injury salvage kinase pathway involving PI3K, Akt and eNOS [171]. Inhibition of ROCK may also be beneficial in I/R injury through attenuating inflammation and preventing the downregulation of the anti-apoptotic protein Bcl-2 [172]. The beneficial effects of ROCK inhibition in I/R injury contrast with the deleterious effect of deletion of cardiomyocyte RhoA, a discrepancy which has been suggested to arise because RhoA and ROCK are expressed in many different cell types in the heart, and the activation of RhoA in cells other than cardiomyocytes may lead to adverse consequences [170].

The inhibition of ROCK also prevents the hypertrophy, macrophage infiltration and endothelial oxidative stress induced by angiotensin II through reducing the upregulation of NADPH oxidase [174]. Increased ROCK activation has also been implicated in the pathogenesis of atherosclerosis and inhibition results in a reduction in atherosclerotic lesions [175]. Research showing the benefits of ROCK inhibition identify ROCK as a target from treatment of various cardiovascular diseases. However, isoform specific inhibitors are yet to be available for routine use.

1.4.3 Current evidence for a role of the RhoA/ROCK pathway in the development of diabetic cardiomyopathy

Previous studies in our lab have demonstrated a role for the RhoA/ROCK pathway in diabetic cardiomyopathy [176]. Activation of ROCK by RhoA phosphorylates LIM kinase 2, an enzyme important in cardiac actin cytoskeletal reorganization [177]. In streptozotocin (STZ)-induced T1D rats, the expression and activity of RhoA in cardiomyocytes is increased, as is the phosphorylation of LIM kinase 2 (p-LIM kinase 2). These observations are associated with increased actin polymerization and the development of diabetic cardiomyopathy. Treatment with ROCK inhibitors reduces both actin polymerization and p-LIM kinase 2 and improves contractile function [176]. Previous reports from our lab also show that in cardiomyocytes isolated from diabetic rats, RhoA expression and ROCK activity as well as ROS production are increased, and the non-specific ROCK inhibitor, Y-27632 abates ROS production [178].

Currently available ROCK inhibitors are non-selective. As such, this limits their use in determining the roles of specific ROCK isoforms in the pathophysiology of diabetic cardiomyopathy. However, we have also shown in the past that under diabetic and insulin-resistant conditions, ROCK 1 protein expression is unchanged but ROCK 2 protein expression is increased and this is associated with the development of cardiac dysfunction [179, 180]. These data implicate ROCK2 and not ROCK1 as the isoform contributing to the development of cardiac dysfunction under diabetic and insulin resistant conditions.

Collectively, further studies are needed to elucidate (1) if the beneficial effects of RhoA/ROCK inhibition are due to cardiomyocyte-specific RhoA/ROCK inhibition or arise in other cell types, and (2) if ROCK2 is the isoform responsible for the cardiac changes that occur with diabetic cardiomyopathy.

1.5 Rationale and research hypothesis

Our lab was the first to show that the RhoA/ROCK pathway contributes to the development of diabetic cardiomyopathy and that acute inhibition of the pathway with a non-isoform selective ROCK inhibitor results in improvement in cardiac function in a rat model of STZ-induced T1D [176]. Zhou et al [181] also showed that chronic treatment of T2D rats with the non-isoform selective inhibitor fasudil hydrochloride resulted in improvement in cardiac contractile function. Both studies hence identify a possible role of the RhoA/ROCK pathway in both T1D and T2D and suggest this pathway as a potential therapeutic target for diabetic cardiomyopathy. However, a number of questions remain. For instance, the unavailability of specific ROCK inhibitors has made it impossible to determine which ROCK isoform contributes to the observed improvements in cardiac function following treatment of diabetic cardiomyocytes with a non-isoform specific ROCK inhibitor. In addition, research has suggested that activation of RhoA and its downstream targets in cardiomyocytes may have differing consequences than its activation in the heart as a whole, depending on the pathological condition. These data hence complicate understanding the role of RhoA and ROCK in diabetic cardiomyopathy.

The purpose of the research undertaken for this thesis was to further investigate the roles of cardiomyocyte RhoA and of ROCK2 in the development of diabetic cardiomyopathy. The overall research hypothesis tested was that '*deletion of ROCK2, or of RhoA in cardiomyocytes will prevent the development of diabetic cardiomyopathy, and this will be associated with reduced fibrosis and hypertrophy'*. Three different studies were undertaken to test this hypothesis. The aim of the *first study was to determine the contribution of ROCK2 to the development of diabetic cardiomyopathy, using CD1 mice with heterozygous knockout of*

ROCK2, made diabetic with STZ. Complete knockout of ROCK2 is embryonically lethal, but heterozygous mice develop normally [182].

Unexpectedly, diabetic wild-type CD1 mice in our first study did not show any overt cardiac dysfunction as measured by echocardiography, even 13 weeks after induction of diabetes. Therefore, in order to allow investigation of the role of RhoA in the diabetic heart, we next sought to determine a suitable mouse model of diabetes or obesity-induced insulin resistance that was associated with the development of cardiac dysfunction in C57Bl/6 mice, the background of the genetically modified floxed RhoA and cre-RhoA mice that we used. As such, the aim of the second study *was to compare the development and progression of cardiac dysfunction in various mouse models of diabetes and obesity.* In order to do so, we compared STZ-treated, high-fat fed, high-fat/high sucrose fed, and high-fat fed/STZ-treated mice. Interestingly in this strain of mice, STZ-treated animals showed the earliest and most severe signs of cardiac dysfunction, establishing this as the model used for our third study.

Lastly, given that the knockdown of RhoA has been found to have differential effects in models of ischemia reperfusion injury [170] and pressure overload [169], the *third aim was to ascertain the role of RhoA in cardiomyocytes in the development of T1D cardiomyopathy, specifically, the development of fibrosis and hypertrophy.* The results of this study demonstrated that knockdown of RhoA protected the diabetic hearts from the development of cardiac contractile dysfunction. This was associated with normalization of signaling through the TGF-β pathway, and the prevention of cardiomyocyte fibrosis, hypertrophy and apoptosis.

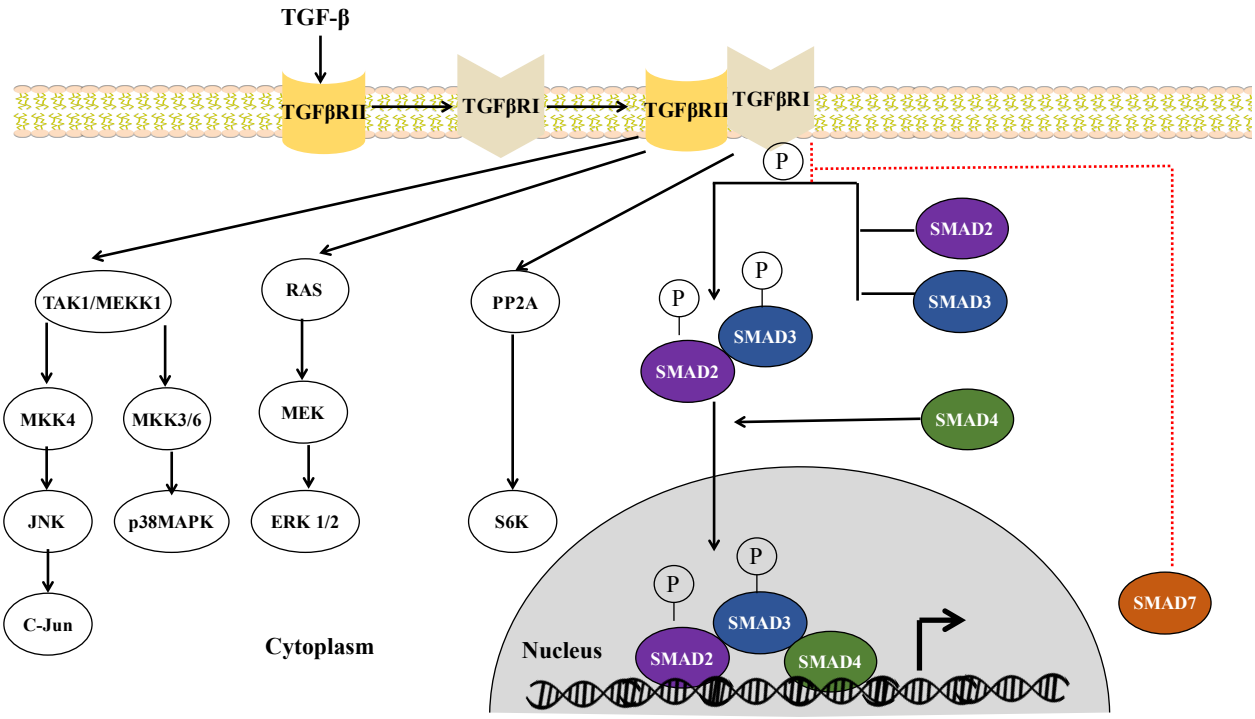

Figure 1: TGF-β signaling pathway.

The TGF-β signaling pathway is implicated in the development of both fibrosis and hypertrophy. Activation of TGF-β by multiple cellular mechanisms, including diabetes-induced oxidative stress, results in binding of TGF-β to its receptor, TGFβRI, which then phosphorylates TGFβRII. Downstream of TGFβRII are multiple targets including TAK1/MEKK1, RAS and PP2A which are involved in the Smad-independent pathway. In addition, TGFβRII phosphorylates both Smad 2 and Smad 3 thereby initiating the Smad-independent pathway. The phosphorylated Smad 2/3 complex associates with Smad 4 and subsequently translocates to the nucleus to modulate the transcription of genes involved in both fibrosis and hypertrophy. Phosphorylation of Smad 2 and 3 is inhibited by Smad7.

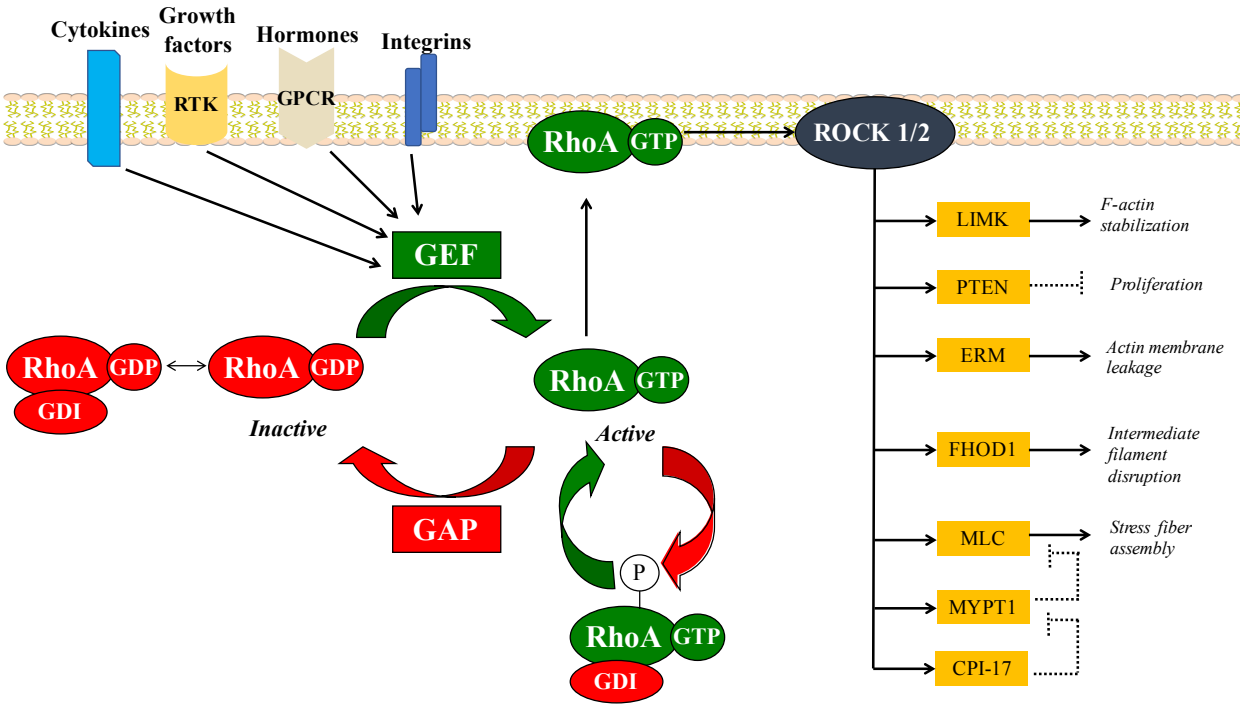

Figure 2: RhoA/ROCK signaling pathway

RhoA is activated when GTP bound and is subsequently translocated to the cell membrane where it activates ROCK1 and ROCK2. Both ROCK1 and ROCK2 have multiple downstream targets including LIMK, PTEN, ERM and MYPT1. In addition to their normal roles in cardiac function, as shown above, PTEN also been implicated in the development of cardiac hypertrophy and LIMK in fibrosis [169].

Chapter 2: The effect of partial ROCK2 deletion on the development of cardiac dysfunction in a model of type 1 diabetes

2.1 Introduction

Diabetes is associated with the development of deleterious chronic comorbidities including cardiovascular disease [183, 184], kidney disease [185, 186], cancers [187] and retinopathy [188]. Of interest, is diabetic cardiomyopathy, which is characterized by diastolic and/or systolic dysfunction independent of coronary artery disease and hypertension [138, 189]. In order to understand the phenomenon of diabetic cardiomyopathy, studies have been carried out *in vivo* [190, 191], *ex vivo* [67] and in isolated cardiomyocytes [192, 193] and these models have shown the disturbances that occur, at the whole heart, cellular and molecular levels. Despite multiple mechanisms being postulated, the exact mechanism contributing to the development and progression of diabetic cardiomyopathy is not completely understood, thereby complicating efforts to develop treatment.

Over-activation of the RhoA/ROCK pathway has been implicated in a number of cardiovascular conditions including ischemia-reperfusion injury [172, 194], hypertension [195, 196], arteriosclerosis [197] and left ventricular hypertrophy [198, 199]. In addition, the RhoA/ROCK pathway has also been associated with the development of diabetic cardiomyopathy. We have previously shown that in cardiomyocytes isolated from STZ-induced diabetic rats, diabetic cardiomyopathy is associated with increased expression of RhoA and ROCK2 (but not ROCK1) [179], and increased phosphorylation of the ROCK targets, MYPT1 and LIM Kinase 2 [176]. Treatment with non-isoform specific ROCK inhibitors inhibits ROCK activity and improves contractile function [176]. The mechanism by which cardiac function is

improved is not completely known but studies from our lab suggest that, under diabetic conditions, activation of the RhoA/ROCK pathway proceeds through a positive feedback loop involving protein kinase C β2 (PKCβ2) and iNOS. Acute inhibition of this loop using non-specific ROCK inhibitors or inhibitors for PKCβ2 and iNOS reduces RhoA/ROCK activity, and also reduces oxidative stress, a contributor to cardiac dysfunction [178].

Given that we and others have previously shown a role for RhoA/ROCK signaling in diabetic cardiomyopathy, and that we have found that the protein expression of ROCK2 and not ROCK1 is increased in diabetic hearts, the aim of this study was to determine if partial deletion of ROCK2 would protect the heart against the development of diabetic cardiomyopathy in a model of chronic T1D. To investigate this, we treated wild-type (WT) mice and mice heterozygous for ROCK2 ($ROCK2^{+/-}$) with citrate buffer (control/non-diabetic) or STZ to induce T1D. The results of this study demonstrated that there were no overt signs of cardiac dysfunction in WT–diabetic compared to WT-citrate mice, as measured by echocardiography, even 13 weeks after induction of diabetes. Diabetic and control WT and $ROCK2^{+/-}$ mice did not show any differences in either diastolic or systolic function despite elevated levels of glucose (>25 mmol/L) in diabetic mice. However, isolation of cardiomyocytes from these animals showed that WT-diabetic animals developed arrhythmias when challenged with high extracellular Ca^{2+}, whereas diabetic $ROCK2^{+/-}$ mice were protected against arrhythmias, thereby indicating a possible role of ROCK2 in arrhythmogenesis in diabetic hearts.

2.2 Methods

2.2.1 Animals

All experiments were conducted in male CD-1 mice housed in a humidity controlled room with a 12 hour light/12 hour dark cycle. Male CD1 ROCK2$^{+/-}$ mice, generated as described by Zhou et al [200], were bred with female WT mice. ROCK2$^{+/-}$ mice were used instead of ROCK2$^{-/-}$ mice, as complete knockouts of ROCK 2 have a low survival rate [200]. Mice born from the same female mouse were housed in the same cage unless they had to be separated to avoid overcrowding (maximum 5 mice/cage). At 3 weeks of age, age-matched mice were weaned and placed on a chow (10% Kcal fat, Lab Diet Inc., St Louis, MO, USA) diet. At 8 weeks of age, mice were randomly assigned to either receive STZ treatment or the vehicle, 0.1M citrate buffer [201]. ROCK2$^{+/+}$ and ROCK2$^{+/-}$ mice received either streptozotocin (STZ, 40 mg Kg^{-1}, intraperitoneal per day for 5 days) [202] or an equal volume of citrate buffer/kg for 5 days. Three weeks following initial injection, mice were tested for persistence of hyperglycemia using a One Touch Glucometer as a sign of development of T1D. Only mice with a blood glucose level over 24 mM were used in subsequent experiments.

2.2.2 Echocardiography

At 13 weeks post STZ treatment, mice underwent echocardiography to measure systolic and diastolic function**.** Echocardiographic image acquisition was carried out using the Vevo 2100 system. Mice were anaesthetized with 4-5% isoflurane in 100% oxygen. Following induction, mice were placed on a heated handling table and anaesthesia and body temperature were maintained at 1-1.5% isoflurane and 37 ± 0.5°C, respectively. Measurements of systolic function included left ventricular ejection fraction, percent fractional shortening, left ventricular mass, stroke volume, cardiac output, and isovolumic contraction time (IVCT). Analysis of the

ratio of early (E)-to-late (atrial, A) ventricular filling velocities (E/A), isovolumic relaxation time (IVRT), duration time of the E and A waves (EAT), and deceleration time of the E wave (EDT) were used to assess diastolic function. The myocardial performance index (MPI) was calculated as a measure of global left ventricular function: MPI = (IVCT + IVRT)/ejection time (ET) [203].

2.2.3 Western blot analysis

Mice were euthanized and their hearts were weighed and rinsed in ice cold PBS and subsequently snap frozen in liquid nitrogen before storage at -80°C. In order to determine protein expression changes, frozen hearts were pulverized using a mortar and pestle and were then homogenized in radioimmunoprecipitation assay buffer (50mM Tris-HCL, pH 7.4, 1% NP-40, 0.5% Na-deoxycholate, 0.1% SDS, 150mM NaCl, 2mM EDTA, 50mM NaF) with 1X protease/phosphatase inhibitors (Cell Signaling Technology, Beverly, MA). Proteins were separated on 8-12% tris-glycine gels and blotted with antibodies against RhoA (sc-418), ROCK2 (sc-5561), Ca^{2+}/calmodulin-dependent protein kinase II (CAMKII, sc-13082), phospholamban (PLB, sc-393990), phospho-PLB^{Thr17} (sc-17024-R) (Santa-Cruz Biotechnology, Dallas, TX), phospho-CAMKII^{Thr286} (#3361, Cell Signaling Technology), ROCK1 (04-1181, EMD Millipore, Etobicoke, ON), ryanodine receptor 2 (RYR2, Sigma-Aldrich, Oakville, ON), pRYR2^{Ser2814} (A0101-31AP, Badrilla Ltd, Leeds, UK). Protein quantity was normalized to GAPDH (sc-47724, Santa-Cruz Biotechnology, Dallas, TX) or ponceau dye. Protein levels were quantified by densitometry using ImageJ software.

2.2.4 Isolation of ventricular cardiomyocytes

Mouse cardiomyocytes were isolated according to the protocol established by Li et al [204]. Briefly, mice were euthanized and their hearts immediately placed in ice cold buffer (113 mM NaCl, 4.7 mM KCl, 0.6 mM KH_2PO_4, 0.6 mM Na_2HPO_4, 1.2 mM $MgSO_4$, 10 mM Na-

HEPES, 12 mM $NaHCO_3$, 10 mM $KHCO_3$, 0.032 mM phenol red, 30 mM taurine, 10 mM 2,3-Butanedione monoxime, and 5.5 mM glucose, pH 7.0). Myocytes were isolated by retrograde perfusion and using collagenase. Calcium tolerant cardiomyocytes were incubated in buffer with low (2.2mM) and high (6mM) Ca^{2+}.

2.2.5 Statistical analysis

All values are shown as mean ± SEM; n denotes the number of animals in each group. Results were analyzed using GraphPad Prism version 6.0 (GraphPad Software, San Diego, CA). Data was analyzed by one-way ANOVA followed by Newman-Keul's test. Differences were considered statistically significant at $p<0.05$.

2.3 Results

2.3.1 Mouse phenotype

Thirteen weeks after either STZ or citrate treatment, both diabetic WT and $ROCK2^{+/-}$ mice weighed less than their corresponding control groups (Fig 3. A). In addition, blood glucose in both the WT-diabetic and $ROCK2^{+/-}$-diabetic mice was higher than that of the vehicle-treated mice (Fig 3. B). However, there were no differences in blood glucose between the two diabetic groups.

2.3.2 Protein expression changes

We assessed expression of ROCK2 and ROCK1 in hearts of the four groups of mice by western blotting. ROCK2 protein expression was elevated in the WT-diabetic group compared to all other groups (Fig. 4A, B). Furthermore, $ROCK2^{+/-}$-citrate animals had an approximately 50% reduction in ROCK2 protein expression compared to their WT counterparts, and there was no

significant increase in ROCK2 expression in ROCK2$^{+/-}$-diabetic mice. Analysis of ROCK1 protein expression (Fig. 4 C) showed no differences amongst the groups.

2.3.3 Assessment of whole heart function

Cardiac function was measured 13 weeks after induction of diabetes (Fig. 5 and 6). Despite the elevated levels of blood glucose, there were no differences in either diastolic or systolic cardiac function (Fig. 5). Calculation of the MPI, a marker of global cardiac function, showed no differences in any of the groups (Fig. 6).

2.3.4 Assessment of cardiomyocyte function

Consistent with our global cardiac function data, cardiomyocytes from both diabetic and nondiabetic WT and ROCK2$^{+/-}$ mice showed no differences in calcium transients and peak Ca^{2+} concentrations when perfused with 2.2 mM Ca^{2+} (Fig. 7). In addition, both non-diabetic WT and ROCK2$^{+/-}$ exhibited similar rates of decay of the Ca^{2+} transient. However, ROCK2$^{+/-}$ diabetic animals showed an improved rate of decay of the Ca^{2+} transient compared to diabetic WT animals (Fig. 7C). However, although no sign of irregular Ca^{2+} transients were detected in either diabetic WT or ROCK2$^{+/-}$ cardiomyocytes in 2.2 mM Ca^{2+}, diabetic WT cardiomyocytes developed arrhythmic Ca^{2+} transients when perfused with 6mM Ca^{2+} (Fig. 8A). On the other hand, diabetic ROCK2$^{+/-}$ mice showed fewer arrhythymic Ca^{2+} transients in comparison to diabetic WT mice (Fig. 8A). Calculation of the number of cells that developed irregular Ca^{2+} transients (Fig. 8B) showed that the number of cells with arrhythmic Ca^{2+} transients was much less in diabetic ROCK2$^{+/-}$ than WT cardiomyocytes.

2.3.5 Determining the contribution of ROCK2 deletion to cardiomyocyte function

Diabetes-induced increased diastolic Ca^{2+} leak, a cause of irregular Ca^{2+} transients, has been suggested to be due to increased phosphorylation of the RYR2 (reviewed in [205]). Hence,

we examined phosphorylation of the RYR2 in hearts from diabetic WT and ROCK2$^{+/-}$ mice (Fig. 9A, B). Phosphorylation of the RYR2 at Ser 2814, the site of CaMKII phosphorylation and activation, was increased in hearts from diabetic WT mice but prevented in hearts from diabetic ROCK2$^{+/-}$ mice. We also determined the phosphorylation of PLB^{Thr17}, a site for CAMKII activation (Fig. 9A, C). No change in PLB^{Thr17}: PLB was detected in WT or ROCK2$^{+/-}$ diabetic mice. Lastly, we measured phosphorylation of CaMKII at Thr287 (Fig. 9A, D). The phosphorylation of CaMKII was significantly increased in hearts from diabetic WT mice, but this increase was prevented in hearts from diabetic ROCK2$^{+/-}$ mice.

2.1 Discussion

Our previous studies in rats indicated that an increase in ROCK activity contributes to diabetic cardiomyopathy, and showed that treatment of animals with a ROCK inhibitor improves cardiac function [179]. In the present study, we investigated the effects of partial deletion of ROCK2 on cardiac contractile function in whole hearts as well as Ca^{2+} transients in cardiomyocytes isolated from diabetic WT and ROCK2$^{+/-}$ hearts. Overall, our data showed that 13 weeks after STZ treatment of WT mice to induce diabetes, there were no overt changes in cardiac function even though ROCK2 expression was elevated in WT-STZ mice hearts. However, analysis of cardiomyocyte function showed that ROCK2 deletion attenuated the development of irregular Ca^{2+} transients induced by increased Ca^{2+} loading in diabetic cardiomyocytes, and in addition, that ROCK2 deletion prevented the increases in phosphorylation of the RYR2 in diabetic mice and this was associated with attenuation of the diabetes-induced increased phosphorylation and activation of CaMKII. These data suggest that ROCK2 contributes to impaired Ca^{2+} homeostasis in diabetic cardiomyocytes, at least in part by

promoting the CaMKII-mediated phosphorylation of the RYR2, increasing its spontaneous release of sarcoplasmic reticulum (SR) Ca^{2+}.

In contrast to our previous observations in diabetic rat hearts, hearts from WT mice with diabetes of 3 months duration did not develop signs of either systolic or diastolic dysfunction *in vivo*. More recent studies in male CD1 mice showed that STZ-induced T1D diabetes induced detectable diastolic dysfunction 12 weeks after STZ treatment, while systolic dysfunction was identified 16 weeks after diabetes induction [151]. Although we were unable to detect significant diastolic dysfunction after 13 weeks of STZ treatment, it is possible that overt cardiac dysfunction would have developed in these mice with time. In contrast, C57Bl/6 mice have been reported to develop cardiac dysfunction as early as 8 weeks after the onset of diabetes [150] suggesting that strain differences may affect the onset of cardiac dysfunction in mice.

To determine the consequences of ROCK2 deletion in diabetic cardiomyocytes, we isolated cardiomyocytes from diabetic WT and $ROCK2^{+/-}$ animals. Several studies have implicated impaired Ca^{2+} homeostasis, an important regulator of cardiac contractility and relaxation, as a contributing factor to the pathogenesis of diabetic cardiomyopathy [11, 206]. For example, Choi et al [206] showed that in a STZ-T1D rat model, animals exhibited both diastolic and systolic dysfunction, which was associated with impaired Ca^{2+} regulation, including depression in the rise and fall of free intracellular Ca^{2+} concentration and impairment in Ca^{2+} reuptake by the SR, as well as a reduction in the rate of Ca^{2+} release by the SR. The SR is the primary store for Ca^{2+} and under normal physiological conditions, for a cardiac contraction to occur, Ca^{2+} has to be released from the SR and consequently bind to troponin C to allow the interaction between actin and myosin and thereby generate force for a contraction. For relaxation

to occur, the cytoplasmic free Ca^{2+} concentration has to be reduced by either its sequestration back into the SR or cellular efflux primarily by the Na-Ca exchanger [11].

Consistent with our contractile data in whole hearts, there were no changes in calcium transients in either diabetic group when measured in the presence of 2.2 mM Ca^{2+}. However, when challenged with high Ca^{2+}, cardiomyocytes from diabetic WT mice showed irregular calcium transients, which were not present in hearts from non-diabetic mice. Fewer cells isolated from $ROCK2^{+/-}$-diabetic mice exhibited irregular calcium transients and, in those that did, the severity was significantly reduced compared to those in WT-diabetic mice. This suggests a role of partial deletion of ROCK2 in reducing the severity and/or occurrence of arrhythmias in a model of type 1 diabetes, as impaired Ca^{2+} handling leading to Ca^{2+} overload has been directly linked to the incidence of arrhythmias in diabetes [207].

Phosphorylation of the RYR2 at Ser2814 by CaMKII increases its sensitivity to Ca^{2+}, resulting in diastolic Ca^{2+} leak [208]. We found that phosphorylation of $RYR2^{Ser2814}$ in cardiomyocytes from diabetic WT mice was significantly increased, and this was attenuated in myocytes from diabetic $ROCK2^{+/-}$ mice. Furthermore, we found that the autophosphorylation and subsequent activation of CaMKII at Thr287 was also increased in diabetic WT but not $ROCK2^{+/-}$ mice. These data imply that under T1D conditions, ROCK2 promotes diastolic Ca^{2+} leak in response to cellular Ca^{2+} overload by promoting the activation of CaMKII. The mechanism by which it does so is currently under investigation.

T1D patients are at an increased risk of sudden death due to arrhythmias following myocardial infarction [209, 210]. Similarly, in T2D patients, diabetes is associated with increased incidence of ventricular fibrillation [211] and diabetes is an independent risk factor for sudden death as shown by epidemiological studies [212]. To our knowledge, the present study is

the first to suggest an anti-arrhythmic effect of ROCK inhibition and may constitute a novel approach to the treatment of diabetes-associated arrhythmias.

Our next project was intended to be an investigation of the role of RhoA/ROCK in an inducible cardiac specific RhoA knockout ($RhoA^{-/-}$) mouse model of diabetes. However, the lack of contractile dysfunction in the WT-diabetic CD1 mouse hearts led us to first compare different models of diabetes and obesity in terms of the development of cardiac dysfunction, in order to choose the most appropriate one. The $RhoA^{-/-}$ mice were on a C57Bl/6 background, therefore we conducted these studies (chapters 3 and 4) in that mouse strain. The projects described in chapters 3 and 4 were run concurrently. However, the results are presented separately because we chose to combine the results related to obesity and type 2 diabetes (chapter 3) as a separate group for publication.

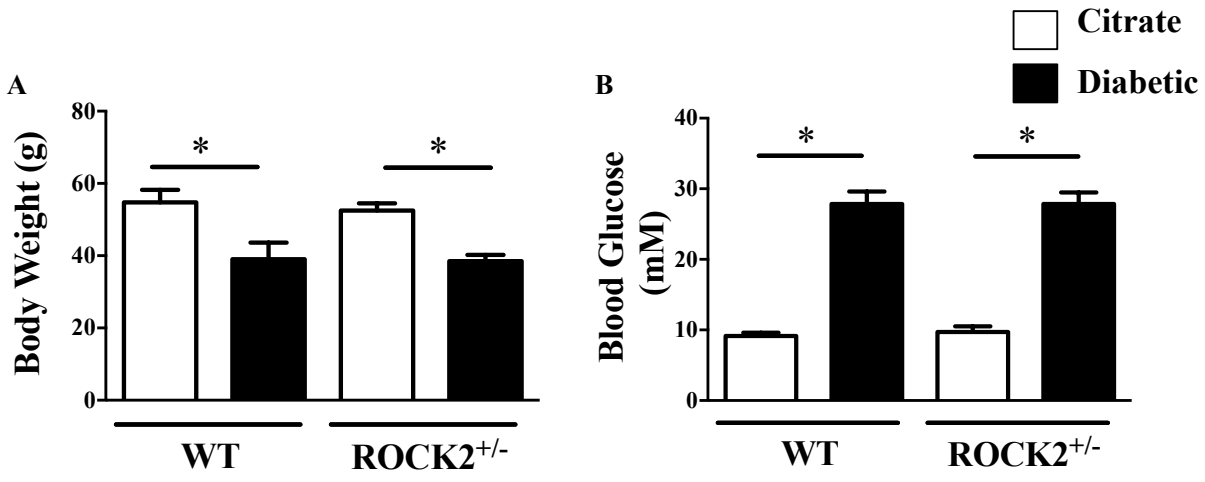

Figure 3: Characteristics of WT and ROCK2$^{+/-}$ mice

WT and ROCK2 mice were treated with STZ (40 mg Kg^{-1}, intraperitoneal per day for 5 days) to induce T1D or were treated with citrate buffer. Whole body weight (A) and blood glucose (B) were measured at termination. *$p<0.05$. Data shown as mean ± S.E.M., n= 5- 7 in each group.

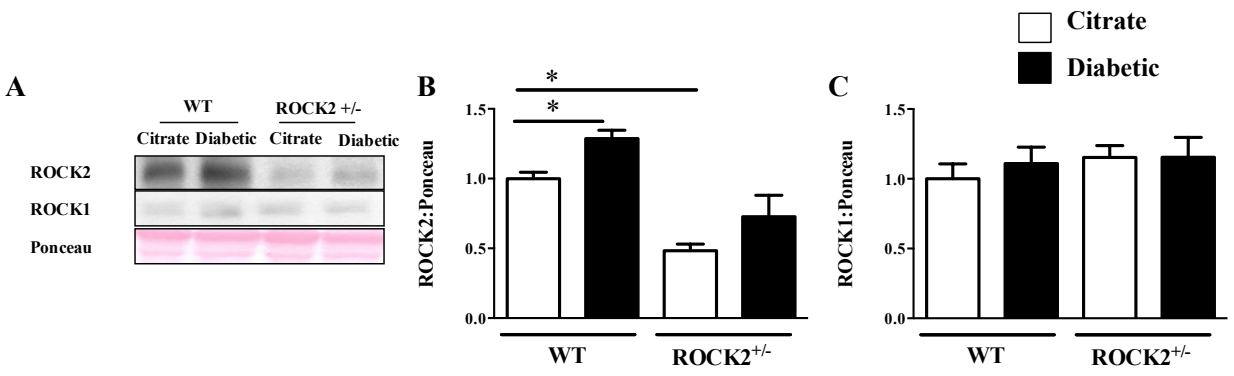

13

Figure 4: Protein expression changes in ROCK2$^{+/-}$ animals

Protein expression levels of ROCK1 and 2 were assessed. Representative blots (A) and calculations of ROCK2 (B) as well as ROCK1 (C) protein expression normalized to ponceau dye are shown. $^{*}p<0.05$. Data shown as mean ± S.E.M., n= 5-7 in each group.

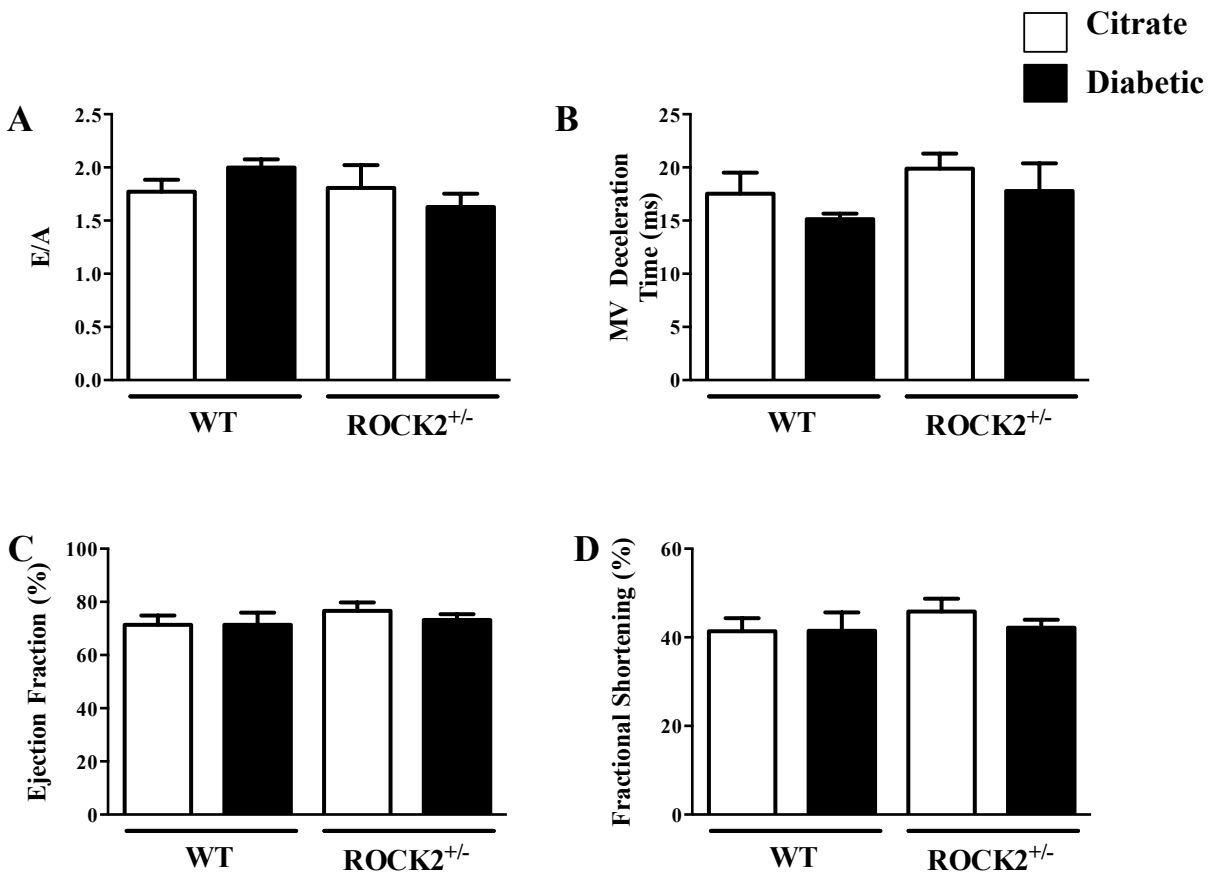

Figure 5: Cardiac function in ROCK2$^{+/-}$ animals

Echocardiography was used to determine E/A (A) and MV deceleration time (B) as markers of diastolic function. Ejection fraction (C) and fractional shortening (D) were measured in order to determine any signs of systolic dysfunction. $^{*}p<0.05$. Data shown as mean ± S.E.M., n= 5-7 in each group.

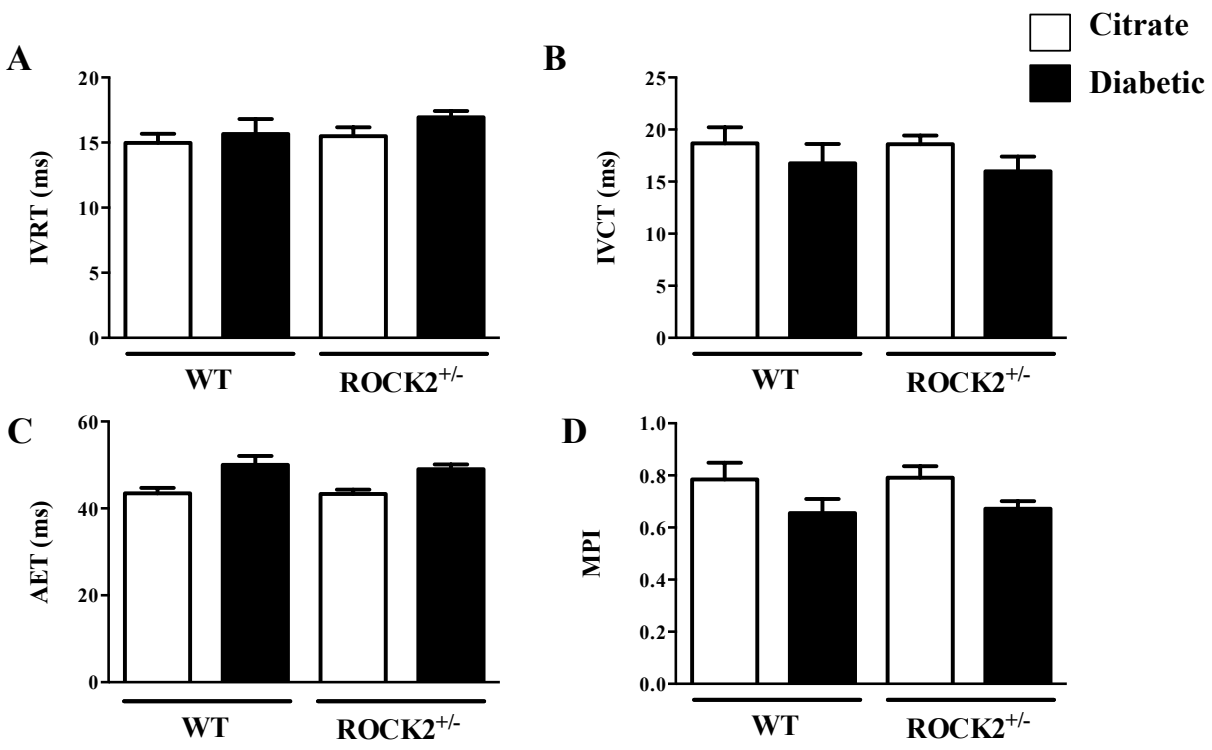

Figure 6: Global cardiac function in ROCK2$^{+/-}$ mice

Measurement of the IVRT (A), IVCT (B) and AET (C) were used to calculate the MPI (D), an indicator of global cardiac function. MPI=(IVRT+IVCT)/AET. $^{*}p<0.05$. Data shown as mean ± S.E.M., n= 5-7 in each group.

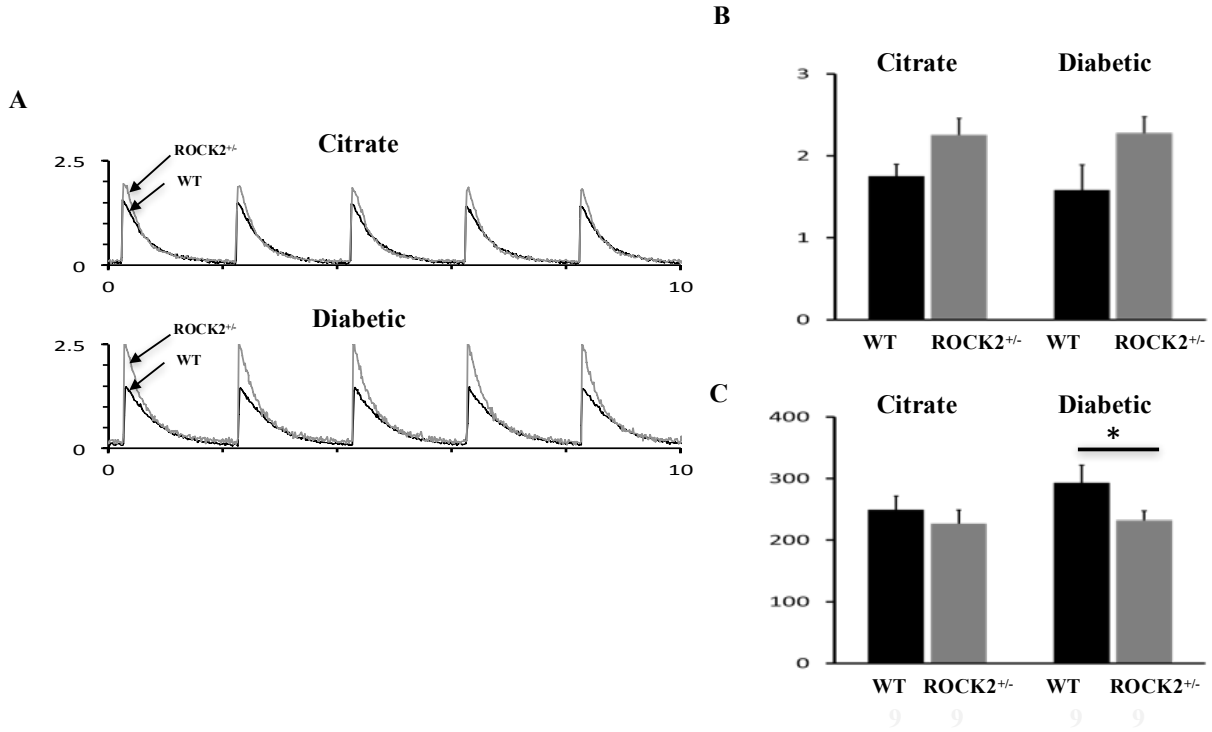

Figure 7: Effect of ROCK inhibition on Ca^{2+} transients in cardiomyocytes isolated from WT and ROCK2$^{+/-}$ mice

Representative Ca^{2+} transients (A), peak intracellular Ca^{2+} concentration (B) and rate of decay of the Ca^{2+} transient (C) in cells isolated from diabetic and control WT and ROCK2$^{+/-}$ mice. *$p<0.05$, n=9 per group.

A

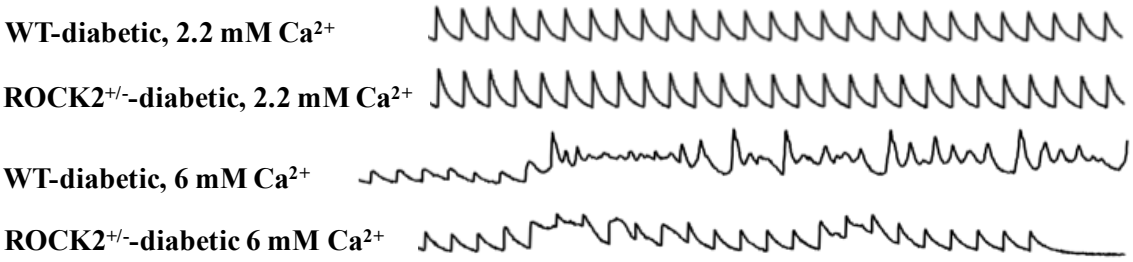

B

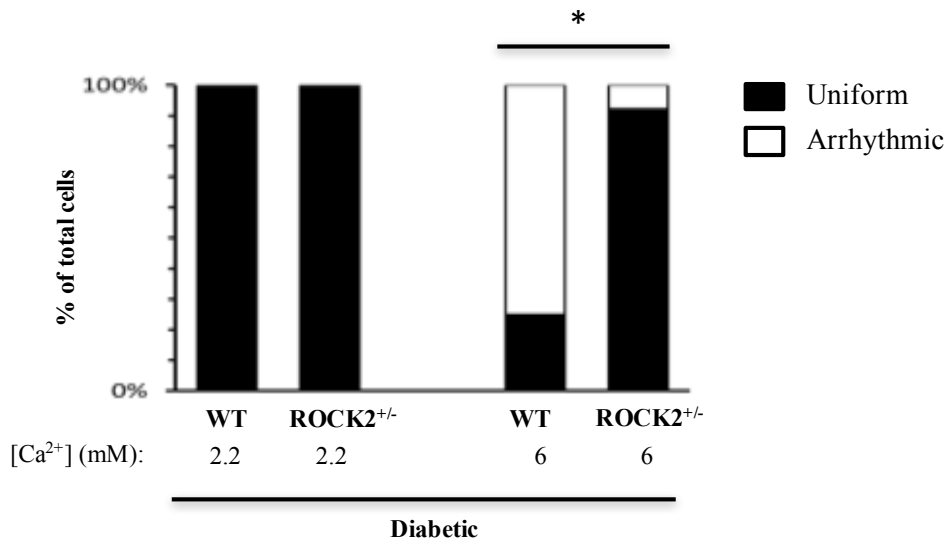

Figure 8: Comparison of Ca^{2+} transients in diabetic WT and ROCK2$^{+/-}$ mice

Cardiomyocytes were isolated from diabetic mice and perfused with 2.2 mM or 6 mM Ca^{2+}. Representative Ca^{2+} transients (A) and calculation of the number of arrhythmic cells (B). *$p<0.05$, n=12-15 per group.

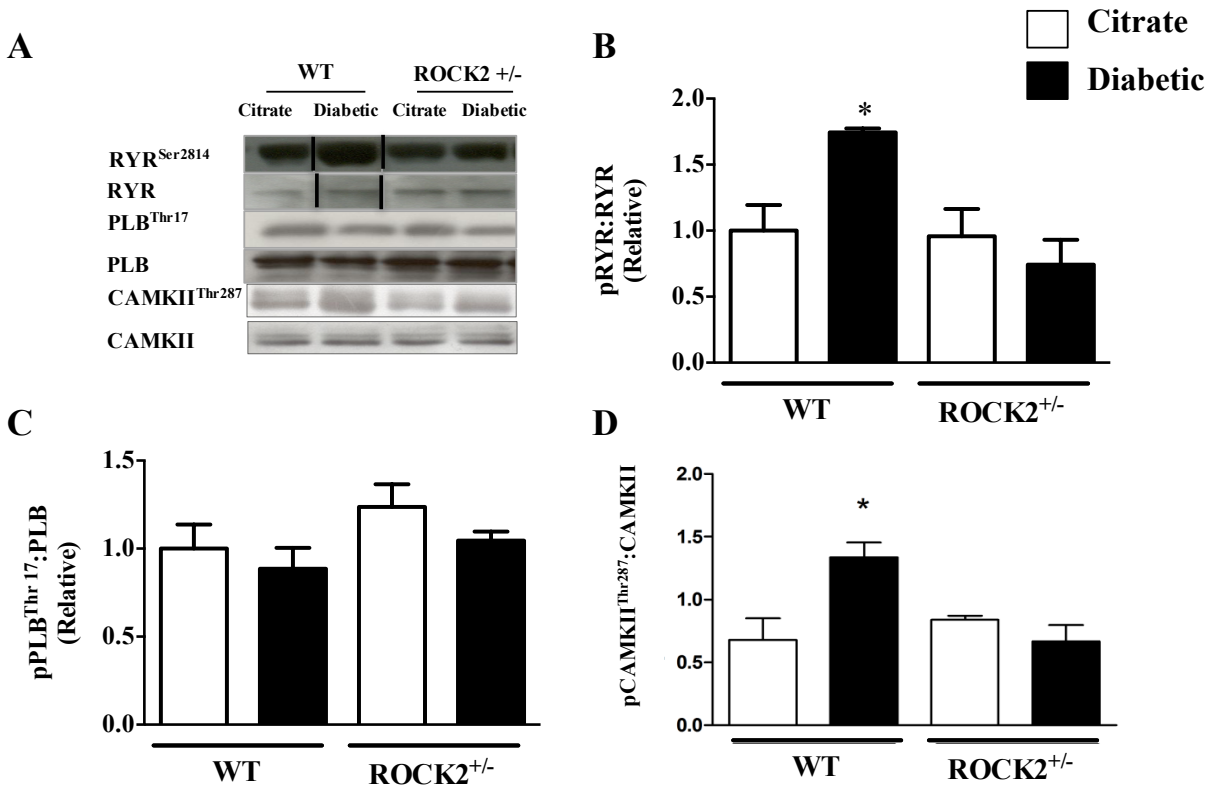

Figure 9: Changes in protein expression and phosphorylation in WT and ROCK2$^{+/-}$ mice

Protein expression levels of pRYR2^{Ser2814}, RYR2, PLB, PLB^{Thr17}, CAMKII and CAMKII^{Thr286} were assessed via western blotting. Representative images are shown (A) as well densitometric analysis of pRYR2^{Ser2814}: RYR2 (B), PLB^{Thr17}: PLB (C) and CAMKII^{Thr286}:CAMKII (D). $^{*}p<0.05$. Data shown as mean ± S.E.M., n= 5-6 in each group.

Chapter 3: Comparison of the development and progression of cardiac dysfunction in mouse models of metabolic stress

3.1 Introduction

Both obesity and diabetes are risk factors for heart failure and acute myocardial infarction [213-215], due at least in part to the development of a cardiomyopathy that is independent of atherosclerosis and hypertension [53, 216]. The progression of diabetic and obesity-induced cardiac dysfunction in humans is normally characterized by the onset of diastolic dysfunction, followed by eventual systolic dysfunction (reviewed in [54]). Multiple mechanisms have been postulated to contribute to the cardiomyopathy, but their contributions are yet to be completely understood.

Small animal models have assisted in further elucidating the mechanisms associated with, and identifying therapeutic targets for, obesity and diabetes-related heart disease and associated comorbidities. Of particular interest is the use of mice, which have similar cardiac developmental sequences as humans [217] and can be manipulated to mimic observations analogous to the pathology and treatment of human heart failure [218, 219]. Recently there has been increasing interest in investigating cardiomyopathy in mouse models of diet-induced obesity and T2D, based on the premise that these will mimic the mechanisms and evolution of diet-induced obesity and diabetes in humans. However, a variety of different regimens have been used and there is lack of consistency between studies in the extent to which heart failure develops, if at all [159, 161, 220]. One major limitation of these studies is that often a single model was studied at only one-time point, and therefore it is not clear whether there are variations in the progression or severity of cardiomyopathy between different regimens.

The purpose of the current study was to concurrently compare the long-term development and progression of cardiac dysfunction in three different models commonly used for the study of obesity and T2D. Specifically, C57Bl6/J mice were fed a high fat diet (HF) in order to mimic human obesity and insulin resistance, or a high fat diet followed by a low dose treatment with streptozotocin (HF-STZ) to induce T2D, or a high fat, high sucrose (HFHS) diet closely resembling a human "Western diet". The results show that despite exhibiting similar metabolic changes, there were variations in the development of cardiac dysfunction amongst the 3 models. HF mice exhibited only a transient decrease in systolic function, whereas HF-STZ mice developed delayed diastolic dysfunction and mice fed a HFHS diet developed sustained decreases in systolic function as well as diastolic dysfunction. These changes in cardiac function were directly correlated with the severity of cardiac fibrosis.

3.2 Methods

3.2.1 Animals

C57Bl/6J mice were obtained from Jackson Laboratories (Bar Harbor, ME, USA) and bred in-house. At 6 weeks of age, male mice were randomly divided into 3 groups. The first group was maintained on a chow (CH) diet (Cat #:5053, 13% kCal from fat (soybean meal and porcine animal fat), LabDiet, St. Louis, MO), the second group was placed on a HF diet (Cat #: D12492, 60% kcal from fat (soybean oil and lard) and 7% kcal from sucrose, Research Diets, New Brunswick, NJ, USA) and the third group on a HFHS diet (Cat #: D12451, Research Diets, New Brunswick, NJ, USA), containing 45% kcal from fat (soybean oil and lard) and 17% kcal from sucrose. Two weeks later, the HF mice were further divided into 2 groups and either injected with 0.1M citrate buffer (pH 3.8) or 40mg/kg STZ in citrate buffer (HF-STZ) for 3

consecutive days. Mice in the CH and HFHS groups were also treated with citrate buffer during this time. Animals were maintained on their respective diets for a further 25 weeks following injection. Cardiac function was measured by echocardiography 12, 18 and 24 weeks post-dietary manipulation. Oral glucose (GTT) and insulin (ITT) tolerance tests were carried out at 25 and 26 weeks, respectively. Mice were euthanized at week 27 and tissues and sera extracted for biochemical analysis and histology. All animal studies were performed in accordance with the Canadian Council for Animal Care's Guide for the Care and Use of Experimental Animals and were approved by the Animal Care Committee of The University of British Columbia.

3.2.2 Echocardiography

To assess cardiac function, transthoracic echocardiography of the left ventricle was carried out in anesthetized mice using a Visualsonics Vevo 2100 ultrasound (Fujifilm Visualsonics, Toronto, ON, Canada) as previously described [180].

3.2.3 Glucose and insulin tolerance tests

Intraperitoneal glucose (GTT) and insulin (ITT) tolerance tests were carried out to assess whole body glucose response and insulin sensitivity, respectively. Briefly, mice were fasted for 6 hours and basal blood glucose was measured via tail vein sampling. For the GTT, glucose (2g/Kg) was injected, and blood glucose was measured 15, 30, 60, 90 and 120 min later using a One Touch Ultra 2 glucometer (LifeScan, Burnaby, BC, Canada). For the ITT, 0.75U/Kg of insulin (Humulin R) was injected and blood glucose was measured 10, 20, 40 and 60 min after injection [180].

3.2.4 Serum profile

Non-fasting serum non-esterified fatty acids were measured by enzymatic analysis using a kit from Zen-Bio (Research Triangle Park, NC). Cholesterol, and triglycerides were also

measured by enzymatic analysis using commercially available kits (Pointe Scientific. Inc., Canton, MI). Insulin levels (EMD Millipore, Etobicoke, ON, Canada) were measured by ELISA using a kit from EMD Millipore (Etobicoke, ON, Canada).

3.2.5 Cardiac triglycerides

Cardiac triglyceride (TG) levels were determined using GPO reagent (Point Scientific. Inc., Canton, MI, USA). Briefly, previously frozen heart sections were homogenized in KOH-EtOH solution. Samples were heated to 70°C for 1 hour and subsequently incubated at room temperature overnight. The next day, 2M Tris-HCL was added to each sample and TG levels were subsequently measured at an absorbance of 500nm [221].

3.2.6 Western blot protein analysis

Hearts were homogenized in radioimmunoprecipitation assay buffer with 1X protease/phosphatase inhibitors (Cell Signaling Technology, Beverly, MA). Proteins were separated by 6-12% SDS-PAGE and immunoblotted using antibodies against ACC, pACC^{Ser79} and GLUT4 (Santa Cruz Biotechnology, Inc., Dallas, TX). Protein band intensity was determined by densitometry and normalized to GAPDH.

3.2.7 Quantitative real-time PCR

Total RNA was extracted from cardiac tissue using TRIzol reagent (Invitrogen, Burlington, ON, Canada) according to the manufacturer's protocol. Reverse transcription was carried out using a SuperScript VILO cDNA synthesis kit (Invitrogen, Carlsbad, CA) in order to generate complementary DNA. Quantitative RT-PCR was performed on an Applied Biosystems StepOnePlus^{TM} PCR system using SYBR Select Master Mix (Applied Biosystems, Foster City, CA). Relative TNF-α and GLUT5 mRNA expression were calculated by the comparative

threshold ($2^{-\Delta\Delta CT}$) method and normalized to the 36b4 endogenous control [180]. The primer sequences used are detailed in Table 1.

3.2.8 Histopathological analysis

Mouse heart apexes were fixed in 10% neutral-buffered formalin and embedded in paraffin. Sections (5μm) were stained with Masson's trichrome stain.

3.2.9 Statistical analysis

All values are shown as mean ± SEM; n denotes the number of animals in each group. Results were analyzed using GraphPad Prism version 6.0 (GraphPad Software, San Diego, CA). The GTT, ITT and repeated cardiac function measurements were analyzed by two-way repeated measures ANOVA followed by a Bonferrroni's post-hoc test. All other data was analyzed by one-way ANOVA followed by Newman-Keul's test. Differences were considered statistically significant at $p<0.05$.

3.3 Results

3.3.1 Mouse phenotype

At termination, all three groups of treated mice weighed more than the CH mice, but there were no significant differences among them (Table 2). The increase in body weight was associated with an increase in epididymal fat pad weight (Fig. 10A) and epididymal fat relative to body weight (Table 2), which was greatest in HF-STZ mice. On the other hand, liver weight was significantly increased in HF and HFHS but not HF-STZ mice (Fig. 10B). There were no differences in heart weight across all groups (Fig. 10C) although hearts from HF and HFHS mice exhibited much higher triglyceride levels than hearts from CH mice. TG levels were not elevated in HF-STZ mouse hearts (Fig. 10D).

Although serum cholesterol levels were increased across all treatment groups by 2-2.5 fold, serum triglycerides were reduced compared to CH mice (Table 2). In addition, circulating free fatty acids were lower in HFHS compared to both HF and HF-STZ mice (Table 2).

An analysis of serum glucose and insulin levels revealed that both HF and HFHS mice were mildly hyperglycemic and were hyperinsulinemic as exhibited by elevated fasting blood glucose and serum insulin levels compared to CH. In contrast, HF-STZ mice exhibited greater hyperglycemia but no elevation in basal serum insulin levels (Table 2).

The effects of the different regimens on glucose and insulin tolerance were examined in GTTs and ITTs, respectively (Fig. 11). In the GTT, blood glucose levels were elevated in all treatment groups compared to CH mice throughout the 120min following glucose injection (Fig. 11A). Calculation of the area under the curve (AUC) of the GTT showed that the treated groups had varying degrees of reduced glucose tolerance, since the AUC of the HF-STZ mice was greater than that of HF mice, which in turn was greater than that of HFHS mice (Fig. 11B). In the ITT, levels of blood glucose were increased in all treated groups compared to CH mice for 60 min after insulin injection (Fig. 11C). Calculation of the AUC showed that the HF, HF-STZ and HFHS groups all had reduced insulin sensitivity compared to CH with no differences amongst them (Fig. 11D).

3.3.2 Development and progression of cardiac dysfunction

Cardiac function in all groups was serially determined by echocardiography 12, 18 and 24 weeks after the change in diet. No significant changes in heart rate or measures of diastolic (E/A, IVRT and MV deceleration time) or systolic (ejection fraction, fractional shortening and IVCT) function were detected in hearts from CH animals over this time (Table 3, Fig. 12). There were no significant changes in heart rate at weeks 12 and 18 (not shown) but by week 24, heart

rates in all high fat-fed groups were reduced significantly compared to CH mice (Table. 3). Furthermore, apart from a small decrease in the IVCT in hearts from HF-STZ mice, no differences were detected in systolic or diastolic function between any of the treatment groups and CH mice at week 12 (Fig. 12). By 18 weeks after beginning the diet, HF mice showed evidence of both diastolic and systolic dysfunction compared to CH mice, with an increase in the E/A (Fig. 12A), and decreases in ejection fraction, fractional shortening and IVCT (Fig. 12D-F). However, these differences were not sustained; by week 24, measures of both diastolic and systolic function for the HF group were restored to the week 12 level and were not different from those of CH mice (Fig. 12).

In contrast, no differences in either diastolic or systolic function were found in the HF-STZ group 18 weeks after beginning high fat feeding (Fig. 12). However, by week 24 these mice exhibited diastolic dysfunction, as indicated by an increase in E/A (Fig. 12A) and a decrease in MV deceleration time (Fig. 12C) compared values recorded at weeks 18 and 12, respectively. Systolic function in these animals remained unchanged at 24 weeks compared to weeks 12 and 18, and compared to CH mice at this time (Fig. 12D-F).

HFHS mice, on the other hand, showed evidence of systolic dysfunction by 18 weeks after beginning the diet, as indicated by significant decreases in both fractional shortening (Fig. 12D) and ejection fraction (Fig. 12E) These differences were still apparent at week 24, and in addition, an increase in the IVCT was detected at this time (Fig. 12F) as were signs of diastolic dysfunction, with increases in both E/A (Fig. 12A) and the MV deceleration time (Fig. 12C) compared to week 12. Additionally, calculation of the MPI ([IVRT + IVCT]/AET), an indicator of global cardiac dysfunction, revealed an increase in the HFHS compared to CH and HF groups at 24 weeks (Table 3).

There were no significant differences between either the HF or HFHS groups and the CH group in LV mass, volume, anterior or posterior wall thickness or internal diameter in diastole or systole at 24 weeks (Table 3). However, LV mass, volume and internal diameter in diastole and systole were significantly lower in HF-STZ compared to both CH and HFHS. This was associated with a significantly lower stroke volume in HF-STZ compared to CH (Table 3).

3.3.3 Development of cardiac fibrosis

Differences in the animal models were further delineated through Masson's trichrome staining of heart tissues at termination (Fig. 13). Vascular accumulation of collagen fibers was higher in all high-fat fed animals compared to the CH group (Fig. 13A and B). The HF (Fig. 13C and D) and HF-STZ mice (Fig. 13E and F) only showed vascular fibrosis (HF lower than HF-STZ), with no apparent interstitial fibrosis. The HFHS group showed the highest levels of both vascular (Fig. 13G) and interstitial (Fig. 13H) fibrosis.

3.3.4 Changes in protein and mRNA expression

To investigate possible reasons for the differences in cardiac function between the different regimens, we examined cardiac protein or mRNA expression of key proteins that have been reported to change in response to high-fat feeding. We first examined levels of total ACC and pACC^{Ser79}, since AMPK-mediated phosphorylation of ACC leads to its inactivation and a reduction in the production of malonyl CoA, contributing to increased fatty acid oxidation. There were no differences in total ACC between the different groups but pACC^{Ser79} was increased by approximately 40% in both HF and HF-STZ compared to CH mice, consistent with an expected increase in fatty acid oxidation (Fig. 14A). However, there were no differences in pACC$^{ser\ 79}$ levels between HFHS and CH mice (Fig. 14A).

In cardiomyocytes, GLUT1 and GLUT4 are the predominant isoforms of glucose transporters, with GLUT4 mainly present in adult hearts and GLUT1 mainly in fetal and neonatal hearts (reviewed in [222]). Protein quantification of whole cell GLUT4 levels showed an increase in hearts from HF-STZ mice compared to both CH and HF groups. There was no statistically significant difference in GLUT4 expression in hearts from HFHS mice compared to any of the other groups (Fig. 14B).

We also measured mRNA expression levels of GLUT5, the main fructose transporter that has been implicated in both obesity and T2D (reviewed in [223]). Interestingly, GLUT5 mRNA expression levels were elevated in hearts from HF-STZ mice compared to all other groups, while there were no differences amongst hearts from CH, HF-STZ and HFHS mice (Fig. 14C).

TNF-α mRNA expression levels were analyzed as an index of changes in inflammatory markers. Levels were low in hearts from HF-STZ and HFHS mice compared to both CH and HF mice hearts. However, there were no significant differences between CH and HF or HF-STZ and HFHS groups (Fig. 14D).

3.4 Discussion

The results of this study demonstrate that, despite similar metabolic derangements, there are clear differences in the development of cardiac dysfunction in mice subjected to different regimens in order to induce obesity or T2D. HF mice developed only a transient decline in cardiac function, while HF-STZ mice exhibited diastolic dysfunction after 24 weeks, but had preserved systolic function, and HFHS mice exhibited the most serious decline in cardiac function, developing sustained systolic dysfunction and eventual diastolic dysfunction.

Furthermore, analysis of cardiac pathological changes revealed that there was a correlation between the extent of cardiac dysfunction and the development of cardiac fibrosis.

Both HF and HFHS mice exhibited mild fasting hyperglycemia, were hyperinsulinemic, and exhibited glucose intolerance and reduced insulin sensitivity in the GTT and ITT, respectively. Thus, these animals can be considered pre-diabetic. HF-STZ mice exhibited more severe hyperglycemia, a greater reduction in glucose tolerance and had low blood insulin levels compared to their HF and HFHS counterparts, indicating a systemic inability to increase insulin secretion as a result of STZ-induced damage to the pancreas. These observations suggest that these mice represent an early T2D model, consistent with previous findings [155].

The changes in serum lipids in response to each of the 3 regimens were similar and were consistent with those previously reported in HF mice when measured in the fed state [224]. The unchanged free fatty acids and decrease in circulating triglycerides seen in treated mice may result from an increase in clearance due to increased mRNA expression of lipoprotein lipase and CD36 in white adipose tissue and/or in liver [225-227]. The increased uptake of triglycerides and fatty acids has been shown to contribute to adipose tissue expansion and to hepatosteatosis, consistent with our observation of increased epididymal fat pad and liver weights in the HF and HFHS mice. Interestingly, in HF-STZ mice epididymal fat pad was increased to a greater extent than in HF and HFHS, but liver weight was not significantly changed compared to CH mice, suggesting differences in the regulation of fatty acid and triglyceride uptake and storage between HF-STZ mice and the other groups.

The development of cardiac dysfunction was delayed for more than 12 weeks in all three treatment groups. In HF mice, the increase in E/A and decreases in both ejection fraction and fractional shortening detected at 18 weeks suggested the onset of both diastolic and systolic

dysfunction. However, this was not sustained, and by 24 weeks after beginning the diet, contractile function had returned to levels similar to week 12. At the same time, there was little evidence of cardiac fibrosis in these animals. These observations may help to explain some of the inconsistencies in the results of previous studies, in which systolic and diastolic dysfunction were detected in C57Bl6/J mice 18-20 weeks [74, 219] but not 28 weeks to 16 months [159, 163] after beginning the same diet. Our data suggest that with continued HF feeding, there are compensatory changes in the heart that lead to restoration of cardiac function.

In contrast to the HF mice, the decline in systolic function seen at 18 weeks of feeding in HFHS mice was maintained and even slightly worsened at 24 weeks, and diastolic dysfunction was also detected at this time. This was associated with the development of extensive cardiac perivascular and interstitial fibrosis. Similarly, others have also reported that feeding C57Bl/6 mice the same diet, for periods ranging from 16-24 weeks, results in the development of both systolic and diastolic dysfunction [162, 163, 228]. These data demonstrate that a diet that is high in a combination of fat and sucrose has substantially greater detrimental effects on cardiac structure and function than a diet high in fat alone. Consistent with this, in a recent study, C57Bl/6 mice fed a diet with a similar proportion of calories from fat, but an even higher percentage from sucrose (30%) were reported to exhibit systolic and diastolic dysfunction as early as 8 weeks after the onset of feeding [161].

Cardiac dysfunction in HF-STZ mice was not seen until 24 weeks after the start of feeding, at which point diastolic dysfunction was detected. This was associated with a moderate degree of fibrosis, but whether cardiac structure and function would continue to decline with time was not examined in this study. Although there is increasing interest in the use of the combination of a high fat diet and low dose STZ to induce T2D in mice, to date there have been

few studies of the effects of this treatment on myocardial structure and function. Our results indicate that despite the presence of greater hyperglycemia, the decline in cardiac function in these mice was delayed compared to the other two models, and less severe than that in the HFHS mice.

The precise mechanisms responsible for the variations in cardiac structural and functional decline amongst the different regimens used in this study are not clear. One of the earliest events reported to occur in the heart in the setting of obesity and T2D is altered energy metabolism, including an increased reliance on fatty acid oxidation for energy production. In addition to reducing cardiac efficiency, the uptake of fatty acids may outstrip the increased capacity of the heart for β-oxidation, leading to the development of cardiac steatosis and lipotoxicity due to the accumulation of triglycerides and lipid intermediates such as ceramides and diacylglycerol. This has been suggested to contribute to cardiac contractile dysfunction by promoting oxidative stress, insulin resistance, cell injury, apoptosis and fibrosis (reviewed in [229]).

Our data demonstrate that cardiac triglycerides were elevated in hearts from both HF and HFHS mice compared to CH and HF-STZ mice. At the same time, the inhibitory phosphorylation of ACC was up-regulated in hearts from HF and HF-STZ mice, but not in hearts from HFHS mice, an indication that the different regimens may have different effects on the pathways that contribute to increased fatty acid oxidation and triglyceride accumulation. ACC promotes the synthesis of malonyl CoA, a regulator of fatty acid oxidation which inhibits fatty acid uptake and oxidation by the mitochondria [230]. Therefore, a decrease in malonyl CoA production due to reduced ACC activity should be accompanied by increased mitochondrial fatty acid uptake and oxidation. That the increased triglyceride accumulation is not accompanied by cardiac contractile dysfunction in HF mice is consistent with the suggestion of others that

triglyceride accumulation itself is not lipotoxic [231]. The lack of change in the inhibitory phosphorylation of ACC in hearts from HFHS mice is in accord with a previous study that showed that fatty acid oxidation is not up-regulated, despite increased expression of CD36 and attenuated glucose oxidation, in these hearts [162]. Although triglyceride levels were not significantly greater in hearts from HFHS than HF mice, it is possible that there is greater accumulation of lipotoxic metabolites in HFHS hearts. Furthermore, the inclusion of sucrose in the diet may also have contributed to the more extensive cardiac dysfunction compared to HF and HF-STZ mice, independent of systemic insulin resistance and triglyceride accumulation. Dietary sucrose is cleaved in the small intestine to its components glucose and fructose, prior to absorption. Increasing evidence suggests that excess fructose uptake into the heart via GLUT5 exerts adverse effects contributing to cardiac dysfunction [232]. The mechanisms involved are likely to be multi-factorial. For instance, fructose-1-phosphate, the product of fructokinase, is a precursor of dihydroxyacetone phosphate, and thus has the potential to further increase the accumulation of triglycerides and lipotoxic compounds in the heart [232]. Furthermore, fructose may promote O-GlcNAcylation of proteins via the hexosamine biosynthetic pathway, and the non-enzymatic glycation of proteins through the formation of fructose-AGE adducts, which are more reactive than glucose-AGE adducts [233]. The latter may contribute to collagen cross-linking, increasing myocardial stiffness and contributing to diastolic dysfunction.

In the present study, the expression of GLUT5 mRNA was unchanged compared to CH in both HFHS and HF hearts, while it was increased in hearts from HF-STZ mice. Thus, the increased supply of dietary sucrose did not modulate the expression of GLUT5 in HFHS hearts. The mechanism underlying the increased expression of GLUT5 in HF-STZ hearts is unclear, as is the significance of this increase in the face of low intake of sucrose. However, since HF-STZ

mice failed to show an increase in cardiac triglyceride accumulation but exhibited an increase in ACC phosphorylation, fatty acid uptake may be in line with fatty acid oxidation in these hearts. Furthermore, HF-STZ mice also exhibited an increase in cardiac GLUT4 protein expression, whereas the expression of GLUT4 was unchanged in hearts from HF and HFHS mice. This suggests that compensatory mechanisms may have developed in hearts from HF-STZ mice, limiting the degree of cardiac dysfunction compared to hearts from HFHS mice.

Ultimately, the disturbances in cardiomyocyte structure and function in response to the 3 regimens appear to be directly correlated to the development of fibrosis in these hearts. Under normal conditions, collagen is significant in maintaining the structural integrity of myofibrils and cardiomyocyte alignment. Previous studies show that collagen synthesis is associated with changes in levels of TNF- α. In acute injury, TNF-α levels are high and induce apoptosis of fibro/adipogenic progenitor cells (FAPs), preventing them from differentiating into matrix producing cells. However, under conditions of chronic organ damage, macrophages release high levels of TGF-β1 and low levels of TNF-α, thereby inhibiting the apoptosis of FAPs and increasing fibrosis [234]. In the present study, TNF-α mRNA expression was reduced and fibrosis was increased in both HFHS and HF-STZ hearts compared to hearts from CH and HF mice after 24 weeks of feeding, suggesting that the same phenomenon might be occurring in cardiac tissue. The differences in levels of fibrosis between HFHS and HF-STZ may be attributable to other factors such as oxidative stress and oxidative post-translational modifications that affect protein expression levels [235].

In conclusion, this study clearly demonstrates the extent to which different regimens used for the induction of obesity and T2D result in different degrees of cardiac pathology. A high fat diet alone, even one containing a very high concentration of fat, does not appear to result in

chronic cardiac dysfunction. On the other hand, a diet that combines a lower but still large amount of fat with sucrose, which most closely resembles the "Western diet" contributing to human obesity, produces very marked adverse effects on cardiac structure and function. Further studies will need to be carried out in order to definitively determine the factors contributing to these differences. To date, the exact causes of cardiac dysfunction associated with both obesity and T2D in humans have not yet been elucidated. The current study suggests that the underlying mechanisms include the adverse effects of the combination of fat and sucrose.

Gene	Primer	Sequence
Glut5	Forward	AGA GCA ACG ATG GAG GAA AA
	Reverse	CCA GAG CAA GGA CCA ATG TC
TNF-α	Forward	AGG TTC TCT TCA AGG GAC AAG
	Reverse	GCA GAG AGG AGG TTG ACT TTC
36b4	Forward	AGA TGC AGC AGA TCC GCA T
	Reverse	GTT CTT GCC CAT CAG CAC C

Table 1: RT-PCR primer sequences used in C57Bl/6 mice

Quantitative real time PCR was carried out on hearts from obese and diabetic C57Bl/6 mice

Measurement	CH	HF	HF-STZ	HFHS
Body weight (g)	33.8 ± 0.7	48.9 ± 1.2*	44.5 ± 1.6*	47.3 ± 1.2*
Epididymal fat/body weight (%)	2.2 ± 0.2	3.3 ± 0.2*	5.4 ± 0.4$^{@}$	3.6 ± 0.2*
Fasting blood glucose (mM)	8.5 ± 0.7	11.3 ± 0.5*	16.1 ± 1.8$^{@}$	10.2 ± 0.3*
Non-fasting blood glucose (mM)	10.9 ± 0.5	9.5 ± 0.9	14.6 ± 0.6$^{@}$	9.1 ± 0.3
Serum insulin (ng/ml)	1.59 ± 0.09	7.60 ± 1.39*	1.65 ± 0.33$^{\#}$	8.13 ± 0.95$^{*\$}$
Serum cholesterol (mg/dL)	107.4 ± 4.3	263.6 ± 9.4*	219.6 ± 16.6$^{*\#}$	236.7 ± 14.9*
Serum free fatty acids (mM)	0.65 ± 0.03	0.81 ± 0.05	0.79 ± 0.10	0.56 ± 0.04$^{\#\$}$
Serum triglycerides (mg/dL)	119.7 ± 8.1	76.6 ± 6.6*	75.0 ± 10.7*	66. 6 ± 4.4*

Table 2: Animal characteristics

Mice were euthanized after high fat feeding for 27 weeks and tissues and sera extracted for biochemical analysis. $^{*}p<0.05$ compared to CH, $^{\#}p<0.05$ compared to HF, $^{\$}$ $p<0.05$ compared to HF-STZ, $^{@}p<0.05$ compared to all groups. Data shown as mean ± S.E.M., n= 7-10 in each group.

Measurement	CH	HF	HF-STZ	HFHS
Heart Rate (bpm)	491 ± 10	456 ± 11*	447 ± 13*	443 ± 8*
AET (ms)	47.6 ± 1.7	50.1 ± 1.5	49.0 ± 1.8	54.3 ± 2.0
MPI	0.62 ± 0.03	0.61 ± 0.02	0.65 ± 0.02	0.72 ± 0.03$^{*\#}$
Stroke Volume (μL)	50.61 ± 1.88	47.69 ± 2.50	39.96 ± 2.89*	47.72 ± 2.30
LV Mass (mg)	122.2 ± 3.9	108.3 ± 5.7	101.0 ± 4.4*	125.8 ± 6.5$^{\$}$
LV Vol; d (μL)	69.9 ± 4.7	64.4 ± 3.6	53.7 ± 5.1*	77.4 ± 2.5$^{\#\$}$
LV Vol; s (μL)	34.4 ± 5.2	27.2 ± 2.8	17.5 ± 3.9*	32.2 ± 3.4$^{\$}$
LVAW; d (mm)	0.99 ± 0.04	0.98 ± 0.05	1.02 ± 0.04	0.98 ± 0.03
LVAW; s (mm)	1.55 ± 0.10	1.65 ± 0.11	1.58 ± 0.09	1.47 ±0.08
LVID; d (mm)	3.98 ± 0.11	3.85 ± 0.09	3.56 ± 0.15*	4.17 ± 0.06$^{\$}$
LVID; s (mm)	2.78 ± 0.23	2.24 ± 0.24	2.01 ± 0.21*	2.87 ± 0.14$^{\$}$
LVPW; d (mm)	0.87 ± 0.03	0.89 ± 0.04	0.93 ±0.06	0.92 ± 0.05
LVAW; s (mm)	1.40 ± 0.10	1.54 ± 0.13	1.41 ± 0.08	1.25 ± 0.07

Table 3: Cardiac function and dimensional measurements at week 24

Cardiac function was assessed by echocardiography. $^{*}p<0.05$ compared to CH, $^{\#}p<0.05$ compared to HF, $^{\$}p<0.05$ compared to HF-STZ, $^{@}p<0.05$ compared to all groups. Data shown as mean ± S.E.M., n= 7-9 in each group.

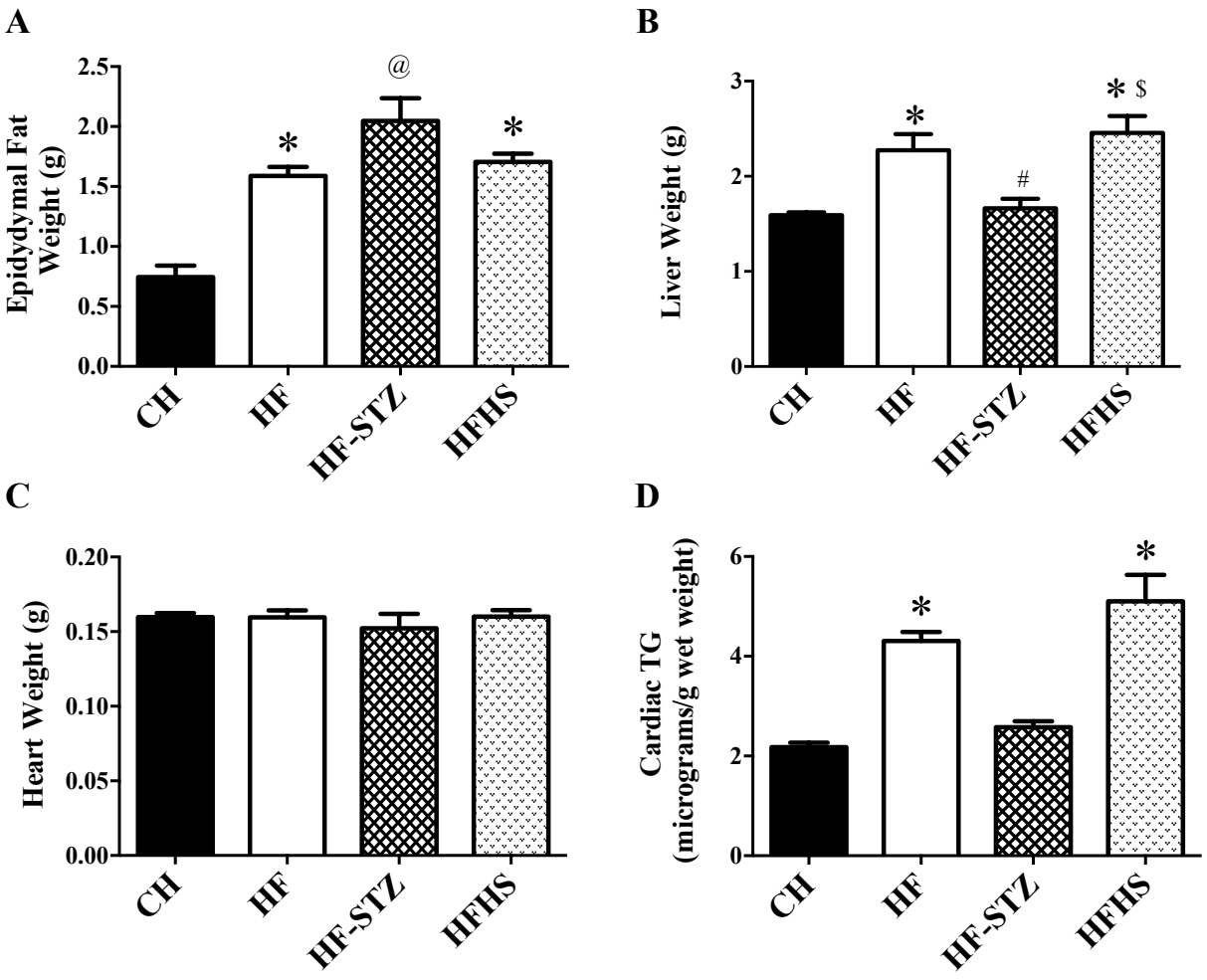

Figure 10: Comparison of organ weights and cardiac TG in different mouse models of metabolic stress

Epidydymal fat (A**),** liver (B) and heart (C) weights, and cardiac TGs (D) in C57Bl/6 mice 27 weeks after treatment with CH, HF, HF-STZ and HFHS. $^{*}p<0.05$ compared to CH, $^{\#}p<0.05$ compared to HF, $^{\$}p<0.05$ compared to HF-STZ, $^{@}p<0.05$ compared to all groups. Data shown as mean ± S.E.M., n= 5-10 in each group.

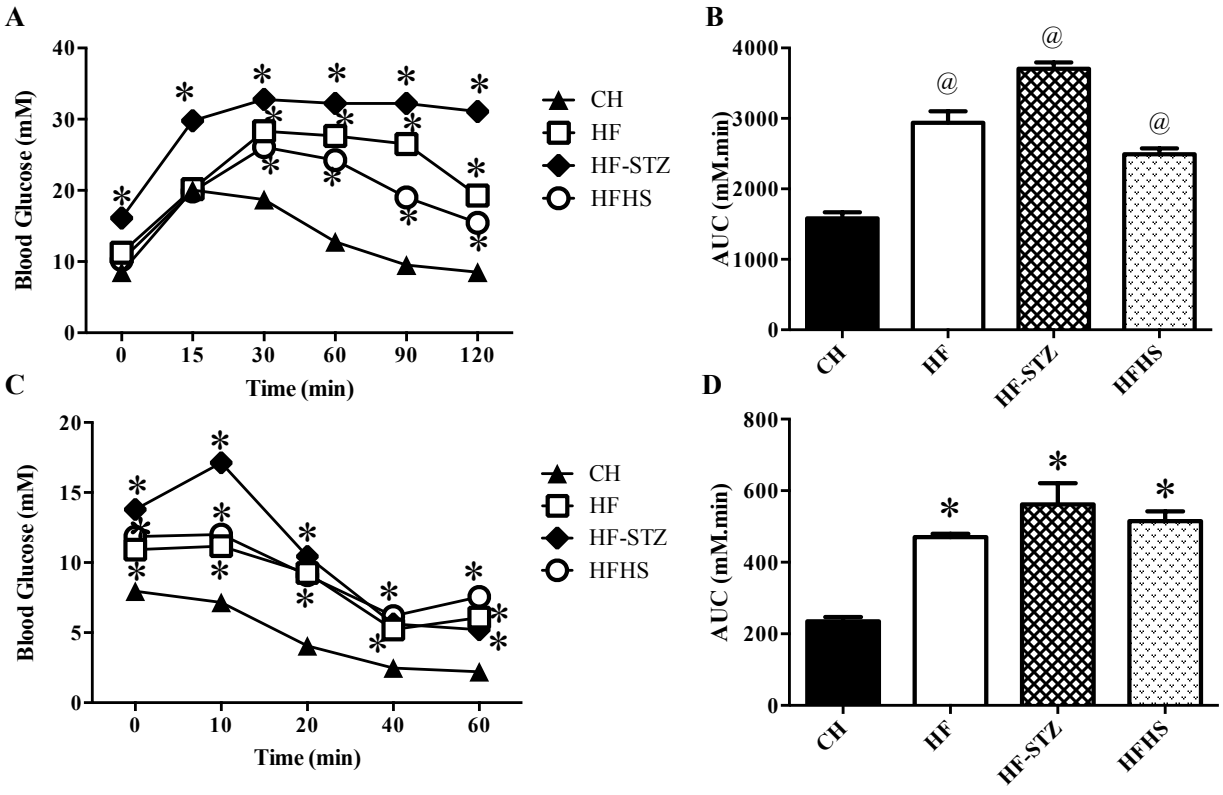

Figure 11: Effect of different models of metabolic stress on glucose and insulin tolerance tests

GTT (A), GTT area under curve (B), ITT (C), ITT area under curve (D) in C57Bl/6 mice following treatment with CH, HF, HF-STZ and HFHS. GTT was performed at week 25 and ITT at week 26. *$p<0.05$ compared to CH, $^{@}p<0.05$ compared to all groups. Data shown as mean ± S.E.M., n= 8-10 in each group.

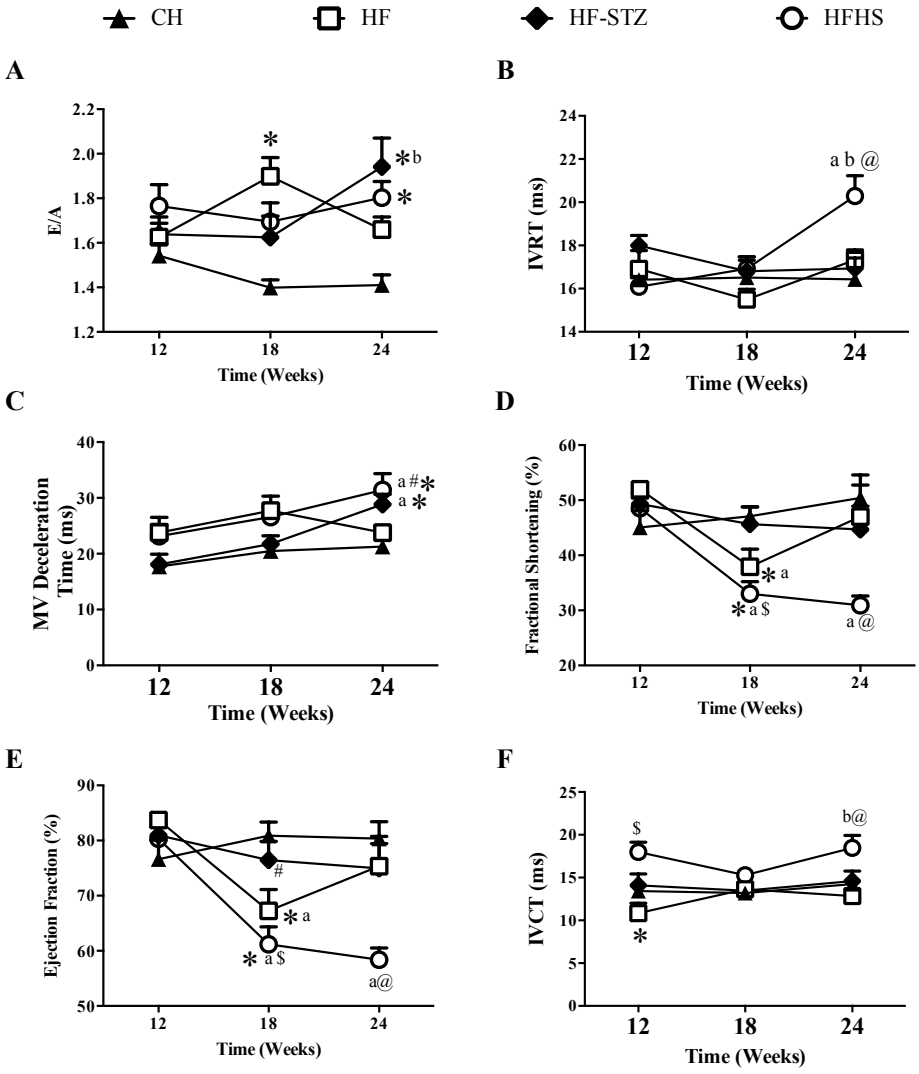

Figure 12: Changes in cardiac function in different mouse models of metabolic stress

E/A (A), IVRT (B) and MV deceleration time (C) were measured at weeks 12, 18 and 24 in order to determine any changes in diastolic function. Fractional shortening (D), ejection fraction (E) and IVCT (F) were assessed to determine changes in systolic function. $^{*}p<0.05$ compared to CH at that time, $^{\#}p<0.05$ compared to HF at that time, $^{@}p<0.05$ compared to all groups at that time, $^{a}p<0.05$ compared to week 12 within the group, $^{b}p<0.05$ compared to week 18 within the group. Data shown as mean ± S.E.M., n= 7-10 in each group**.**

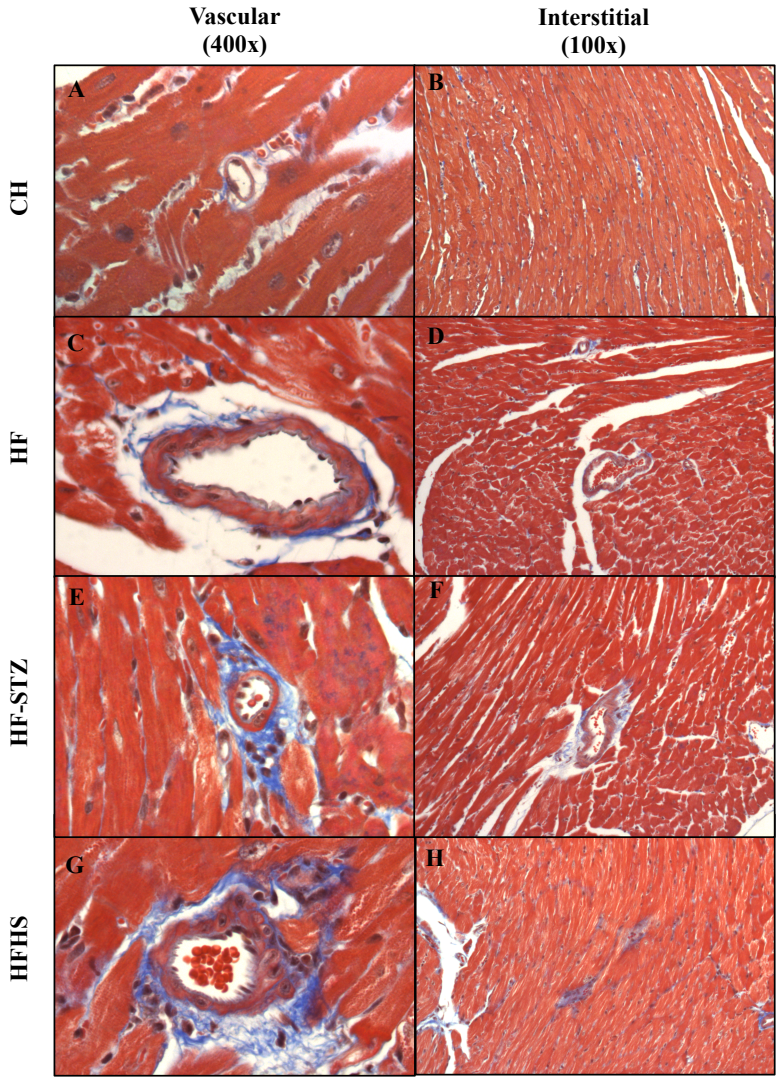

Figure 13: Effect of different high fat feeding models on the development of cardiac fibrosis

Heart tissue from CH (A and B), HF (C and D), HF-STZ (E and F) and HFHS (G and H) was stained with Masson's trichrome stain and visualized at both 100x and 400x magnifications.

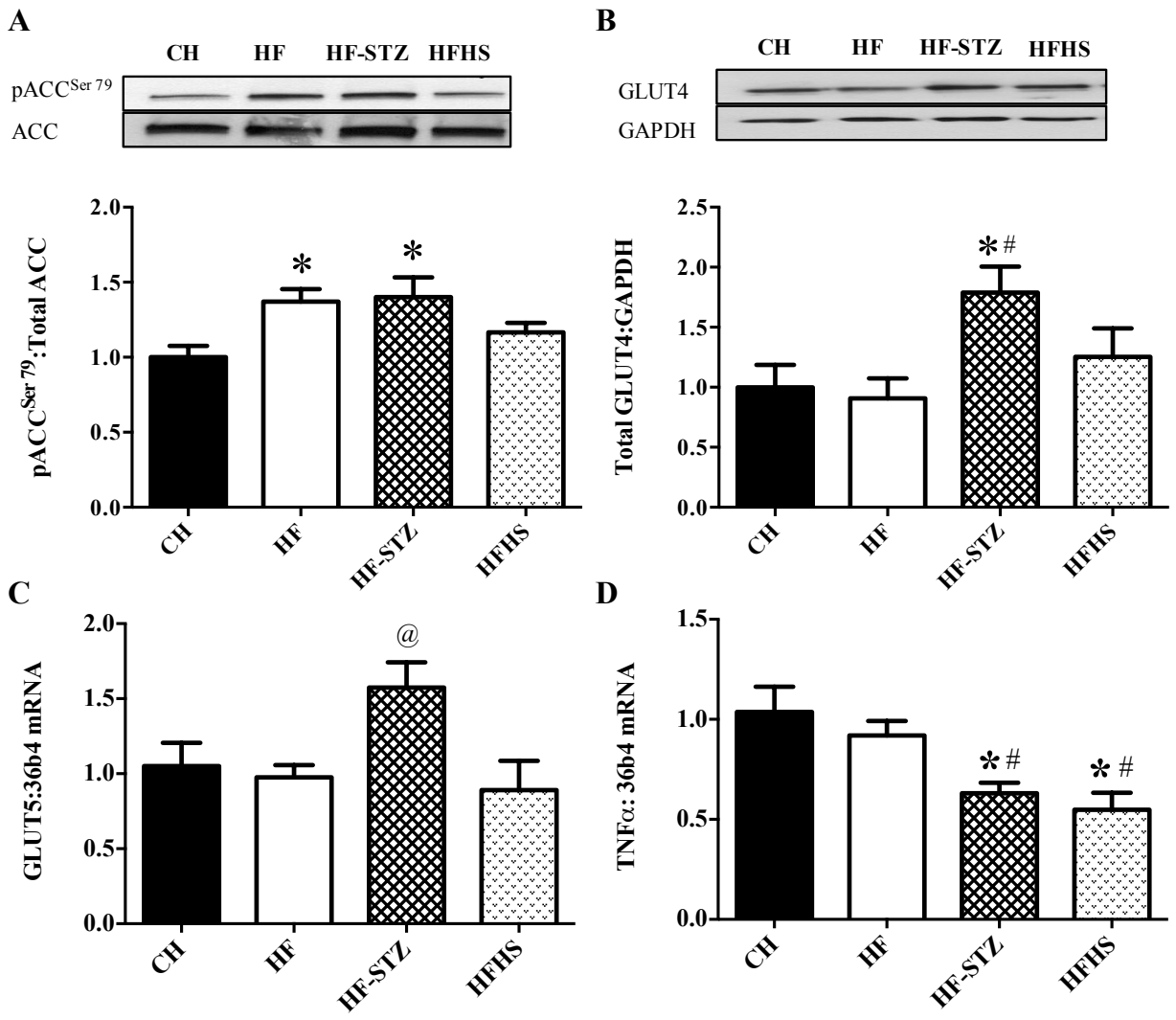

Figure 14: Changes in cardiac protein and mRNA expression in different mouse models of metabolic stress

Protein expression levels of ACC phosphorylated at Ser79 normalized to total ACC (A) and total GLUT4 normalized to GAPDH (B) were measured in heart samples. Cardiac mRNA expression levels of GLUT5 (C) and TNFα (D) normalized to the endogenous control 36b4 were also determined. $^{*}p<0.05$ compared to CH, $^{\#}p<0.05$ compared to HF, $^{@}p<0.05$ compared to all groups. Data shown as mean ± S.E.M., n= 7-8 in each group.

Chapter 4: Development and progression of cardiac dysfunction in a mouse model of type 1 diabetes

4.1 Introduction

STZ treated mice have been used for decades to understand the mechanisms associated with the development of T1D [236, 237]. The use of STZ is particularly attractive as the model is relatively inexpensive, simple and results in onset of symptoms of diabetes in as little as 7-10 days [152, 238]. STZ is a pancreatic β cell toxin that, in a dose-dependent manner, induces hyperglycemia and hypoinsulinemia, the hallmarks of T1D [139].

Cardiovascular complications, including diabetic cardiomyopathy, which is characterized by diastolic and/or systolic dysfunction, have been identified in several studies using the STZ mouse model. Yu et al [149] showed that a single moderate dose of STZ in C57Bl/6 mice (100mg/Kg) results in both diastolic and systolic dysfunction that can be detected after 4 weeks using magnetic resonance imaging and echocardiography. In contrast, in a separate study, treatment of FVB/N mice with multiple low dose injections of STZ (55 mg/Kg, 5 days) resulted in induction of early left ventricular dysfunction, as exhibited by a reduction in E/A with preserved IVRT and MV deceleration time, 8 weeks after the last injection [239]. In addition, in C57Bl/6 mice injected with a single high dose of STZ (150mg/kg), both diastolic and systolic dysfunction were observed 12 weeks after treatment and this was accompanied by oxidative stress and cardiac fibrosis [150]. This suggests that the time point at which cardiac function is assessed after STZ treatment, the STZ dosage and the mouse strain are important variables in the induction of cardiac dysfunction associated with STZ treatment.

In this study, which as noted above was run concurrently with the project outlined in chapter 3, C57Bl/6J mice were treated with STZ to induce type 1 diabetes to confirm whether and when they developed overt cardiomyopathy so that the model could be applied to transgenic mice with altered cardiac expression of RhoA. We used multiple low dose STZ injections as previous studies have indicated that at high doses, STZ induces both renal and hepatic toxicity [240-242]. Both diastolic and systolic dysfunction were observed 12 weeks after treatment.

4.2 Methods

At 6 weeks of age, male C57Bl/6J mice (Jackson Laboratories, Bar Harbor, ME, USA) mice were randomly divided into 2 groups and either injected with 0.1M citrate buffer (pH 3.8) or 50mg/kg STZ in citrate buffer (diabetic) for 5 consecutive days. Three weeks following the initial injection, mice were tested for the presence of hyperglycemia using a One Touch glucometer as a sign of development of T1D. Animals with blood glucose over 20mM were considered diabetic and used in the study. At 12 weeks post STZ treatment, cardiac systolic and diastolic function were measured by echocardiography as detailed in chapter 2**.**

4.3 Results

4.3.1 Animal characteristics

Twelve weeks following STZ treatment, diabetic animals exhibited lower whole body (Fig. 15A) and heart weight (Fig. 15B) compared to their citrate-injected counterparts. However, when the heart weights were normalized to body weight (Fig. 15C), there were no differences between the groups. Measurement of blood glucose levels showed that diabetic mice had much higher blood glucose compared to citrate animals (Fig. 15D).

4.3.2 Cardiac function

Measurement of cardiac function at 12 weeks after treatment revealed both diastolic and systolic dysfunction in the STZ-treated mice (Fig. 16). E/A (Fig. 16A) was increased and IVRT (Fig. 16B) was decreased in the STZ-treated group, showing evidence of diastolic dysfunction in this group. In addition, diabetic mice showed reduced ejection fraction (Fig. 16C) and fractional shortening (Fig. 16D), and elongated IVCT (Fig. 16E). The MPI (Fig. 16F) was also higher in diabetic animals.

4.4 Discussion

Various STZ-induced type 1 diabetic mouse models have been implemented to assess the mechanisms involved in the development and progression of type 1 diabetes. Our observations of hyperglycemia and reductions in both heart and body weights in 12 week diabetic mice are consistent with findings by Chaudhry et al [148] who treated C57Bl/6 mice with low dose STZ over 5 consecutive days in order to induce diabetes. The systolic and diastolic dysfunction that we detected at this time is consistent with the results of Liu et al [150], who showed a reduction in ejection fraction and fractional shortening, as well as elongated IVRT as measured by echocardiography 12 weeks after treatment of mice with a single high dose of STZ compared to citrate injected mice. Our data demonstrate that the use of multiple low dose STZ induces diabetic cardiomyopathy without increasing the risk of either hepatic or renal toxicity.

These data show that in contrast to CD-1 mice (Chapter 2), treatment of C57Bl/6 mice with STZ resulted in detectable cardiac dysfunction by 12 weeks after induction of diabetes. The reason for this difference between strains is unclear. Although a slightly higher dose of STZ was used in the present study compared to the previous one, blood glucose was similarly elevated in

the two strains of animals. One possibility is that compensatory mechanisms delay or prevent the development of cardiomyopathy in hearts of diabetic CD-1 mice, but are not present in those of C57Bl/6 mice. In addition, the results suggested that induction of diabetes with STZ is a reliable and cost-effective approach for studying the role of cardiomyocyte RhoA in the development of diabetic cardiomyopathy in C57Bl/6 mice, and thus this model was used in our final study.

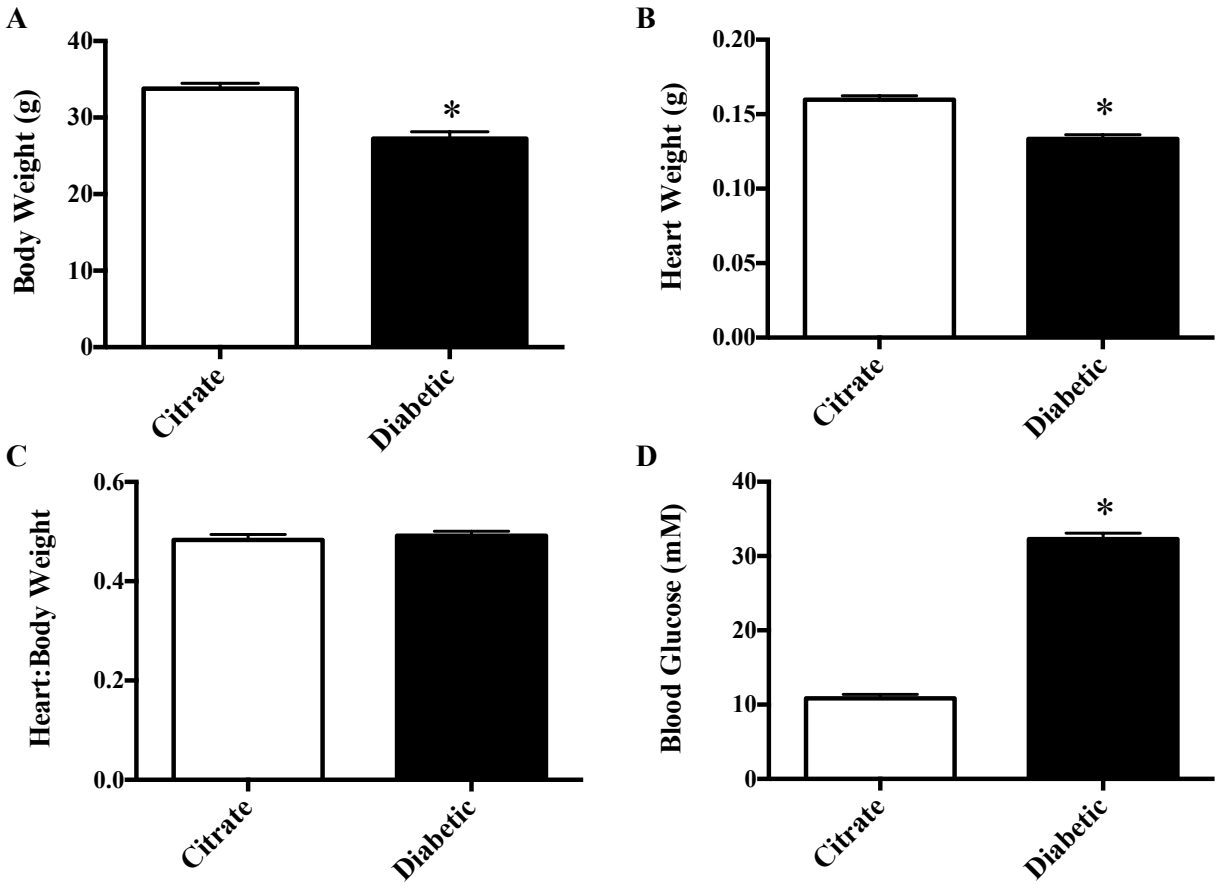

Figure 15: Animal characteristics of T1D C57Bl/6 mice

Twelve weeks after STZ treatment body weight (A), heart weight (B), heart weight relative to body weight (C) and blood glucose (D) were determined. $^{*}p<0.05$. Data shown as mean ± S.E.M., n= 7-10 in each group.

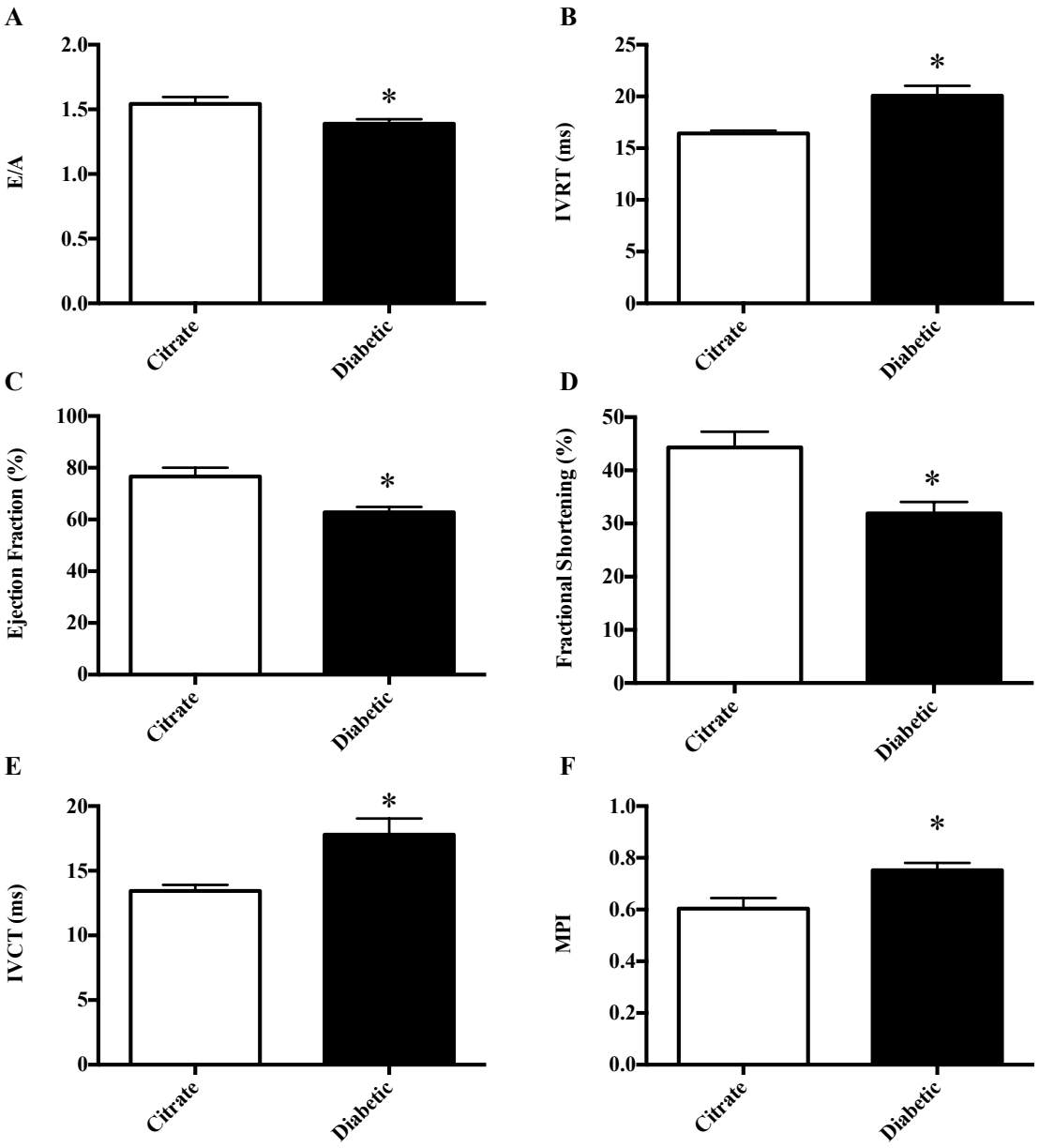

Figure 16: Changes in cardiac function in TID C57Bl/6 mice

E/A (A) and IVRT (B) were measured in order to determine any changes in diastolic function. Ejection fraction (C), Fractional shortening (D), and IVCT (E) were assessed to determine changes in systolic function. MPI (F) was calculated as a measure of global cardiac dysfunction. $^{*}p<0.05$. Data shown as mean ± S.E.M., n= 5-10 in each group**.**

Chapter 5: Deletion of RhoA in cardiomyocytes protects the heart from contractile dysfunction and associated fibrosis in a mouse model of type 1 diabetes

5.1 Introduction

The small GTPase protein RhoA is involved in a number of cellular activities including migration [243], cell cycle progression [244], adhesion [245] and modulation of gene expression [246]. Through activation of its downstream effectors, in particular Rho kinase (ROCK), RhoA has also been implicated in many forms of cardiovascular disease including hypertension [247], ischemia reperfusion (I/R) injury [172] and atherosclerosis [248]. However, due in part to its numerous effectors and its expression in many cell types, the role of RhoA in the heart has not been clearly defined. For example, recent studies by Lauriol et al [169] have shown that cardiomyocyte deletion of RhoA protects the heart from fibrosis but promotes the development of heart failure associated with pressure overload produced by transverse aortic constriction (TAC). RhoA appears to contribute to compensatory hypertrophy in TAC by increasing the activity of ERK1/2 and Akt. In addition, through its ability to activate LIM kinase, thereby decreasing cardiac contractility, as well as to activate pro-fibrotic transcriptional regulators such as myocardin response transcription factor (MRTF) and serum response factor (SRF), RhoA contributed to both fibrosis and impaired cardiac function [169]. In contrast, Xiang et al [170] show that cardiomyocyte overexpression of RhoA is not associated with deleterious effects. In fact, the over-expression of RhoA resulted in cardioprotection from I/R injury, with no changes in either ERK or Akt, or the pro-apoptotic proteins Bax and Bak, but an increase in activation of protein kinase D. Mice with cardiac specific knockout of RhoA showed a decreased tolerance to I/R injury as shown by an increase in cardiac infarct size compared to wild type control animals

[170]. These studies suggest that the role of RhoA may vary depending on the cell type and on the disease state, and that its activation may either be protective or deleterious through multiple downstream pathways that are not completely understood.

Previous studies from this lab and others have demonstrated that increased activation of the RhoA-ROCK pathway contributes to diabetic cardiomyopathy and that inhibition of ROCK improves cardiac function, reduces ROS production, and over the longer time, reduces fibrosis [176, 181]. Because the adverse effects of activation of the pathway could arise from its actions in a number of cell types in the heart or elsewhere, the aim of the current study was to determine the specific contribution of RhoA in cardiomyocytes to the development of diabetic cardiomyopathy, using mice with cardiomyocyte knockdown of RhoA. Our results show that in a model of type 1 diabetes, deletion of cardiomyocyte RhoA prevented cardiac dysfunction by inhibiting the development of fibrosis, hypertrophy and apoptosis through mechanisms involving the regulation of the TGF-β signaling pathway.

5.2 Methods

5.2.1 Generation of RhoA floxed mice

To investigate the role of RhoA in the pathophysiology of diabetic cardiomyopathy, an inducible cardiac specific RhoA knockout mouse was used. The cardiac specific floxed RhoA and MerCreMer mice used in this study were generated in the laboratory of Dr. Jeffery Molkentin of the University of Cincinatti. Mice homozygous for floxed RhoA (RhoA flanked by two LoxP sites) were mated with knock-in mice expressing tamoxifen-inducible alpha myosin heavy chain (α-MHC) Cre recombinase (MerCreMer) to produce mice expressing both α-MHC Cre recombinase and floxed RhoA. Inducible Cre recombinase has (i) two mutated ligand-

binding domains (LBD) of the mouse estrogen receptor, Mer, and (ii) Cre recombinase. The mutated LBD binds to tamoxifen but not to estrogen or progesterone [249]. The α-MHC promoter controls cardiac tissue cre-recombinase expression specifically [250]. In the absence of tamoxifen, Cre recombinase is not expressed but RhoA is expressed. Upon binding of tamoxifen to Mer, Cre recombinase is transcribed and excises the gene flanked by the Loxp sites, in this case RhoA, thereby inhibiting RhoA gene transcription.

In order to generate the mice used in experiments, male C57Bl/6-SV129 RhoA-floxed mice ($RhoA^{fl/fl}$) were mated with female C57Bl/6 mice expressing α-MHC Cre recombinase (cre-$RhoA^{-/-}$). The resulting offspring were heterozygous for the floxed gene ($RhoA^{fl/-}$) with or without the cardiac-specific MerCreMer. In order to generate cre-$RhoA^{fl/fl}$ mice, the heterozygous RhoA-Loxp-MerCreMer mice ($RhoA^{fl/-}$) were mated with $RhoA^{fl/fl}$ mice. The resulting $RhoA^{fl/fl}$ and cre-$RhoA^{fl/fl}$ mice were then bred for 4-5 generations to generate litters with greater genetic uniformity and were then used in subsequent experiments.

5.2.2 Tamoxifen treatment and induction of diabetes

At 10 weeks of age, both $RhoA^{fl/fl}$ and their cre-$RhoA^{fl/fl}$ littermates were injected with 30mg/kg Tamoxifen for 5 consecutive days to generate mice expressing cardiomyocyte RhoA (referred to as $RhoA^{+/+}$) and mice with cardiomyocyte RhoA deletion (referred to as $RhoA^{-/-}$), respectively. Three weeks later, mice from each group were further randomly divided into 2 groups and either injected with citrate buffer (pH 3.8) or 50mg/kg STZ in citrate buffer per day for 5 consecutive days. Three weeks following initial STZ injection, mice were tested for the persistence of hyperglycemia as a sign of the development of T1D. Mice with blood glucose levels over 18mM were considered diabetic and used in the experiments. At 12 weeks post-STZ treatment, mice underwent echocardiography to measure systolic and diastolic function. One

week later, mice were weighed and euthanized and their hearts extracted and either quick frozen in liquid nitrogen or used for isolated cardiomyocyte studies. Details of the experimental procedure are outlined in Fig. 17.

5.2.3 Echocardiography

To assess cardiac function, transthoracic echocardiography of the left ventricle was carried out using a Visualsonics Vevo 2100 ultrasound (Fujifilm Visualsonics, Toronto, ON, Canada) as previously described (Chapter 2). Briefly, mice were anaesthetized with 4-5% isoflurane in 100% oxygen. Following induction, mice were placed on a heated handling table and anaesthesia and body temperature were maintained at 1-1.5% isoflurane and 37 ± 0.5°C, respectively. Using pulse-wave Doppler of the apical four-chamber view, the E/A, MV deceleration time, AET, IVCT, IVRT, and MPI were determined. M-mode scans of the two-dimensional parasternal short-axis were acquired in order to determine fractional shortening, ejection fraction and cross-sectional dimensions.

5.2.4 Whole heart studies

5.2.4.1 Western blot

Following euthanasia, whole hearts were weighed and rinsed in ice cold PBS and subsequently snap frozen in liquid nitrogen before storage at -80°C. In order to determine protein expression changes, frozen hearts were pulverized using a mortar and pestle and were then homogenized in radioimmunoprecipitation assay buffer (details outlined in Chapter 2). Proteins were separated on 6-12% Tris-glycine gels and blotted with antibodies against RhoA (sc-418), ROCK2 (sc-5561) Smad7 (sc-365846), Col1A1 (sc-8784-R) (Santa-Cruz Biotechnology, Dallas, TX), ROCK1 (04-1181, EMD Millipore, Etobicoke, ON), cleaved caspase 3 (#9662S), Bax (#2772), Smad 2/3 (#3102S) and phospho-Smad2 (Ser465/467)/Smad3 (Ser423/425) (#8828S)

(Cell Signaling Technology, Beverly, MA). Protein quantity was normalized to GAPDH (sc-47724, Santa-Cruz Biotechnology, Dallas, TX) or ponceau stain.

5.2.4.2 ROCK activity assay

To determine ROCK activity, a portion of the pulverized sample was homogenized in lysis buffer (50mM Tris-HCl, pH 7.5, 150mM NaCl, 1mM EDTA, 1MM EGTA, 1mM Na_3VO_4, 1mM 2-glycerol-phosphate, 1% NP-40 and 1X protease/phosphatase inhibitors). 90μg of protein was then incubated in the ROCK assay buffer (250mM Tris-HCl, pH 7.5, 100mM $MgCl_2$, 50mM glycerol-2-phosphate, 1mM Na_3VO_4, 10mM DTT) with 5mM ATP and 0.5 μg of purified MYPT substrate at 30°C for 30min. The phosphophorylation of $MYPT^{Thr853}$, an indicator of ROCK activity, was analyzed by Western blotting using the $MYPT^{Thr853}$ antibody (#4563, Cell Signaling Technology, Beverly, MA). Protein quantity was normalized to total MYPT (sc-25618, Santa-Cruz Biotechnology, Dallas, TX).

5.2.4.3 Histology

Mouse heart apexes were fixed in 10% neutral-buffered formalin immediately after harvest. After 24 h of fixation, samples were paraffin embedded and 5μm-thick sections were stained with Masson's trichrome stain for the visualization of collagenous connective tissue. Tissue sections were imaged using a Nikon Eclipse TI microscope.

5.2.4.4 Quantitative real time PCR

Total RNA was extracted from cardiac tissue and quantitative-PCR was performed as detailed in Chapter 3. Relative TGF-β, COL1A1, Col3A1 and Smad7 mRNA expression were calculated by the comparative threshold ($2^{-\Delta\Delta CT}$) method and normalized to the 36b4 endogenous control. Details of the primer sequences used are shown in Table 4.

5.2.5 Isolated cardiomyocytes

Following echocardiography, mice were euthanized and cardiomyocytes isolated from freshly excised hearts through heart retrograde perfusion as previously described [204]. Cardiomyocyte cell size was also determined via live-cell confocal imaging using a Zeiss LSM 700 microscope (Carl Zeiss Canada Ltd., Toronto, ON).

5.2.6 Statistical analysis

All values are shown as mean ± SEM; n denotes the number of animals in each group. Results were analyzed using GraphPad Prism version 6.0 (GraphPad Software, San Diego, CA). Data were analyzed by one-way ANOVA followed by Newman-Keul's test. Differences were considered statistically significant at $p<0.05$.

5.3 Results

5.3.1 Animal characteristics

Twelve weeks after induction of diabetes, both body weights (Fig. 18A) and heart weights (Fig. 18B) were similar across all treatment groups. However, heart weight relative to tibial length (Fig. 18C) was significantly lower in diabetic-RhoA$^{+/+}$ mice compared to non-diabetic RhoA$^{+/+}$ animals. Blood glucose was significantly elevated in the diabetic groups compared to the non-diabetic animals, with no differences between RhoA$^{+/+}$ and RhoA$^{-/-}$ mice (Fig. 18D).

RhoA protein expression was approximately 50% lower in whole hearts from non-diabetic RhoA$^{-/-}$ compared to RhoA$^{+/+}$ mice (Fig. 19A, B). The remaining RhoA expression in RhoA$^{-/-}$ hearts represents the sum of incomplete deletion of RhoA in cardiomyocytes following tamoxifen treatment (which at best reduces expression by approximately 80%) [250] and RhoA

expression in other cell types in the heart. Induction of diabetes increased RhoA expression by about 25% in hearts from both $RhoA^{+/+}$ and $RhoA^{-/-}$ mice, but these differences were not significant compared to their corresponding non-diabetic controls. Interestingly, no diabetes-induced changes in ROCK1 (Fig. 19A, C) or ROCK2 expression (Fig. 19A, D) or in total ROCK activity (Fig. 19A, E) were detected in hearts from either $RhoA^{+/+}$ or $RhoA^{-/-}$ mice.

5.3.2 Cardiac function

No differences in either systolic or diastolic function were detected between the non-diabetic $RhoA^{+/+}$ and $RhoA^{-/-}$ mice. However, by 12 weeks after induction of diabetes, overt systolic dysfunction was evident in $RhoA^{+/+}$ mice, as indicated by decreases in both ejection fraction (Fig. 20A) and fractional shortening (Fig. 20B) compared to the non-diabetic $RhoA^{+/+}$ animals. Similarly, the IVCT was significantly increased in diabetic compared to non-diabetic $RhoA^{+/+}$ mice (Fig. 20C). On the other hand, diabetic $RhoA^{-/-}$ diabetic animals were protected from cardiac systolic dysfunction, since no changes in ejection fraction, fractional shortening or IVCT could be detected in these animals (Fig. 20A-C). Although diabetic $RhoA^{+/+}$ mice did not manifest any significant changes in E/A (Fig. 20D) or MV deceleration time (Fig. 20E), the IVRT was significantly increased in these mice compared to non-diabetic $RhoA^{+/+}$ mice (Fig. 20F), suggesting the presence of diastolic dysfunction in these hearts. On the other hand, hearts from diabetic $RhoA^{-/-}$ mice did not show any significant change in IVRT (Fig. 20F), suggesting that they were also protected against the development of diastolic dysfunction. Interestingly, MV deceleration time was somewhat lower in $RhoA^{-/-}$ mice than in $RhoA^{+/+}$ mice, but there was no difference in this parameter between non-diabetic and diabetic $RhoA^{-/-}$ mice (Fig. 20E).

There were no differences in heart rate or in AET between any of the groups (Table 5). However, consistent with the increase in both IVCT and IVRT in diabetic $RhoA^{+/+}$ mice, calculation of the MPI (Table 5) revealed a higher value in this group compared to non-diabetic $RhoA^{+/+}$ animals, indicating the presence of global cardiac dysfunction. This change was not apparent in hearts from diabetic $RhoA^{-/-}$ mice (Table 5).

No significant differences in cardiac dimensions were detected in diabetic $RhoA^{+/+}$ or diabetic $RhoA^{-/-}$ mice and their respective non-diabetic controls (Table 5). In particular, there were no significant changes in echocardiographic assessments of LV mass in diabetic compared to non-diabetic hearts (Table 5).

5.3.3 Fibrosis in whole hearts

Contractile dysfunction in diabetic hearts has been linked at least in part to the development of fibrosis. Therefore, mouse heart sections were stained with Masson's trichrome stain to assess the diabetes-induced degree of fibrosis (Fig 21). No differences in levels of fibrosis between the hearts from non-diabetic $RhoA^{+/+}$ (Fig. 21A) and $RhoA^{-/-}$ (Fig. 21C) animals were detected on microscopic evaluation. However, there were signs of extensive fibrosis in the diabetic $RhoA^{+/+}$ hearts (Fig. 21B) compared to hearts from non-diabetic $RhoA^{+/+}$ mice (Fig. 21A), and calculation of fibrotic area revealed a significant increase in these hearts compared to non-diabetic mice (Fig. 21E). In contrast, there was no significant increase in fibrosis in hearts from diabetic $RhoA^{-/-}$ animals (Fig. 21D, E).

Consistent with the increased fibrosis in hearts from diabetic $RhoA^{+/+}$ mice, the mRNA expression of both Col1A1 (Fig. 22A) and Col3A1 (Fig. 22B), as well as protein expression of Col1A1 (Fig. 22C) were elevated in hearts from diabetic compared to non-diabetic $RhoA^{+/+}$ mice. On the other hand, there were no significant changes in collagen mRNA or protein

expression in hearts from diabetic RhoA$^{-/-}$ mice compared to non-diabetic RhoA$^{+/+}$ or RhoA$^{-/-}$ mice (Fig. 22).

5.3.4 Evaluation of hypertrophy and apoptosis

In addition to fibrosis, remodeling of the heart in diabetic cardiomyopathy is associated with cardiomyocyte hypertrophy and increased apoptosis. Accordingly, we evaluated these parameters in hearts from diabetic compared to non-diabetic RhoA$^{+/+}$ and RhoA$^{-/-}$ mice. Cardiomyocyte area was determined in isolated cardiomyocytes by live-cell confocal imaging (Fig. 23). There were no differences in cardiomyocyte area between non-diabetic RhoA$^{+/+}$ and RhoA$^{-/-}$ mice. However, there was a marked increase in the area of cardiomyocytes from diabetic RhoA$^{+/+}$ hearts compared to their corresponding non-diabetic counterparts, consistent with the development of cellular hypertrophy. This increase was completely prevented in cardiomyocytes from diabetic RhoA$^{-/-}$ hearts, in which cell area was normalized to that of the non-diabetic mice.

The presence of cellular hypertrophy without an overall increase in absolute or relative heart weight (Fig. 18B, C) or left ventricular mass (Table 5) suggests that cell death must also be increased in diabetic RhoA$^{+/+}$ hearts. Consistent with this, levels of both Bax (Fig. 24A) and cleaved caspase 3 (Fig. 24B), markers of apoptosis, were significantly increased in these hearts compared to non-diabetic RhoA$^{+/+}$ hearts. In contrast, there was no change in the expression of either marker of apoptosis in hearts from diabetic RhoA$^{-/-}$ mice (Fig. 24).

5.3.5 Changes in the TGF-β signaling pathway

The TGF-β signaling pathway has been established as a significant contributor to the modulation of both fibrosis and hypertrophy in the diabetic heart [129, 251]. Therefore, we next examined the effects of cardiomyocyte RhoA deletion on this pathway. There was no difference in mRNA expression of TGF-β1 between hearts of non-diabetic RhoA$^{+/+}$ and RhoA$^{-/-}$ mice (Fig.

25A). Furthermore, there was no difference in TGF-β1 mRNA expression between the non-diabetic and diabetic RhoA$^{+/+}$ hearts (Fig. 25A). However, hearts from diabetic RhoA$^{-/-}$ mice showed much lower levels of TGF-β1 mRNA expression compared to hearts from both the diabetic RhoA$^{+/+}$ and non-diabetic RhoA$^{-/-}$ mice (Fig. 25A).

To assess whether TGF-β signaling was altered in diabetic hearts, we determined if there were any changes in phosphorylation of its downstream targets, Smad2 and 3, since up-regulation of phospho-Smad2 (Ser465/467)/Smad3 (Ser423/425) relative to total Smad 2/3 is a marker of increased TGF-β signaling. There was a marked increase in the phosphorylation of Smad2/3 in hearts from diabetic RhoA$^{+/+}$ mice compared non-diabetic RhoA$^{+/+}$ mice, consistent with increased activation of TGF-β (Fig. 25B). However, this was not observed in hearts from diabetic RhoA$^{-/-}$ animals, in which phospho-Smad2/3 levels were unchanged relative to non-diabetic mice (Fig. 25B).

We also measured the mRNA and protein expression levels of Smad7, which is an inhibitor of the TGF-β1 signaling pathway. Hearts from diabetic RhoA$^{+/+}$ animals exhibited significantly lower levels of Smad7 mRNA and protein compared to non-diabetic animals (Fig. 25C, D). This was not observed in hearts from diabetic RhoA$^{-/-}$ mice, in which Smad7 mRNA and protein expression levels were similar to those of non-diabetic RhoA$^{-/-}$ animals (Fig. 25C, D).

5.4 Discussion

We have previously demonstrated that, in models of diabetes, acute inhibition of the RhoA-ROCK pathway results in an improvement in cardiac function [176, 178] while in other studies, chronic inhibition of RhoA/ROCK signaling was shown to attenuate cardiac fibrosis in

the diabetic heart [181, 252]. The results of the current study demonstrate that in a T1D model of diabetic cardiomyopathy, RhoA in cardiomyocytes: 1) contributes to the development of cardiac dysfunction; 2) promotes fibrosis, hypertrophy and apoptosis; and 3) increases signaling through the TGF-β pathway, specifically, by upregulating Smad2/3 phosphorylation and downregulating Smad7 mRNA and protein expression. Cardiomyocyte specific deletion of RhoA prevented the development of diabetic cardiomyopathy and this was associated with the upregulation of TGF-β signaling and diminishing fibrosis, hypertrophy and apoptosis.

Much of what is known about the role of RhoA in the diabetic heart is through inhibition of its downstream effectors, particularly ROCK. Both RhoA and ROCK are expressed in multiple cell types in the heart, including cardiomyocytes, vascular smooth muscle cells and fibroblasts. In the current study, we assessed the role of RhoA specifically in cardiomyocytes in the development of diabetic cardiomyopathy, using a cardiac specific αMHC-cre recombinase expressing mouse model, in order to establish its contribution to the development of diabetic contractile dysfunction.

The reduction of RhoA protein expression in non-diabetic hearts did not result in any differences in cardiac dimensions, structure or function, consistent with previous reports that knockdown of cardiomyocyte RhoA does not result in overt changes in the heart [169]. However, cardiomyocyte specific deletion of RhoA prevented the development of both diastolic and systolic dysfunction in diabetic hearts, establishing an important role of cardiomyocyte RhoA in the development of diabetic cardiomyopathy.

Diabetic cardiomyopathy is associated with cardiac remodeling including fibrosis and hypertrophy. Fibrosis contributes to cardiac stiffness and decreased ventricular compliance, which subsequently leads to contractile dysfunction [253, 254]. Both diabetic patients and

animal models of diabetes exhibit increased levels of interstitial and perivascular fibrosis [65, 255]. Upregulation of the TGF-β canonical signaling pathway has been implicated as a contributor to the observed cardiac dysfunction and cardiac fibrosis associated with T1D [256]. In this pathway, TGF-β binds to the TGF-β receptor II which then recruits TGF-β receptor I to form a heterometric receptor complex. TGF-β receptor I subsequently directly phosphorylates Smad2 and Smad3 in their carboxyl terminal serine residues. Upon phosphorylation, Smad2 and 3 form a complex with Smad4 which enters the nucleus to regulate gene expression, including genes involved in fibrosis including those for collagens I and III (reviewed in [257]).

Previous studies have shown that cardiac contractile dysfunction and fibrosis is accompanied by upregulation of TGF-β signaling in hearts from models of both T1D and T2D rodents [181, 258]. This was associated with increases in TGF-β1 protein expression as well as in the phosphorylation of both Smad2 and 3. In the current study, we found that diabetic $RhoA^{+/+}$ animals developed marked perivascular and interstitial fibrosis, accompanied by increases in Col1A1 and Col3A1 mRNA expression as well as Col1A1 protein expression. At the same time, although TGF-β mRNA expression was not increased, Smad2/3 phosphorylation was enhanced, suggesting that TGF-β signaling is enhanced in these hearts. Interestingly, in hearts from diabetic-$RhoA^{-/-}$ mice, TGF-β1 mRNA expression was markedly depressed compared to their non-diabetic controls, and this was associated with normalization of pSmad2/3 levels. At the same time, Col1A1 and Coll3A1 mRNA as well as Col1A1 protein expression were lower in diabetic $RhoA^{-/-}$ than in diabetic $RhoA^{+/+}$ hearts, and were not significantly different from those in non-diabetic $RhoA^{-/-}$ hearts. These data suggest that cardiomyocyte RhoA plays a significant role in the development of cardiac fibrosis in diabetes by enhancing TGF-β activity, and that it may also be required to sustain the expression of TGF-β in the diabetic heart.

TGF-β signaling is negatively regulated by Smad7, which by binding to the TGF-β receptor I through its MH2 domain leads to inhibition of Smad2 and 3 phosphorylation [126], or by binding to nuclear DNA, interferes with the binding of the Smad2/3/4 complex to DNA [259]. A decrease in Smad7 expression has been reported in both hearts and kidneys of diabetic rodents, in association with upregulation of TGF-β/Smad2/3 signaling and the development of fibrosis, respectively [257, 260]. Furthermore, knocking out Smad7 results in a further increase in activation of the TGF-β/Smad2/3 pathway, while Smad7 overexpression attenuates Smad2/3 phosphorylation and reduces fibrosis in T1D renal injury [260]. In the present study, diabetic $RhoA^{+/+}$ animals exhibited reduced levels of cardiac Smad7 mRNA and protein expression compared to the non-diabetic $RhoA^{+/+}$ mice, consistent with loss of its inhibitory effect. Interestingly, our data also shows that in diabetic $RhoA^{-/-}$ mice, the expression of Smad7 mRNA and protein in the heart were not different from those of non-diabetic $RhoA^{+/+}$ or $RhoA^{-/-}$ mice. Thus, one possible mechanism by which RhoA enhances TGF-β activity and the phosphorylation of Smad2/3 in the diabetic heart is by removing the inhibitory effect of Smad7. Cardiomyocyte deletion of RhoA prevented the decrease in Smad7 expression, thereby maintaining the negative feedback regulation of Smad2/3 phosphorylation and preventing the development of fibrosis.

TGF-β upregulation has also been shown to induce cardiac hypertrophy through Smad dependent pathways. In a model of T1D, indirectly reducing pSmad2 using a PKCβ inhibitor results in prevention of cardiac hypertrophy and preserved contractility [261], while direct inhibition of Smad2 phosphorylation also inhibits cardiac hypertrophy in a model of pressure overload [262]. In the present study, the increase in Smad2/3 phosphorylation and decrease in Smad7 expression were associated with cardiomyocyte hypertrophy as well as fibrosis in hearts from diabetic-$RhoA^{+/+}$ mice. This observation is closely related to RhoA signaling as

cardiomyocyte specific deletion of RhoA, which prevented the changes in Smad, also prevented the development of cardiomyocyte hypertrophy suggesting that through its regulation of Smad2/3 phosphorylation, RhoA modulates cardiomyocyte hypertrophy. RhoA may also mediate cardiac hypertrophy by activating PI3K and subsequently Akt, which is involved in the initiation of hypertrophy [169].

Cardiomyocyte hypertrophy was observed in the diabetic $RhoA^{+/+}$ heart with no overall increase in heart weight, which is suggestive of cell death occurring concurrently with cellular hypertrophy. As such, we analyzed changes in the pro-apoptotic proteins Bax and caspase 3, both of which were elevated in diabetic $RhoA^{+/+}$ hearts compared to all other groups. This may also be attributable to an increase in TGF-β signaling, since in ventricular cardiomyocytes, Smad 3 and 4 induce apoptosis and inhibition of the Smad proteins prevents TGF-β induced apoptosis [263]. Furthermore, TGF-β induced apoptosis is associated with an increase in caspase activation [264].

The exact mechanisms by which cardiomyocyte RhoA is activated in the diabetic heart, and how it modulates TGF-β signaling are not yet clear. In a recent study, it was suggested that in cardiomyocytes, RhoA is upstream of TGF-β, since mechanical stretch-induced activation of RhoA in neonatal rat ventricular myocytes resulted in increased production of TGF-β [265]. On the other hand, vascular smooth muscle cell differentiation studies suggest that RhoA is downstream of TGF-β since addition of TGF-β1 *in vitro* resulted in a steady increase in RhoA protein expression, while treatment with the RhoA inhibitor C3 transferase or dominant negative RhoA resulted in inhibition of Smad2/3 phosphorylation and Smad-dependent gene transcription [266].

Previous studies have implicated ROCK downstream of RhoA in mediating the pro-fibrotic effects of diabetes in rat heart, based on the inhibitory effects of treatment with the non-isoform selective ROCK inhibitor fasudil [181]. Indeed, there is strong evidence for a role for ROCK, and in particular ROCK1, in the development of cardiac fibrosis associated with pressure overload [267, 268]. In contrast, in the present study, we were unable to detect changes in either ROCK1 or ROCK2 protein expression, or in total ROCK activity hearts from diabetic-RhoA$^{+/+}$ mice. Although it is possible that we were unable to detect a small isoform-specific change in ROCK activity in these hearts, it is also possible that RhoA promotes cardiac fibrosis in diabetic hearts through one of its other downstream targets.

In conclusion, in a model of type 1 diabetes, deletion of cardiomyocyte RhoA prevented cardiac dysfunction by inhibiting the development of fibrosis, hypertrophy, and apoptosis through mechanisms that include the regulation of Smad2 and 3 phosphorylation and Smad7 protein expression. Our data show, for the first time, that RhoA in cardiomyocytes is a major driver of cardiac dysfunction in diabetes. Further research is needed to identify the downstream targets that are responsible for this effect.

Gene	Primer	Sequence
Col1a1	Forward	GAG CGG AGA GTA CTG GAT CG
	Reverse	GCT TCT TTT CCT TGG GGT TC
Col3a1	Forward	GCC CAC AGC CTT CTA CAC
	Reverse	CCA GGG TCA CCA TTT CTC
TGF-ß1	Forward	CAA CAA TTC CTG GCG TTA CCT TGG
	Reverse	GAA AGC CCT GTA TTC CGT CTC CTT
Smad7	Forward	ACT CTG TGA ACT AGA GTC TCC
	Reverse	GTC TTC TCC TCC CAG TAT G
36b4	Forward	AGA TGC AGC AGA TCC GCA T
	Reverse	GTT CTT GCC CAT CAG CAC C

Table 4: Primer sequences used for RT-PCR in mice with cardiomyocyte RhoA deletion

After 12 weeks of STZ treatment, RT-PCR was carried out on hearts from both $RhoA^{+/+}$ and $RhoA^{-/-}$ animals.

Measurement	**RhoA$^{+/+}$**		**RhoA$^{-/-}$**	
	Non-diabetic	*Diabetic*	*Non-diabetic*	*Diabetic*
Heart Rate (bpm)	482.6 ± 23.9	443.1 ± 18.6	459.5 ± 14.9	475.5 ± 4.2
AET (ms)	51.9 ± 1.1	54.7 ± 2.0	55.86 ± 2.2	56.2 ± 1.6
MPI	0.5 ± 0.0	0.8 ± 0.1$^{@}$	0.4 ± 0.0	0.5 ± 0.0
LV Mass (mg)	118.3 ± 5.5	95.3 ± 12.3	125.0 ± 11.9	108.0 ± 7.1
LVAW; d (mm)	1.0 ± 0.0	1.0 ± 0.1	1.1 ± 0.1	1.0 ± 0.0
LVAW; s (mm)	1.7 ± 0.1	1.6 ± 0.1	1.8 ± 0.1	1.6 ± 0.0
LVID; d (mm)	4.0 ± 0.2	3.6 ± 0.2	3.9 ± 0.2	3.8 ± 0.1
LVID; s (mm)	2.0 ± 0.2	1.8 ± 0.2	2.1 ± 0.1	2.1 ± 0.1
LVPW; d (mm)	0.8 ± 0.1	0.8 ± 0.0	0.9 ± 0.0	0.8 ± 0.0
LVPW; s (mm)	1.5 ±0.1	1.3 ± 0.1	1.4 ± 0.1	1.3 ± 0.0

Table 5: Cardiac changes in mice with deletion of RhoA

12 weeks after STZ injection, cardiac functional and dimensional changes were determined. $^{@}p<0.05$ compared to all other groups. Data shown as mean ± S.E.M., n= 5-11 in each group.

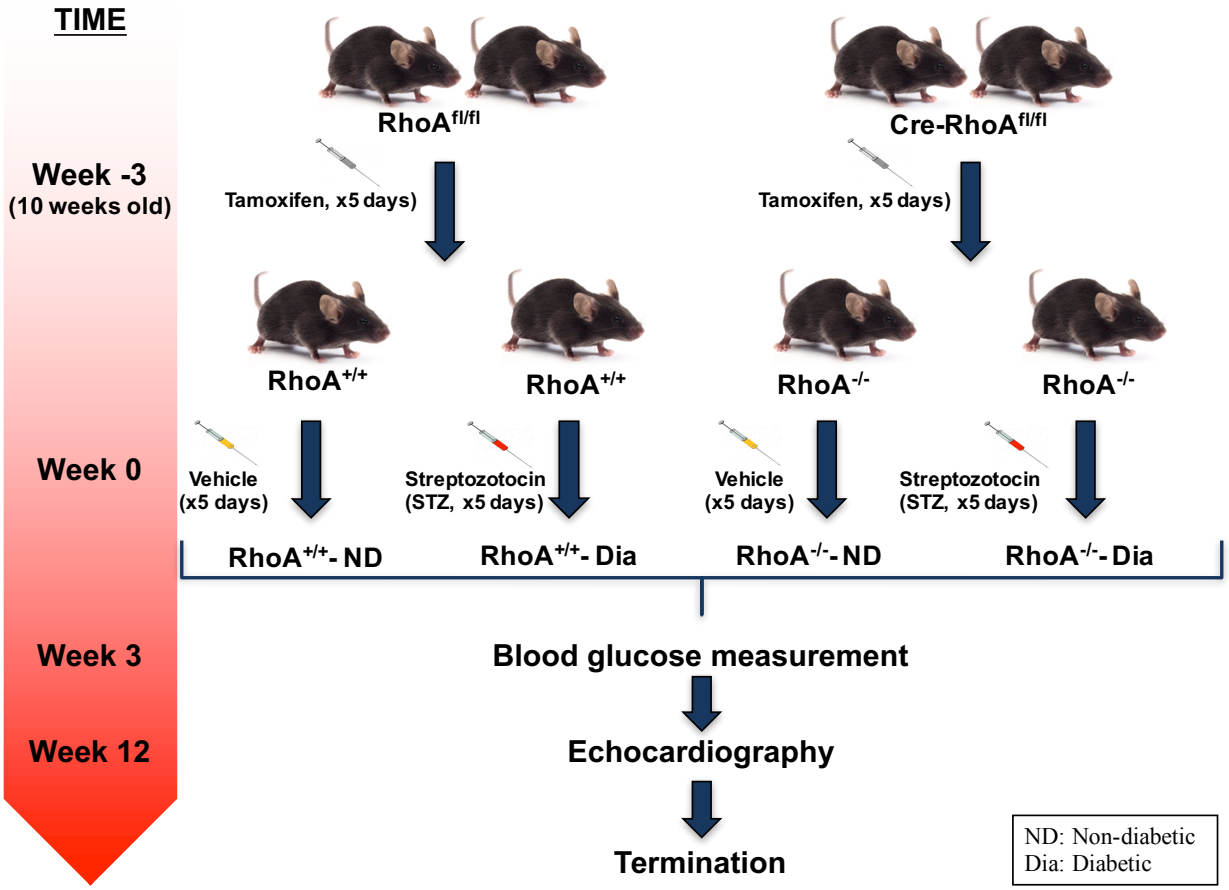

Figure 17: Animal experimental model

Mice were treated with tamoxifen to induce cardiomyocyte specific deletion of RhoA in mice with the cre promoter. Both $RhoA^{+/+}$ and $RhoA^{-/-}$ animals were then treated with STZ in order to induce type 1 diabetes. Cardiac function was measured via echocardiography 12 weeks after STZ treatment.

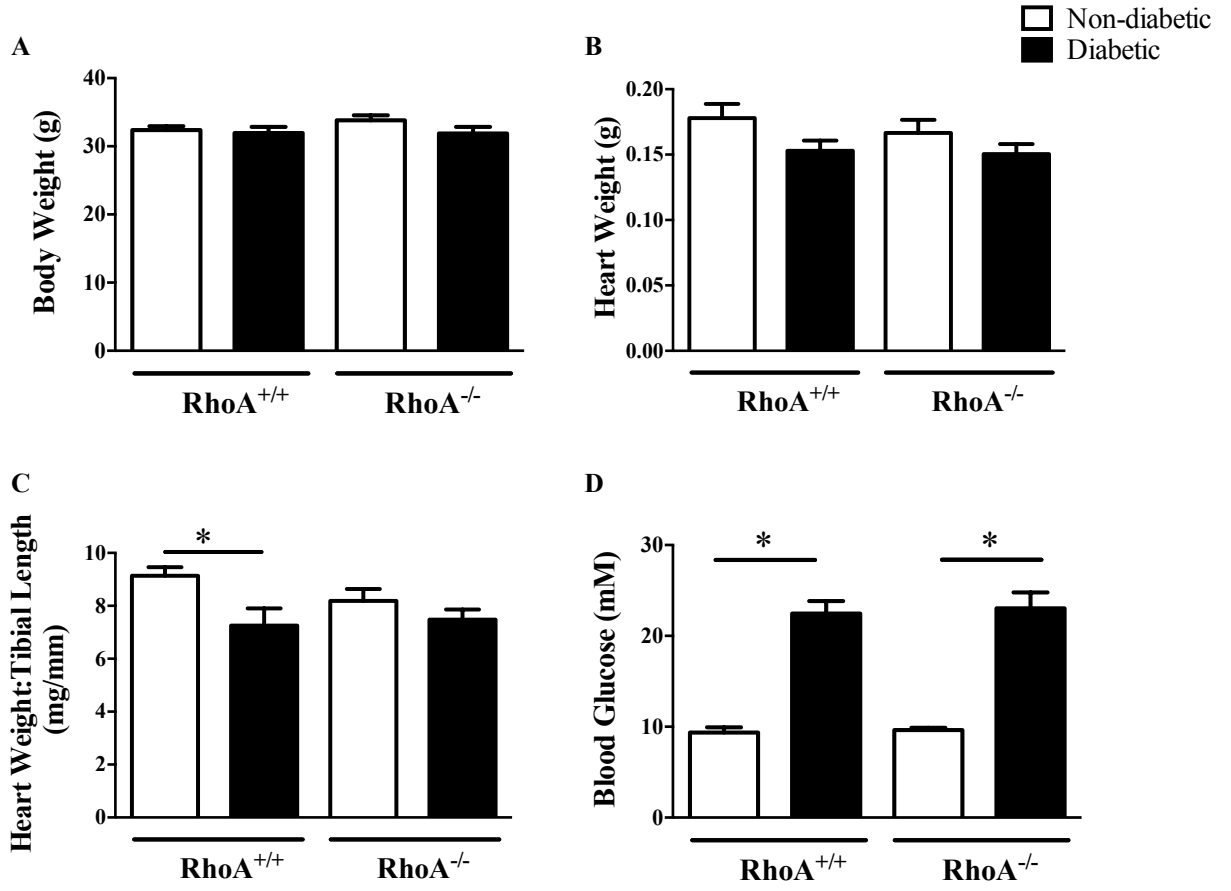

Figure 18: Characteristics of mice with deletion of RhoA

12 Weeks after STZ treatment, whole body weight (A), heart weight (B), heart weight relative to tibial length (C) and blood glucose (D) were determined. $^{*}p<0.05$. Data shown as mean ± S.E.M., n= 7-10 in each group.

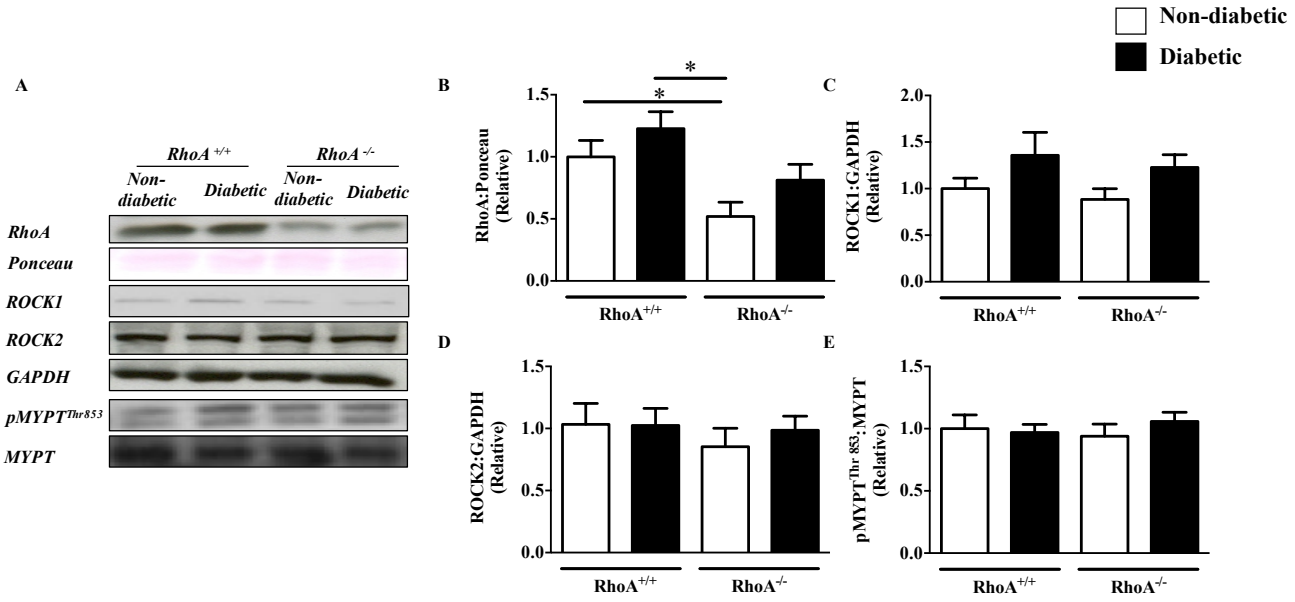

Figure 19: RhoA/ROCK pathway protein expression changes

Representative western blot images for RhoA, ROCK1 ROCK2 and pMYPT^{Thr853}relative to GAPDH or ponceau dye (A) and relative protein expression quantification of RhoA (B), ROCK1 (C), ROCK2 (D), pMYPT^{Thr853} (E). $^{*}p<0.05$. Data shown as mean ± S.E.M., n= 6-9 in each group.

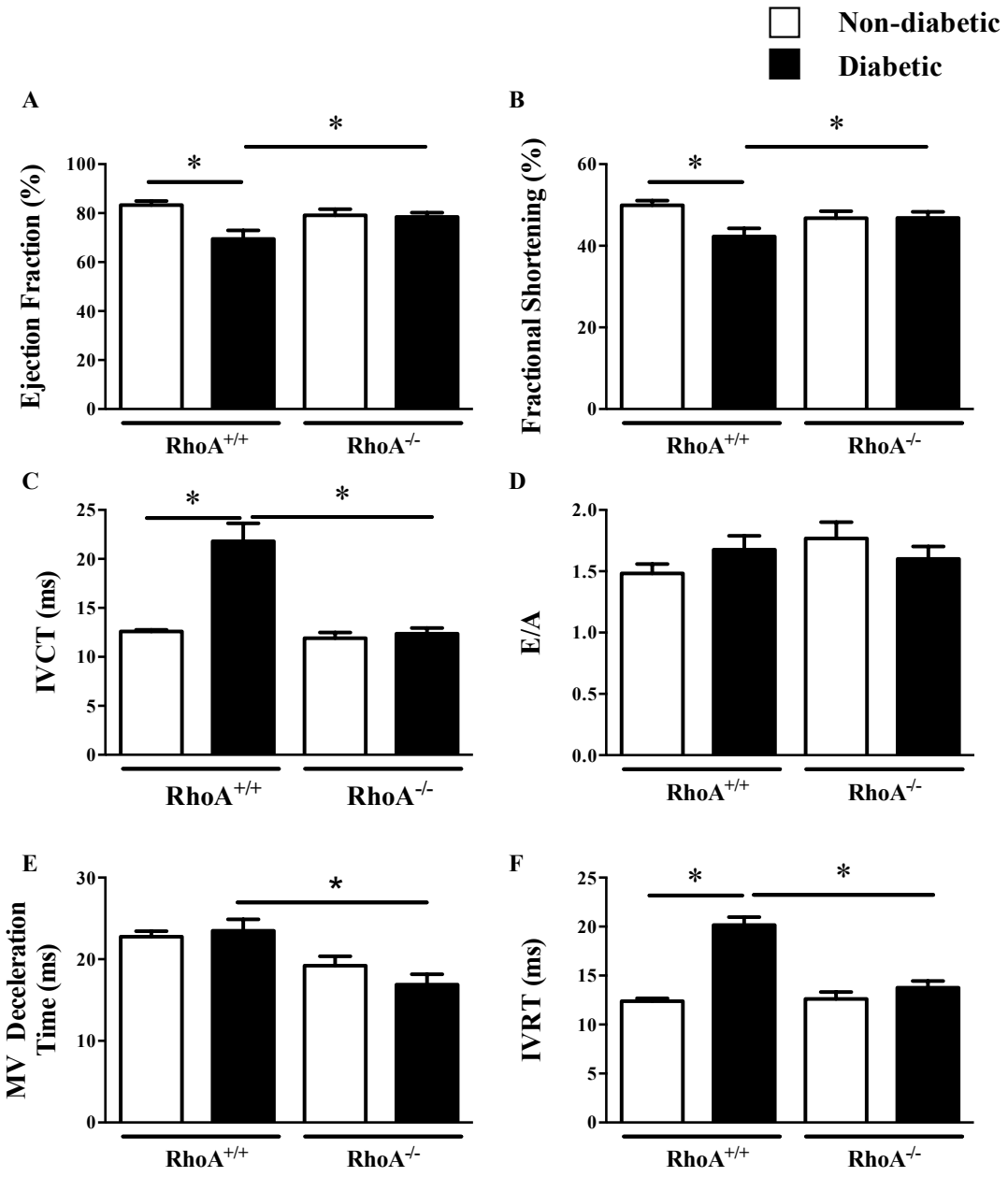

Figure 20: Cardiac diastolic and systolic function

Echocardiography was used to determine ejection fraction (A), fractional shortening (B) and IVCT (C) as markers of systolic function; and, E/A (D), MV deceleration time (E) as well as IVRT (D) as markers of diastolic function, $^{*}p<0.05$. Data shown as mean ± S.E.M., n= 7-10 in each group.

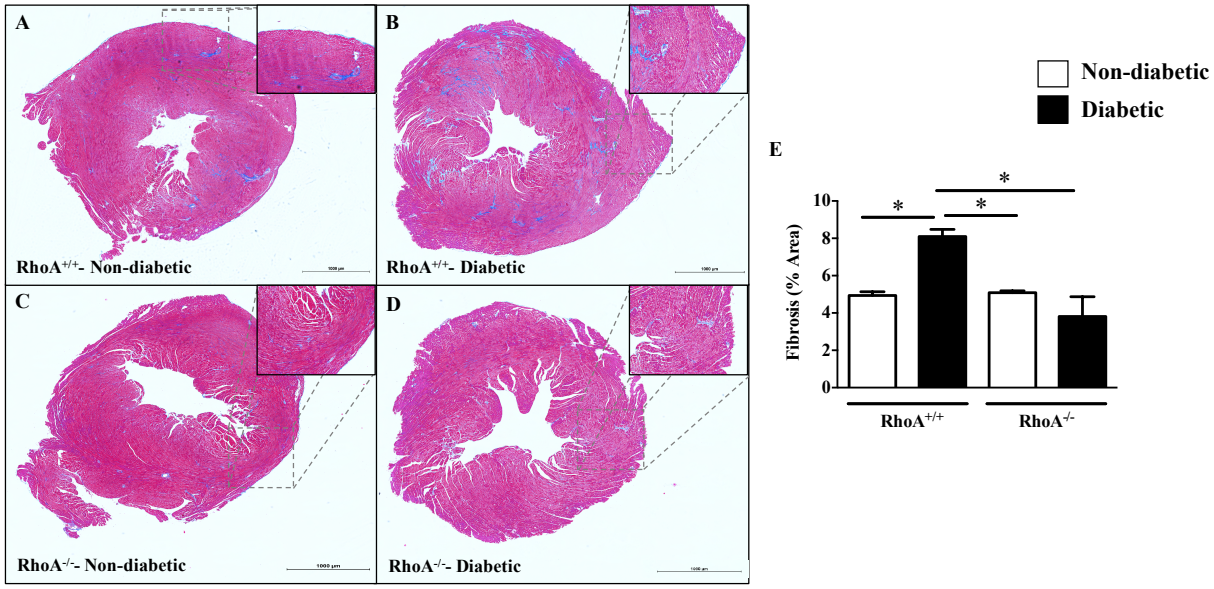

Figure 21: Assessment of cardiac fibrosis

Hearts from for non-diabetic $RhoA^{+/+}$ (A), diabetic $RhoA^{+/+}$ (B), non-diabetic $RhoA^{-/-}$ (C) and diabetic $RhoA^{-/-}$ (D) mice were stained with Masson's trichrome stain. Areas of fibrosis were calculated as a function of the total cross-sectional area visualized (E). $^{*}p<0.05$. Data shown as mean ± S.E.M., n=3 in each group.

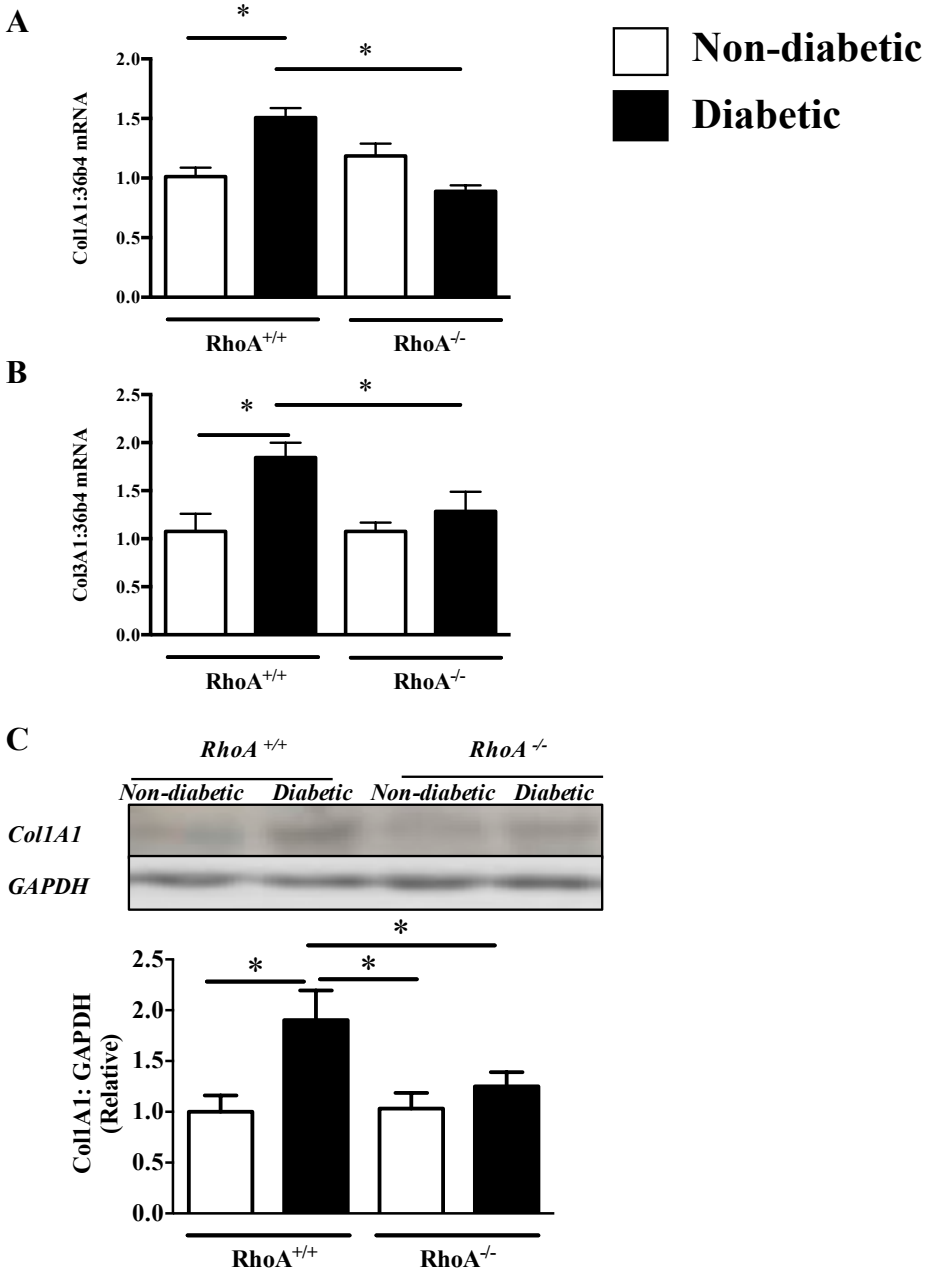

Figure 22: Collagen messenger RNA and protein expression levels

Messenger RNA expression levels for Col1A1 (A), Col3A1 (B) and protein expression for Col1A1 (C) were determined. $^{*}p<0.05$. Data shown as mean ± S.E.M., n= 6-9 in each group.

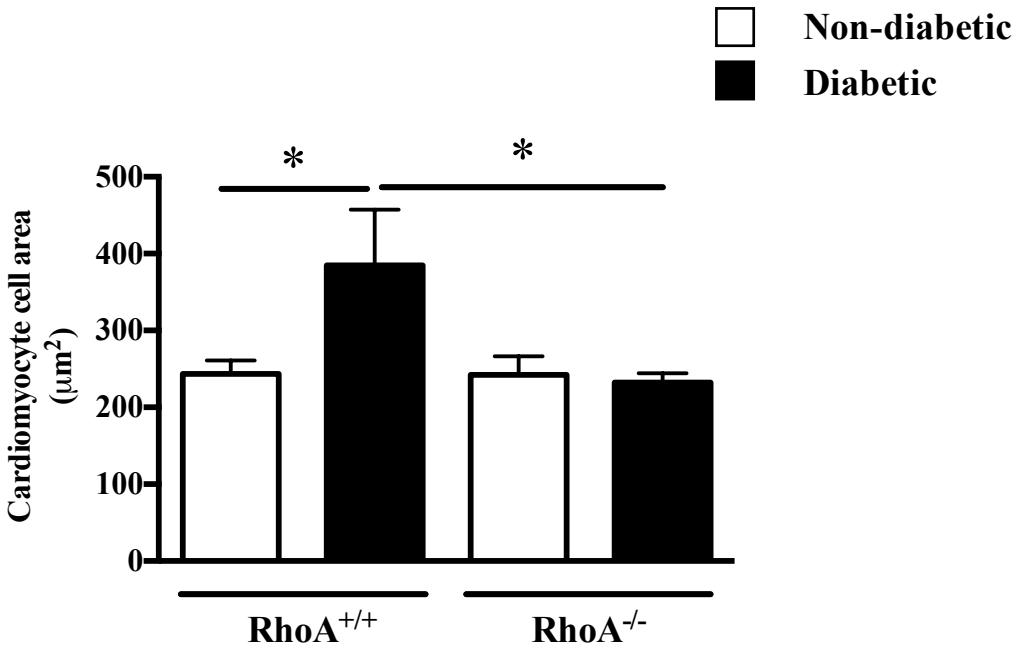

Figure 23: Calculation of the cross-sectional area of isolated cardiomyocytes

After 12 weeks of STZ treatment, cardiomyocytes were isolated and their cell size was determined. $^{*}p<0.05$. Data shown as mean ± S.E.M., n=5-8 in each group.

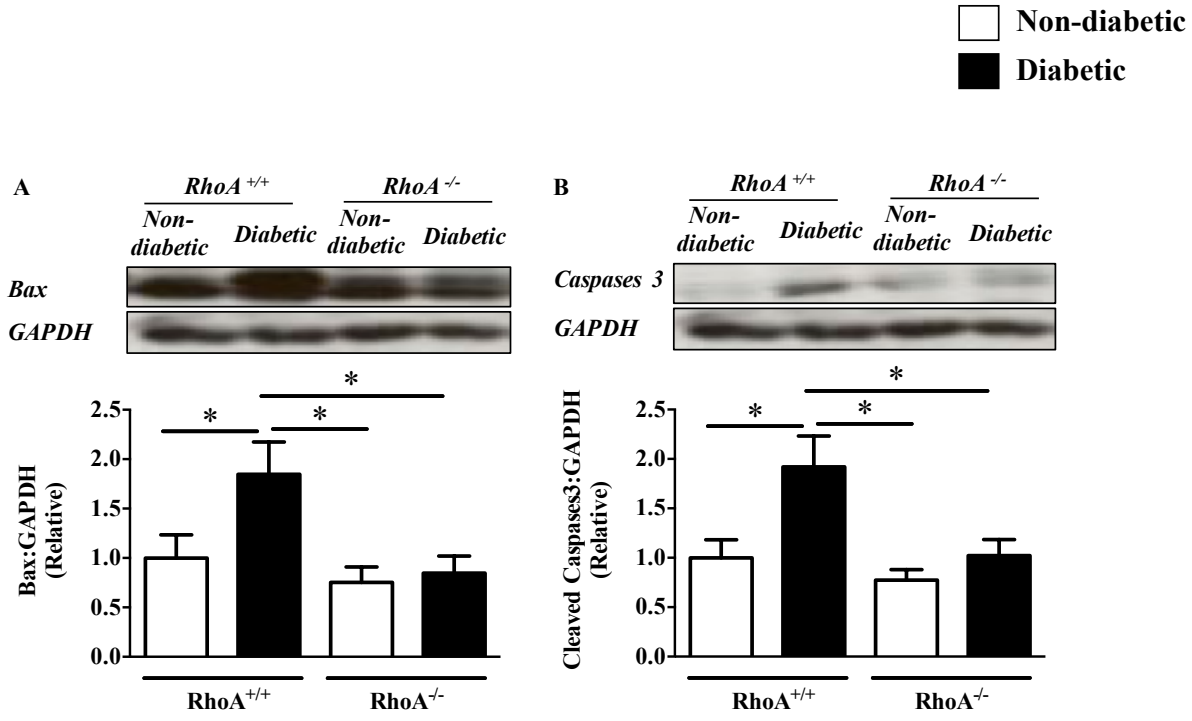

Figure 24: Changes in expression levels for proteins involved in apoptosis

Representative western blot images for Bax and cleaved caspases 3 relative to GAPDH or (A); and, relative protein expression quantification of Bax (B) and cleaved caspase 3 (C). $^{*}p<0.05$. Data shown as mean ± S.E.M., n= 7-10 in each group.

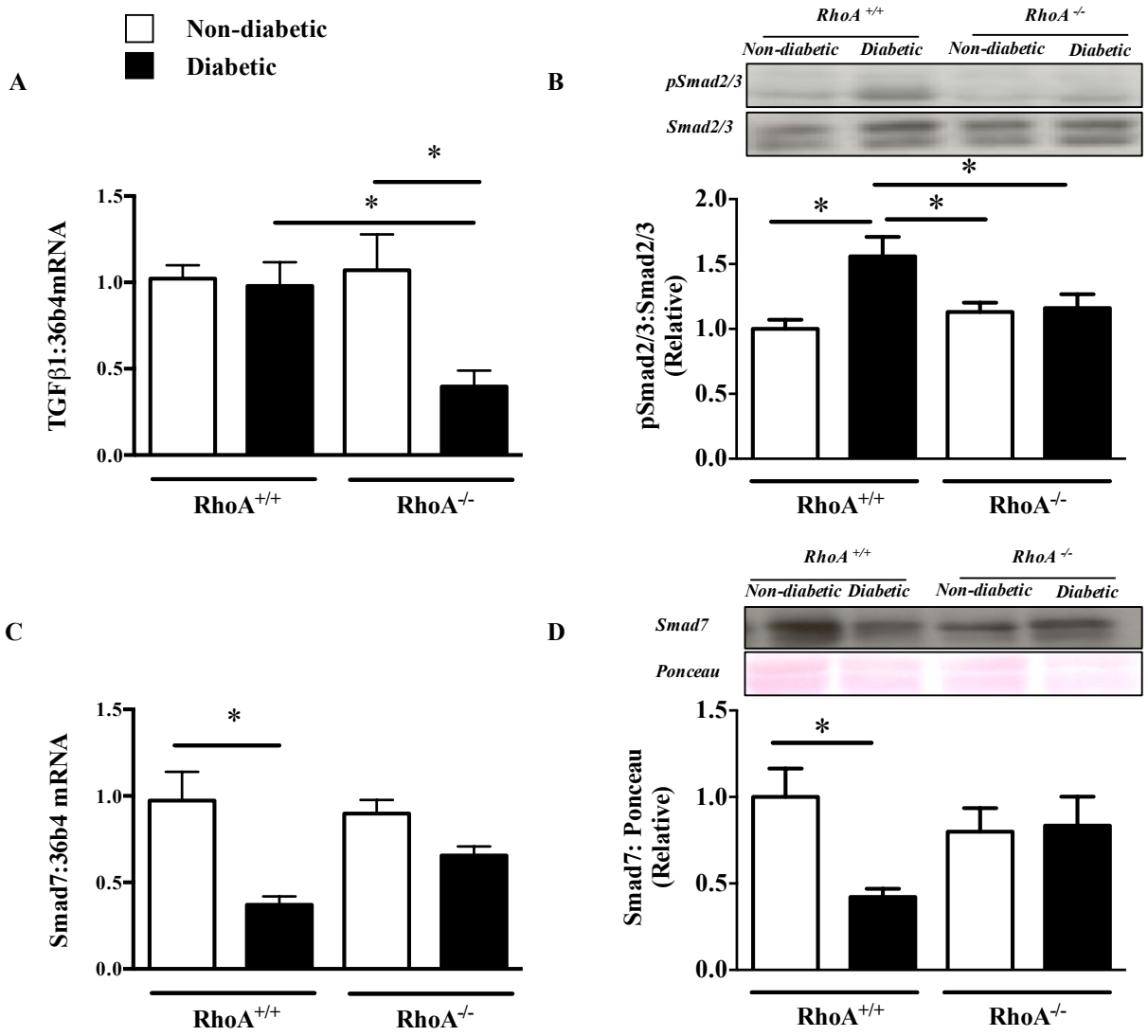

Figure 25: Changes in expression levels for mRNA and proteins involved in TGF-β signaling

Changes in TGF-β1 mRNA (A), Smad2/3 protein phosphorylation (B), Smad7 mRNA (C) and Smad7 protein expression (D) were determined 12 weeks after diabetes induction. $^{*}p<0.05$. Data shown as mean ± S.E.M., n= 7-10 in each group.

Chapter 6: Conclusions

6.1 Summary and conclusions

Cardiovascular complications including hypertension and atherosclerosis are a leading cause of death in diabetic patients [269]. In fact, diabetic patients are 3-5 times more likely to develop heart failure compared to non-diabetics [53]. Of particular interest is diabetic cardiomyopathy which is defined by diastolic and/or systolic dysfunction, independent of other risk factors such as hypertension, coronary artery and valvular disease [65, 81]. Multiple mechanisms have been postulated to contribute to diabetic cardiomyopathy, including oxidative stress, fibrosis, hypertrophy and apoptosis [62].

Over-activation of the RhoA/ROCK pathway has been implicated as a contributor to the cardiac dysfunction observed in diabetic cardiomyopathy. There are 2 isoforms of ROCK: ROCK1 and ROCK2, and inhibiting both isoforms with a non-specific inhibitor prevents the development of overt left ventricular cardiac dysfunction in diabetic rat models [176]. Although the potential benefits of RhoA/ROCK signaling inhibition in diabetic cardiomyopathy have begun to be realized, it remains unclear (1) if the beneficial effects of RhoA/ROCK inhibition are due to cardiomyocyte-specific RhoA/ROCK inhibition or arise in other cell types, and (2) which isoform of ROCK, ROCK1 or ROCK2, is responsible for the cardiac changes that occur with diabetic cardiomyopathy.

In order to address these issues, our first study was aimed at determining the role of ROCK2 in the development of diabetic cardiomyopathy in a model of T1D. In order to do so, we used CD1 mice with partial deletion of ROCK2 that were nondiabetic or treated to become diabetic. Thirteen weeks after diabetes induction, there were no differences in global cardiac function between the non-diabetic and diabetic WT or ROCK2$^{+/-}$ mice even though STZ treated

animals were overtly diabetic with blood glucose levels >25mmol/L. We attributed this to the time at which cardiac function was measured after diabetes induction.

We further isolated cardiomyocytes from these animals in order to determine if there were any changes at the cardiomyocyte level. Consistent with the global cardiac function data, cardiomyocytes from all groups showed no differences in Ca^{2+} transients when subjected to low Ca^{2+} concentrations of 2.2mM. However, when exposed to high concentrations of 6mM Ca^{2+}, diabetic WT animals showed irregular Ca^{2+} transients that were more severe and occurred in more cells compared to cardiomyocytes isolated from $ROCK2^{+/-}$ mice. The reduced occurrence of arrhythmic transients in cardiomyocytes from $ROCK2^{+/-}$ mice was associated with prevention of the increased phosphorylation of RYR2 and activation CAMKII, both of which are increased in WT mice and result in diastolic Ca^{2+} leak. These data suggest that ROCK2 plays a role in calcium handling under conditions of calcium overload and partial deletion of ROCK2 may be beneficial in preventing the number and severity of arrhythmic events associated with diabetic cardiomyopathy.

In our next project, we intended investigate the role of RhoA/ROCK in cardimyocytes using a cardiac-specific RhoA knockout mouse model of diabetes. However, given that we did not observe any signs of global cardiac dysfunction in the diabetic WT CD1 mice, we first assessed different models of diabetes and obesity order to determine the most appropriate one to induce cardiac dysfunction. The $RhoA^{-/-}$ mice were on a C57Bl/6 background, therefore we conducted experiments in that mouse strain.

Using models for obesity and T2D, C57Bl/6 mice were placed on a chow (CH), high fat (HF) or high fat-high sucrose (HFHS) diet. After 2 weeks, half of the HF mice were injected with STZ (HF-STZ) for 3 days in order to induce T2D. After 18 and 24 weeks, HFHS mice

showed signs of both diastolic and systolic dysfunction, while HF-STZ mice exhibited only diastolic dysfunction. In contrast, cardiac function was largely preserved in HF mice at both time points. All 3 treatment groups had comparable decreases in glucose tolerance and insulin sensitivity as measured by intraperitoneal glucose and insulin tolerance tests, respectively. Changes in serum triglycerides and cholesterol were also comparable, while no differences in free fatty acids compared to CH were detected. These data indicate that HFHS diet, which resembles a 'Western' diet high in fat and sugar, induced the most severe cardiac dysfunction. This is not due to differences in weight gain or in glucose or insulin tolerance or circulating lipids, suggesting that other mechanisms contribute to the deleterious cardiac effects of HFHS.

We also used a model of T1D whereby C57Bl/6 mice were either treated with citrate buffer (controls) or injected with STZ. Twelve weeks after diabetes induction, the diabetic mice showed signs of both diastolic and systolic dysfunction. As such, this model was chosen for our subsequent studies as it showed more severe contractile dysfunction compared to the obesity and T2D models and this occurred at an earlier time.

Our next study was aimed at determining if the benefits of RhoA/ROCK inhibition are due to downregulation of the pathway in cardiomyocytes. Mice with cardiomyocyte-specific deletion of RhoA were employed. $RhoA^{+/+}$ and $RhoA^{-/-}$ mice were treated with STZ to become diabetic or injected with vehicle so that they remained nondiabetic. Twelve weeks after the induction of diabetes, diabetic $RhoA^{+/+}$ mice showed both diastolic and systolic contractile dysfunction, which was associated with increased fibrosis, cardiomyocyte hypertrophy and apoptosis. Our data suggests that these observations may be due to an increase in the activity of the TGF-β signaling pathway as shown by an increase in Smad2/3 phosphorylation, which is associated with activation, as well as a decrease in the protein expression of Smad7, an important

regulator in the negative feedback of TGF-β signaling. In contrast diabetic $RhoA^{-/-}$ mice showed no signs of development of cardiac dysfunction and both Smad2/3 phosphorylation and Smad7 protein expression were unchanged compared to the nondiabetic mice. These results identify the downregulation of RhoA specifically in cardiomyocytes as a therapeutic approach for preventing diabetic cardiomyopathy.

The studies described herein collectively identify RhoA as well as its downstream target ROCK2 as playing a role in the development of cardiac dysfunction associated with diabetes. Reducing RhoA and ROCK2 expression specifically in cardiomyocytes provides beneficial effects probably through preventing over-activation of downstream targets. Previous studies have failed to ascertain the differential roles of ROCK1 and ROCK2 in diabetic cardiac dysfunction. This is, in part, due to the absence of commercially available isoform specific ROCK inhibitors. In addition, previous studies showing the effects of ROCK inhibition were carried out in whole hearts hence the beneficial effects were not well defined as RhoA and ROCK are expressed in other cell types other than cardiomyocytes including fibroblasts and vascular endothelial cells. In the studies we described herein, the major findings were that:

- In mouse models of high fat feeding, HFHS produces the most severe diastolic and systolic dysfunction compared to HF alone or HF-STZ.
- When considering mouse models of diabetes, strain differences contribute to variations in onset of diabetic cardiomyopathy. In T1D mouse models, CD1 mice have delayed onset of cardiac dysfunction compared to C57Bl/6 mice.
- Diabetes is associated with an increase in cardiomyocyte arrhythmic events in response to Ca^{2+} overload, which can be attributed to the presence of ROCK2.

- Partial deletion of ROCK2 improves the incidence and severity of arrhythmias produced by Ca^{2+} loading in cardiomyocytes from diabetic hearts, by reducing diastolic Ca^{2+} leaks through preventing RYR2 phosphorylation by CAMKII.
- ROCK2 deletion prevents increases in CAMKII autophosphorylation in hearts from diabetic mice.
- RhoA contributes to diabetic cardiac dysfunction by increasing activation of the TGF-β pathway, specifically, through increasing Smad2/3 phosphorylation and reducing Smad7 expression, an inhibitor of TGF-β/Smad2/3 pathway.
- Cardiomyocyte specific RhoA knockdown also prevents hypertrophy and apoptosis in diabetic hearts, possibly through inhibiting the activation of the TGF-β pathway.

Although the findings describe above are novel, there were some limitations to the studies conducted here. First, we were unable to detect any diastolic or systolic cardiac dysfunction in the CD1 mice, mostly likely due to the duration of the diabetic period that we assessed. Recent studies show that extending the diabetic period to 16 weeks may have proved to be informative [151], and allowed us to examine the contribution of ROCK2 to impaired systolic and diastolic function. Furthermore, all our experiments were carried out using animal models, specifically, male mice of CD1 and C57Bl/6 background, hence species differences may impede the development of therapeutic RhoA or ROCK2 inhibitors for use in humans. In addition, it is unknown if the observations made in both CD1 and C57Bl/6 male also occur in female mice or if using other mouse strains. Lastly, in the study described in Chapter 5, experiments were not carried out in cre-$RhoA^{-/-}$ mice in order to determine if there are off-target effects as a result of the presence of cre recombinase.

In conclusion, this study identifies RhoA and ROCK2 as potential therapeutic targets for diabetic cardiomyopathy. Inhibition of both produces beneficial effects by modulating various cellular mechanisms.

6.2 Future directions

6.2.1 Determining the mechanisms contributing to changes in phosphorylation of RYR2 and CAMKII

We identified RhoA/ROCK2 signaling as a modulator of CAMKII phosphorylation and subsequently RYR2 phosphorylation and hence Ca^{2+} regulation. However, we did not identify the exact mechanism by which this occurred. It will be important to identify the changes that occur to these proteins in order to determine if this can be translated to other cardiovascular diseases.

6.2.2 Determining the contribution of RhoA/ROCK signaling to diabetes and diet-induced cardiac dysfunction

The data in Chapter 3 suggests that a HFHS diet induces the most severe form of cardiac dysfunction compared to both HF and HF-STZ. Furthermore, STZ-induced diabetes (Chapter 4) resulted in early onset (12 weeks) of cardiac dysfunction. Given our data implicating RhoA and ROCK2 in diabetes-induced cardiac dysfunction (Chapters 2 and 5), as well as previously in diabetic rat hearts, it would be of interest to determine whether there are differences in RhoA/ROCK signaling in the heart between the various models of metabolic stress, and whether these contribute to the differences in cardiac function that were observed.

6.2.3 Confirmation of the role of ROCK2 in diabetic cardiomyocytes

In this study, we used a whole body ROCK2 knockdown model to identify the benefits of partial ROCK2 deletion. We recently acquired mice with cardiac specific deletion of ROCK2, which could be used to reduce ROCK2 expression by more than 50%. These mice would assist with determining the effects of further decreases in ROCK2 as well as determining the effects of ROCK2 inhibition in cardiomyocytes only, without inhibiting expression in other cell types.

6.2.4 Assessment of mechanisms contributing to increased Smad2/3 phosphorylation and reduced Smad7 expression

Although we showed that cardiomyocyte RhoA deletion prevents Smad2/3 phosphorylation in T1D, it is unknown which downstream targets of RhoA regulate this mechanism. Furthermore, we show that RhoA regulates Smad7 expression. Further studies are needed to identify the targets that link RhoA and Smad7 regulation.

Bibliography

1. Ahmad SI, SpringerLink ebooks - Biomedical and Life Sciences (2013): *Diabetes : an old disease, a new insight.* New York; Austin, Tex.: Springer Science+Business Media; Landes Bioscience; 2012.
2. Hansen SS, Aasum E, Hafstad AD: **The role of NADPH oxidases in diabetic cardiomyopathy.** *Biochim Biophys Acta* 2017, DOI: 10.1016/j.bbadis.2017.07.025 [Epub ahead of print].
3. Duh EJ, Sun JK, Stitt AW: **Diabetic retinopathy: current understanding, mechanisms, and treatment strategies.** *JCI Insight* 2017, **2**, DOI: 10.1172/jci.insight.93751 [Epub ahead of print].
4. Bodman M, Dulebohn S: **Neuropathy, diabetic.** In *StatPearls*. Treasure Island (FL); 2017, https://www.ncbi.nlm.nih.gov/pubmed/28723038 [Accessed August 4, 2017].
5. Ko GJ, Kalantar-Zadeh K, Goldstein-Fuchs J, Rhee CM: **Dietary approaches in the management of diabetic patients with kidney disease.** *Nutrients* 2017, **9**, DOI: 10.3390/nu9080824.
6. Fakhruddin S, Alanazi W, Jackson KE: **Diabetes-induced reactive oxygen species: mechanism of their generation and role in renal injury.** *J Diabetes Res* 2017, **2017:**8379327, DOI: 10.1155/2017/8379327.
7. Guilbaud A, Niquet-Leridon C, Boulanger E, Tessier FJ: **How can diet affect the accumulation of advanced glycation end-products in the human body?** *Foods* 2016, **5**, DOI: 10.3390/foods5040084.

8. Sochett E, Noone D, Grattan M, Slorach C, Moineddin R, Elia Y, Mahmud FH, Dunger DB, Dalton N, Cherney D, Scholey J, Reich H, Deanfield J: **Relationship between serum inflammatory markers and vascular function in a cohort of adolescents with type 1 diabetes.** *Cytokine* 2017, DOI: 10.1016/j.cyto.2017.07.013 [Epub ahead of print].

9. Bulani Y, Sharma SS: **Argatroban attenuates diabetic cardiomyopathy in rats by reducing fibrosis, inflammation, apoptosis, and protease-activated receptor expression.** *Cardiovasc Drugs Ther* 2017, DOI: 10.1007/s10557-017-6732-3 [Epub ahead of print].

10. Eguchi K, Boden-Albala B, Jin Z, Rundek T, Sacco RL, Homma S, Di Tullio MR: **Association between diabetes mellitus and left ventricular hypertrophy in a multiethnic population.** *Am J Cardiol* 2008, **101:**1787-1791.

11. Belke DD, Dillmann WH: **Altered cardiac calcium handling in diabetes.** *Curr Hypertens Rep* 2004, **6:**424-429.

12. Kitada M, Zhang Z, Mima A, King GL: **Molecular mechanisms of diabetic vascular complications.** *J Diabetes Investig* 2010, **1:**77-89.

13. Buse MG: **Hexosamines, insulin resistance, and the complications of diabetes: current status.** *Am J Physiol Endocrinol Metab* 2006, **290:**E1-E8.

14. Roglic G, World Health Organization: *Global report on diabetes.* Geneva, Switzerland: World Health Organization; 2016.

15. MacCracken J, Hoel D: **From ants to analogues. Puzzles and promises in diabetes management.** *Postgrad Med* 1997, **101:**138-150.

16. Keck FS, Duntas LH: **Brunner's missing 'Aha experience' delayed progress in diabetes research by 200 years.** *Hormones (Athens)* 2007, **6:**251-254.

17. American Diabetes A: **Diagnosis and classification of diabetes mellitus.** *Diabetes Care* 2014, **37 Suppl 1:**S81-90.

18. Yeung WC, Rawlinson WD, Craig ME: **Enterovirus infection and type 1 diabetes mellitus: systematic review and meta-analysis of observational molecular studies.** *BMJ* 2011, **342:**d35.

19. Lonnrot M, Lynch KF, Elding Larsson H, Lernmark A, Rewers MJ, Torn C, Burkhardt BR, Briese T, Hagopian WA, She JX, Simell OG, Toppari J, Ziegler AG, Akolkar B, Krischer JP, Hyoty H, Group TS: **Respiratory infections are temporally associated with initiation of type 1 diabetes autoimmunity: the TEDDY study.** *Diabetologia* 2017, DOI: 10.1007/s00125-017-4365-5 [Epub ahead of print].

20. Mustonen N, Siljander H, Peet A, Tillmann V, Harkonen T, Ilonen J, Hyoty H, Knip M, Group DS: **Early childhood infections precede development of beta-cell autoimmunity and type 1 diabetes in children with HLA-conferred disease risk.** *Pediatr Diabetes* 2017, DOI: 10.1111/pedi.12547 [Epub ahead of print].

21. Hanafusa T, Imagawa A: **Fulminant type 1 diabetes: a novel clinical entity requiring special attention by all medical practitioners.** *Nat Clin Pract Endocrinol Metab* 2007, **3:**36-45.

22. Ghosh S, Collier A, Krentz AJ: *Diabetes.* 2nd edn. Edinburgh ; New York: Elsevier; 2012.

23. Wu J, Ward E, Threatt T, Lu ZK: **Progression to type 2 diabetes and its effect on health care costs in low-income and insured patients with prediabetes: A retrospective study using medicaid claims data.** *J Manag Care Spec Pharm* 2017, **23:**309-316.

24. Tancredi M, Rosengren A, Svensson AM, Kosiborod M, Pivodic A, Gudbjornsdottir S, Wedel H, Clements M, Dahlqvist S, Lind M: **Excess mortality among persons with type 2 diabetes.** *N Engl J Med* 2015, **373:**1720-1732.

25. Boden G: **Role of fatty acids in the pathogenesis of insulin resistance and NIDDM.** *Diabetes* 1997, **46:**3-10.

26. Yu C, Chen Y, Cline GW, Zhang D, Zong H, Wang Y, Bergeron R, Kim JK, Cushman SW, Cooney GJ, Atcheson B, White MF, Kraegen EW, Shulman GI: **Mechanism by which fatty acids inhibit insulin activation of insulin receptor substrate-1 (IRS-1)-associated phosphatidylinositol 3-kinase activity in muscle.** *J Biol Chem* 2002, **277:**50230-50236.

27. Boden G, Chen X, Ruiz J, White JV, Rossetti L: **Mechanisms of fatty acid-induced inhibition of glucose uptake.** *J Clin Invest* 1994, **93:**2438-2446.

28. Randle PJ, Newsholme EA, Garland PB: **Regulation of glucose uptake by muscle. 8. Effects of fatty acids, ketone bodies and pyruvate, and of alloxan-diabetes and starvation, on the uptake and metabolic fate of glucose in rat heart and diaphragm muscles.** *Biochem J* 1964, **93:**652-665.

29. Wellen KE, Hotamisligil GS: **Inflammation, stress, and diabetes.** *J Clin Invest* 2005, **115:**1111-1119.

30. Sprague AH, Khalil RA: **Inflammatory cytokines in vascular dysfunction and vascular disease.** *Biochem Pharmacol* 2009, **78:**539-552.

31. Taylor-Fishwick DA, Weaver JR, Grzesik W, Chakrabarti S, Green-Mitchell S, Imai Y, Kuhn N, Nadler JL: **Production and function of IL-12 in islets and beta cells.** *Diabetologia* 2013, **56:**126-135.

32. O'Sullivan JB, Mahan CM: **Criteria for the oral glucose tolerance test in pregnancy.** *Diabetes* 1964, **13:**278-285.

33. Montoro MN, Kjos SL, Chandler M, Peters RK, Xiang AH, Buchanan TA: **Insulin resistance and preeclampsia in gestational diabetes mellitus.** *Diabetes Care* 2005, **28:**1995-2000.

34. Sermer M, Naylor CD, Gare DJ, Kenshole AB, Ritchie JW, Farine D, Cohen HR, McArthur K, Holzapfel S, Biringer A, et al.: **Impact of increasing carbohydrate intolerance on maternal-fetal outcomes in 3637 women without gestational diabetes. The Toronto Tri-Hospital Gestational Diabetes Project.** *Am J Obstet Gynecol* 1995, **173:**146-156.

35. Wahlberg J, Ekman B, Nystrom L, Hanson U, Persson B, Arnqvist HJ: **Gestational diabetes: Glycaemic predictors for fetal macrosomia and maternal risk of future diabetes.** *Diabetes Res Clin Pract* 2016, **114:**99-105.

36. Hillier TA, Pedula KL, Schmidt MM, Mullen JA, Charles MA, Pettitt DJ: **Childhood obesity and metabolic imprinting: the ongoing effects of maternal hyperglycemia.** *Diabetes Care* 2007, **30:**2287-2292.

37. Catalano PM, Huston L, Amini SB, Kalhan SC: **Longitudinal changes in glucose metabolism during pregnancy in obese women with normal glucose tolerance and gestational diabetes mellitus.** *Am J Obstet Gynecol* 1999, **180:**903-916.

38. Buchanan TA, Xiang AH: **Gestational diabetes mellitus.** *J Clin Invest* 2005, **115:**485-491.

39. Guo CC, Jin YM, Lee KK, Yang G, Jing CX, Yang X: **The relationships between HLA class II alleles and antigens with gestational diabetes mellitus: A meta-analysis.** *Sci Rep* 2016, **6:**35005.

40. McCance DR, Hanson RL, Charles MA, Jacobsson LT, Pettitt DJ, Bennett PH, Knowler WC: **Comparison of tests for glycated haemoglobin and fasting and two hour plasma glucose concentrations as diagnostic methods for diabetes.** *BMJ* 1994, **308:**1323-1328.

41. Engelgau MM, Thompson TJ, Herman WH, Boyle JP, Aubert RE, Kenny SJ, Badran A, Sous ES, Ali MA: **Comparison of fasting and 2-hour glucose and HbA1c levels for diagnosing diabetes. Diagnostic criteria and performance revisited.** *Diabetes Care* 1997, **20:**785-791.

42. Colagiuri S, Lee CM, Wong TY, Balkau B, Shaw JE, Borch-Johnsen K, Group D-CW: **Glycemic thresholds for diabetes-specific retinopathy: implications for diagnostic criteria for diabetes.** *Diabetes Care* 2011, **34:**145-150.

43. Pai JK, Cahill LE, Hu FB, Rexrode KM, Manson JE, Rimm EB: **Hemoglobin a1c is associated with increased risk of incident coronary heart disease among apparently healthy, nondiabetic men and women.** *J Am Heart Assoc* 2013, **2:**e000077.

44. Goto A, Noda M, Matsushita Y, Goto M, Kato M, Isogawa A, Takahashi Y, Kurotani K, Oba S, Nanri A, Mizoue T, Yamagishi K, Yatsuya H, Saito I, Kokubo Y, Sawada N, Inoue M, Iso H, Kadowaki T, Tsugane S, Group JS: **Hemoglobin a1c levels and the risk of cardiovascular disease in people without known diabetes: a population-based cohort study in Japan.** *Medicine (Baltimore)* 2015, **94:**e785.

45. Kennelly PJ, Rodwell VW, Rodwell VW, Bender DA, Botham KM, Kennelly PJ, Weil PA: **Proteins: Myoglobin & hemoglobin.** In *Harper's Illustrated Biochemistry, 30e*. New York, NY: McGraw-Hill Education; 2015.

46. WHO: **Use of glycated haemoglobin (HbA1c) in the diagnosis of diabetes mellitus.** *Diabetes Res Clin Pract* 2011, **93:**299-309.

47. Sacks DB: **A1C versus glucose testing: a comparison.** *Diabetes Care* 2011, **34:**518-523.

48. Sasongko MB, Widyaputri F, Agni AN, Wardhana FS, Kotha S, Gupta P, Widayanti TW, Haryanto S, Widyaningrum R, Wong TY, Kawasaki R, Wang JJ: **Prevalence of diabetic retinopathy and blindness in Indonesian adults with type 2 diabetes.** *Am J Ophthalmol* 2017, DOI: 10.1016/j.ajo.2017.06.019 [Epub ahead of print].

49. Fenwick EK, Xie J, Man REK, Sabanayagam C, Lim L, Rees G, Wong TY, Lamoureux EL: **Combined poor diabetes control indicators are associated with higher risks of diabetic retinopathy and macular edema than poor glycemic control alone.** *PLoS One* 2017, **12:**e0180252.

50. Jaiswal M, Divers J, Dabelea D, Isom S, Bell RA, Martin CL, Pettitt DJ, Saydah S, Pihoker C, Standiford DA, Dolan LM, Marcovina S, Linder B, Liese AD, Pop-Busui R, Feldman EL: **Prevalence of and risk factors for diabetic peripheral neuropathy in youth with type 1 and type 2 diabetes: SEARCH for diabetes in youth study.** *Diabetes Care* 2017, DIO: 10.2337/dc17-0179 [Epub ahead of print].

51. Bahety P, Agarwal G, Khandelwal D, Dutta D, Kalra S, Taparia P, Singhal V: **Occurrence and predictors of depression and poor quality of life among patients**

with type-2 diabetes: A northern India perspective. *Indian J Endocrinol Metab* 2017, **21:**564-569.

52. Mozaffarian D, Benjamin EJ, Go AS, Arnett DK, Blaha MJ, Cushman M, de Ferranti S, Despres JP, Fullerton HJ, Howard VJ, Huffman MD, Judd SE, Kissela BM, Lackland DT, Lichtman JH, Lisabeth LD, Liu S, Mackey RH, Matchar DB, McGuire DK, Mohler ER, 3rd, Moy CS, Muntner P, Mussolino ME, Nasir K, Neumar RW, Nichol G, Palaniappan L, Pandey DK, Reeves MJ, Rodriguez CJ, Sorlie PD, Stein J, Towfighi A, Turan TN, Virani SS, Willey JZ, Woo D, Yeh RW, Turner MB, American Heart Association Statistics C, Stroke Statistics S: **Heart disease and stroke statistics--2015 update: a report from the American Heart Association.** *Circulation* 2015, **131:**e29-322.

53. Kannel WB, McGee DL: **Diabetes and cardiovascular disease. The Framingham study.** *JAMA* 1979, **241:**2035-2038.

54. Boudina S, Abel ED: **Diabetic cardiomyopathy, causes and effects.** *Rev Endocr Metab Disord* 2010, **11:**31-39.

55. Mandavia CH, Aroor AR, Demarco VG, Sowers JR: **Molecular and metabolic mechanisms of cardiac dysfunction in diabetes.** *Life sciences* 2013, **92:**601-608.

56. Ernande L, Bergerot C, Rietzschel ER, De Buyzere ML, Thibault H, Pignonblanc PG, Croisille P, Ovize M, Groisne L, Moulin P, Gillebert TC, Derumeaux G: **Diastolic dysfunction in patients with type 2 diabetes mellitus: is it really the first marker of diabetic cardiomyopathy?** *J Am Soc Echocardiogr* 2011, **24:**1268-1275 e1261.

57. Andersson C, Vasan RS: **Epidemiology of heart failure with preserved ejection fraction.** *Heart Fail Clin* 2014, **10:**377-388.

58. Altara R, Giordano M, Norden ES, Cataliotti A, Kurdi M, Bajestani SN, Booz GW: **Targeting obesity and diabetes to treat heart failure with preserved ejection fraction.** *Front Endocrinol (Lausanne)* 2017, **8:**160.

59. Zile MR, Baicu CF, Ikonomidis JS, Stroud RE, Nietert PJ, Bradshaw AD, Slater R, Palmer BM, Van Buren P, Meyer M, Redfield MM, Bull DA, Granzier HL, LeWinter MM: **Myocardial stiffness in patients with heart failure and a preserved ejection fraction: contributions of collagen and titin.** *Circulation* 2015, **131:**1247-1259.

60. Schannwell CM, Schneppenheim M, Perings S, Plehn G, Strauer BE: **Left ventricular diastolic dysfunction as an early manifestation of diabetic cardiomyopathy.** *Cardiology* 2002, **98:**33-39.

61. Ehl NF, Kuhne M, Brinkert M, Muller-Brand J, Zellweger MJ: **Diabetes reduces left ventricular ejection fraction--irrespective of presence and extent of coronary artery disease.** *Eur J Endocrinol* 2011, **165:**945-951.

62. Miki T, Yuda S, Kouzu H, Miura T: **Diabetic cardiomyopathy: pathophysiology and clinical features.** *Heart Fail Rev* 2013, **18:**149-166.

63. Ingwall JS, SpringerLink (Online service), SpringerLINK eBooks - English/International Collection (Archive): *ATP and the Heart.* S.l.: Springer US; 2002.

64. Doenst T, Nguyen TD, Abel ED: **Cardiac metabolism in heart failure: implications beyond ATP production.** *Circ Res* 2013, **113:**709-724.

65. Regan TJ, Lyons MM, Ahmed SS, Levinson GE, Oldewurtel HA, Ahmad MR, Haider B: **Evidence for cardiomyopathy in familial diabetes mellitus.** *J Clin Invest* 1977, **60:**884-899.

66. Rijzewijk LJ, van der Meer RW, Smit JW, Diamant M, Bax JJ, Hammer S, Romijn JA, de Roos A, Lamb HJ: **Myocardial steatosis is an independent predictor of diastolic dysfunction in type 2 diabetes mellitus.** *J Am Coll Cardiol* 2008, **52:**1793-1799.

67. Belke DD, Larsen TS, Gibbs EM, Severson DL: **Altered metabolism causes cardiac dysfunction in perfused hearts from diabetic (db/db) mice.** *Am J Physiol Endocrinol Metab* 2000, **279:**E1104-1113.

68. Zhou YT, Grayburn P, Karim A, Shimabukuro M, Higa M, Baetens D, Orci L, Unger RH: **Lipotoxic heart disease in obese rats: implications for human obesity.** *Proc Natl Acad Sci U S A* 2000, **97:**1784-1789.

69. Lopaschuk GD, Tsang H: **Metabolism of palmitate in isolated working hearts from spontaneously diabetic "BB" Wistar rats.** *Circ Res* 1987, **61:**853-858.

70. Pulinilkunnil T, Kienesberger PC, Nagendran J, Waller TJ, Young ME, Kershaw EE, Korbutt G, Haemmerle G, Zechner R, Dyck JR: **Myocardial adipose triglyceride lipase overexpression protects diabetic mice from the development of lipotoxic cardiomyopathy.** *Diabetes* 2013, **62:**1464-1477.

71. Wang ZV, Li DL, Hill JA: **Heart failure and loss of metabolic control.** *J Cardiovasc Pharmacol* 2014, **63:**302-313.

72. Shao D, Tian R: **Glucose transporters in cardiac metabolism and hypertrophy.** *Compr Physiol* 2015, **6:**331-351.

73. Gray S, Kim JK: **New insights into insulin resistance in the diabetic heart.** *Trends Endocrinol Metab* 2011, **22:**394-403.

74. Park SY, Cho YR, Kim HJ, Higashimori T, Danton C, Lee MK, Dey A, Rothermel B, Kim YB, Kalinowski A, Russell KS, Kim JK: **Unraveling the temporal pattern of diet-**

induced insulin resistance in individual organs and cardiac dysfunction in C57BL/6 mice. *Diabetes* 2005, **54:**3530-3540.

75. Huang JP, Huang SS, Deng JY, Hung LM: **Impairment of insulin-stimulated Akt/GLUT4 signaling is associated with cardiac contractile dysfunction and aggravates I/R injury in STZ-diabetic rats.** *J Biomed Sci* 2009, **16:**77.

76. Yagyu H, Chen G, Yokoyama M, Hirata K, Augustus A, Kako Y, Seo T, Hu Y, Lutz EP, Merkel M, Bensadoun A, Homma S, Goldberg IJ: **Lipoprotein lipase (LpL) on the surface of cardiomyocytes increases lipid uptake and produces a cardiomyopathy.** *J Clin Invest* 2003, **111:**419-426.

77. Pulinilkunnil T, Abrahani A, Varghese J, Chan N, Tang I, Ghosh S, Kulpa J, Allard M, Brownsey R, Rodrigues B: **Evidence for rapid "metabolic switching" through lipoprotein lipase occupation of endothelial-binding sites.** *J Mol Cell Cardiol* 2003, **35:**1093-1103.

78. Rodrigues B, Cam MC, Jian K, Lim F, Sambandam N, Shepherd G: **Differential effects of streptozotocin-induced diabetes on cardiac lipoprotein lipase activity.** *Diabetes* 1997, **46:**1346-1353.

79. Elkeles RS, Hambley J: **The effects of fasting and streptozotocin diabetes on hepatic triglyceride lipase activity in the rat.** *Diabetes* 1977, **26:**58-60.

80. O'Looney P, Vander Maten M, Vahouny GV: **Insulin-mediated modifications of myocardial lipoprotein lipase and lipoprotein metabolism.** *J Biol Chem* 1983, **258:**12994-13001.

81. Rodrigues B, Cam MC, McNeill JH: **Metabolic disturbances in diabetic cardiomyopathy.** *Mol Cell Biochem* 1998, **180:**53-57.

82. Finck BN, Lehman JJ, Leone TC, Welch MJ, Bennett MJ, Kovacs A, Han X, Gross RW, Kozak R, Lopaschuk GD, Kelly DP: **The cardiac phenotype induced by PPARalpha overexpression mimics that caused by diabetes mellitus.** *J Clin Invest* 2002, **109:**121-130.

83. Finck BN, Han X, Courtois M, Aimond F, Nerbonne JM, Kovacs A, Gross RW, Kelly DP: **A critical role for PPARalpha-mediated lipotoxicity in the pathogenesis of diabetic cardiomyopathy: modulation by dietary fat content.** *Proc Natl Acad Sci U S A* 2003, **100:**1226-1231.

84. Glatz JF, Luiken JJ, Bonen A: **Membrane fatty acid transporters as regulators of lipid metabolism: implications for metabolic disease.** *Physiol Rev* 2010, **90:**367-417.

85. Luiken JJ, Koonen DP, Willems J, Zorzano A, Becker C, Fischer Y, Tandon NN, Van Der Vusse GJ, Bonen A, Glatz JF: **Insulin stimulates long-chain fatty acid utilization by rat cardiac myocytes through cellular redistribution of FAT/CD36.** *Diabetes* 2002, **51:**3113-3119.

86. Luiken JJ, Coort SL, Willems J, Coumans WA, Bonen A, van der Vusse GJ, Glatz JF: **Contraction-induced fatty acid translocase/CD36 translocation in rat cardiac myocytes is mediated through AMP-activated protein kinase signaling.** *Diabetes* 2003, **52:**1627-1634.

87. Ouwens DM, Diamant M, Fodor M, Habets DD, Pelsers MM, El Hasnaoui M, Dang ZC, van den Brom CE, Vlasblom R, Rietdijk A, Boer C, Coort SL, Glatz JF, Luiken JJ: **Cardiac contractile dysfunction in insulin-resistant rats fed a high-fat diet is associated with elevated CD36-mediated fatty acid uptake and esterification.** *Diabetologia* 2007, **50:**1938-1948.

88. Luiken JJ, Arumugam Y, Bell RC, Calles-Escandon J, Tandon NN, Glatz JF, Bonen A: **Changes in fatty acid transport and transporters are related to the severity of insulin deficiency.** *Am J Physiol Endocrinol Metab* 2002, **283:**E612-621.

89. Christoffersen C, Bollano E, Lindegaard ML, Bartels ED, Goetze JP, Andersen CB, Nielsen LB: **Cardiac lipid accumulation associated with diastolic dysfunction in obese mice.** *Endocrinology* 2003, **144:**3483-3490.

90. Sena LA, Chandel NS: **Physiological roles of mitochondrial reactive oxygen species.** *Mol Cell* 2012, **48:**158-167.

91. Kang DH, Kang SW: **Targeting cellular antioxidant enzymes for treating atherosclerotic vascular disease.** *Biomol Ther (Seoul)* 2013, **21:**89-96.

92. Matough FA, Budin SB, Hamid ZA, Alwahaibi N, Mohamed J: **The role of oxidative stress and antioxidants in diabetic complications.** *Sultan Qaboos Univ Med J* 2012, **12:**5-18.

93. Nishikawa T, Edelstein D, Du XL, Yamagishi S, Matsumura T, Kaneda Y, Yorek MA, Beebe D, Oates PJ, Hammes HP, Giardino I, Brownlee M: **Normalizing mitochondrial superoxide production blocks three pathways of hyperglycaemic damage.** *Nature* 2000, **404:**787-790.

94. Turrens JF, Alexandre A, Lehninger AL: **Ubisemiquinone is the electron donor for superoxide formation by complex III of heart mitochondria.** *Arch Biochem Biophys* 1985, **237:**408-414.

95. Sivitz WI, Yorek MA: **Mitochondrial dysfunction in diabetes: from molecular mechanisms to functional significance and therapeutic opportunities.** *Antioxid Redox Signal* 2010, **12:**537-577.

96. Brand MD: **The sites and topology of mitochondrial superoxide production.** *Exp Gerontol* 2010, **45:**466-472.

97. Muller FL, Liu Y, Van Remmen H: **Complex III releases superoxide to both sides of the inner mitochondrial membrane.** *J Biol Chem* 2004, **279:**49064-49073.

98. Touyz RM, Briones AM, Sedeek M, Burger D, Montezano AC: **NOX isoforms and reactive oxygen species in vascular health.** *Mol Interv* 2011, **11:**27-35.

99. Maalouf RM, Eid AA, Gorin YC, Block K, Escobar GP, Bailey S, Abboud HE: **Nox4-derived reactive oxygen species mediate cardiomyocyte injury in early type 1 diabetes.** *American journal of physiology Cell physiology* 2012, **302:**C597-604.

100. Incalza MA, D'Oria R, Natalicchio A, Perrini S, Laviola L, Giorgino F: **Oxidative stress and reactive oxygen species in endothelial dysfunction associated with cardiovascular and metabolic diseases.** *Vascul Pharmacol* 2017, DOI: 10.1016/j.vph.2017.05.005 [Epub ahead of print].

101. Desco MC, Asensi M, Marquez R, Martinez-Valls J, Vento M, Pallardo FV, Sastre J, Vina J: **Xanthine oxidase is involved in free radical production in type 1 diabetes: protection by allopurinol.** *Diabetes* 2002, **51:**1118-1124.

102. Kuppusamy UR, Indran M, Rokiah P: **Glycaemic control in relation to xanthine oxidase and antioxidant indices in Malaysian Type 2 diabetes patients.** *Diabet Med* 2005, **22:**1343-1346.

103. Rajesh M, Mukhopadhyay P, Batkai S, Mukhopadhyay B, Patel V, Hasko G, Szabo C, Mabley JG, Liaudet L, Pacher P: **Xanthine oxidase inhibitor allopurinol attenuates the development of diabetic cardiomyopathy.** *J Cell Mol Med* 2009, **13:**2330-2341.

104. Maejima Y, Kuroda J, Matsushima S, Ago T, Sadoshima J: **Regulation of myocardial growth and death by NADPH oxidase.** *J Mol Cell Cardiol* 2011, **50:**408-416.

105. Riojas-Hernandez A, Bernal-Ramirez J, Rodriguez-Mier D, Morales-Marroquin FE, Dominguez-Barragan EM, Borja-Villa C, Rivera-Alvarez I, Garcia-Rivas G, Altamirano J, Garcia N: **Enhanced oxidative stress sensitizes the mitochondrial permeability transition pore to opening in heart from Zucker Fa/fa rats with type 2 diabetes.** *Life Sci* 2015, **141:**32-43.

106. Kranias EG, Hajjar RJ: **Modulation of cardiac contractility by the phospholamban/SERCA2a regulatome.** *Circ Res* 2012, **110:**1646-1660.

107. Norton GR, Candy G, Woodiwiss AJ: **Aminoguanidine prevents the decreased myocardial compliance produced by streptozotocin-induced diabetes mellitus in rats.** *Circulation* 1996, **93:**1905-1912.

108. Aragno M, Mastrocola R, Medana C, Catalano MG, Vercellinatto I, Danni O, Boccuzzi G: **Oxidative stress-dependent impairment of cardiac-specific transcription factors in experimental diabetes.** *Endocrinology* 2006, **147:**5967-5974.

109. Bidasee KR, Zhang Y, Shao CH, Wang M, Patel KP, Dincer UD, Besch HR, Jr.: **Diabetes increases formation of advanced glycation end products on Sarco(endo)plasmic reticulum Ca2+-ATPase.** *Diabetes* 2004, **53:**463-473.

110. Teupe C, Rosak C: **Diabetic cardiomyopathy and diastolic heart failure -- difficulties with relaxation.** *Diabetes research and clinical practice* 2012, **97:**185-194.

111. Krenning G, Zeisberg EM, Kalluri R: **The origin of fibroblasts and mechanism of cardiac fibrosis.** *Journal of cellular physiology* 2010, **225:**631-637.

112. Fujiu K, Nagai R: **Contributions of cardiomyocyte-cardiac fibroblast-immune cell interactions in heart failure development.** *Basic research in cardiology* 2013, **108:**357.

113. Liu RM, Gaston Pravia KA: **Oxidative stress and glutathione in TGF-beta-mediated fibrogenesis.** *Free radical biology & medicine* 2010, **48:**1-15.

114. Bujak M, Frangogiannis NG: **The role of TGF-beta signaling in myocardial infarction and cardiac remodeling.** *Cardiovascular research* 2007, **74:**184-195.

115. Khalil N: **TGF-beta: from latent to active.** *Microbes Infect* 1999, **1:**1255-1263.

116. Kluwe J, Pradere JP, Gwak GY, Mencin A, De Minicis S, Osterreicher CH, Colmenero J, Bataller R, Schwabe RF: **Modulation of hepatic fibrosis by c-Jun-N-terminal kinase inhibition.** *Gastroenterology* 2010, **138:**347-359.

117. Zhou J, Deo BK, Hosoya K, Terasaki T, Obrosova IG, Brosius FC, 3rd, Kumagai AK: **Increased JNK phosphorylation and oxidative stress in response to increased glucose flux through increased GLUT1 expression in rat retinal endothelial cells.** *Investigative ophthalmology & visual science* 2005, **46:**3403-3410.

118. Hocevar BA, Brown TL, Howe PH: **TGF-beta induces fibronectin synthesis through a c-Jun N-terminal kinase-dependent, Smad4-independent pathway.** *The EMBO journal* 1999, **18:**1345-1356.

119. Zhang YE: **Non-Smad pathways in TGF-beta signaling.** *Cell Res* 2009, **19:**128-139.

120. Kretzschmar M, Doody J, Timokhina I, Massague J: **A mechanism of repression of TGFbeta/ Smad signaling by oncogenic Ras.** *Genes Dev* 1999, **13:**804-816.

121. Petritsch C, Beug H, Balmain A, Oft M: **TGF-beta inhibits p70 S6 kinase via protein phosphatase 2A to induce G(1) arrest.** *Genes Dev* 2000, **14:**3093-3101.

122. Rastogi S, Sentex E, Elimban V, Dhalla NS, Netticadan T: **Elevated levels of protein phosphatase 1 and phosphatase 2A may contribute to cardiac dysfunction in diabetes.** *Biochim Biophys Acta* 2003, **1638:**273-277.

123. Lakos G, Takagawa S, Chen SJ, Ferreira AM, Han G, Masuda K, Wang XJ, DiPietro LA, Varga J: **Targeted disruption of TGF-beta/Smad3 signaling modulates skin fibrosis in a mouse model of scleroderma.** *Am J Pathol* 2004, **165:**203-217.

124. Khan R, Sheppard R: **Fibrosis in heart disease: understanding the role of transforming growth factor-beta in cardiomyopathy, valvular disease and arrhythmia.** *Immunology* 2006, **118:**10-24.

125. Nakao A, Afrakhte M, Moren A, Nakayama T, Christian JL, Heuchel R, Itoh S, Kawabata M, Heldin NE, Heldin CH, ten Dijke P: **Identification of Smad7, a TGFbeta-inducible antagonist of TGF-beta signalling.** *Nature* 1997, **389:**631-635.

126. Hayashi H, Abdollah S, Qiu Y, Cai J, Xu YY, Grinnell BW, Richardson MA, Topper JN, Gimbrone MA, Jr., Wrana JL, Falb D: **The MAD-related protein Smad7 associates with the TGFbeta receptor and functions as an antagonist of TGFbeta signaling.** *Cell* 1997, **89:**1165-1173.

127. Wang B, Hao J, Jones SC, Yee MS, Roth JC, Dixon IM: **Decreased Smad 7 expression contributes to cardiac fibrosis in the infarcted rat heart.** *Am J Physiol Heart Circ Physiol* 2002, **282:**H1685-1696.

128. Wang X, Mu C, Mu T, Gao L, Zhao Y, Zhang Y, Zhang Z: **Effects of Tongxinluo on myocardial fibrosis in diabetic rats.** *J Chin Med Assoc* 2016, **79:**130-136.

129. Rosenkranz S, Flesch M, Amann K, Haeuseler C, Kilter H, Seeland U, Schluter KD, Bohm M: **Alterations of beta-adrenergic signaling and cardiac hypertrophy in**

transgenic mice overexpressing TGF-beta(1). *Am J Physiol Heart Circ Physiol* 2002, **283:**H1253-1262.

130. Dobaczewski M, Chen W, Frangogiannis NG: **Transforming growth factor (TGF)-beta signaling in cardiac remodeling.** *J Mol Cell Cardiol* 2011, **51:**600-606.

131. Fredj S, Bescond J, Louault C, Potreau D: **Interactions between cardiac cells enhance cardiomyocyte hypertrophy and increase fibroblast proliferation.** *Journal of cellular physiology* 2005, **202:**891-899.

132. Zhang P, Su J, Mende U: **Cross talk between cardiac myocytes and fibroblasts: from multiscale investigative approaches to mechanisms and functional consequences.** *American journal of physiology Heart and circulatory physiology* 2012, **303:**H1385-1396.

133. Westermann D, Rutschow S, Van Linthout S, Linderer A, Bucker-Gartner C, Sobirey M, Riad A, Pauschinger M, Schultheiss HP, Tschope C: **Inhibition of p38 mitogen-activated protein kinase attenuates left ventricular dysfunction by mediating pro-inflammatory cardiac cytokine levels in a mouse model of diabetes mellitus.** *Diabetologia* 2006, **49:**2507-2513.

134. Lowe G, Woodward M, Hillis G, Rumley A, Li Q, Harrap S, Marre M, Hamet P, Patel A, Poulter N, Chalmers J: **Circulating inflammatory markers and the risk of vascular complications and mortality in people with type 2 diabetes mellitus and cardiovascular disease or risk factors: The Advance Study.** *Diabetes* 2013, DOI: 10.2337/db12-1625 [Epub ahead of print].

135. Wagner MA, Siddiqui MA: **The JAK-STAT pathway in hypertrophic stress signaling and genomic stress response.** *Jak-Stat* 2012, **1:**131-141.

136. Sano M, Fukuda K, Kodama H, Pan J, Saito M, Matsuzaki J, Takahashi T, Makino S, Kato T, Ogawa S: **Interleukin-6 family of cytokines mediate angiotensin II-induced cardiac hypertrophy in rodent cardiomyocytes.** *The Journal of biological chemistry* 2000, **275:**29717-29723.

137. Kim NN, Villarreal FJ, Printz MP, Lee AA, Dillmann WH: **Trophic effects of angiotensin II on neonatal rat cardiac myocytes are mediated by cardiac fibroblasts.** *The American journal of physiology* 1995, **269:**E426-437.

138. Sharma V, McNeill JH: **Diabetic cardiomyopathy: where are we 40 years later?** *Can J Cardiol* 2006, **22:**305-308.

139. Lenzen S: **The mechanisms of alloxan- and streptozotocin-induced diabetes.** *Diabetologia* 2008, **51:**216-226.

140. Dufrane D, van Steenberghe M, Guiot Y, Goebbels RM, Saliez A, Gianello P: **Streptozotocin-induced diabetes in large animals (pigs/primates): role of GLUT2 transporter and beta-cell plasticity.** *Transplantation* 2006, **81:**36-45.

141. Wilson GL, Patton NJ, McCord JM, Mullins DW, Mossman BT: **Mechanisms of streptozotocin- and alloxan-induced damage in rat B cells.** *Diabetologia* 1984, **27:**587-591.

142. Crouch R, Kimsey G, Priest DG, Sarda A, Buse MG: **Effect of streptozotocin on erythrocyte and retinal superoxide dismutase.** *Diabetologia* 1978, **15:**53-57.

143. Slonim AE, Fletcher T, Burke V, Burr IM: **Effect of streptozotocin on red-blood-cell-reduced glutathione: modification by glucose, nicotinamide, and epinephrine.** *Diabetes* 1976, **25:**216-222.

144. Robbins MJ, Sharp RA, Slonim AE, Burr IM: **Protection against streptozotocin-induced diabetes by superoxide dismutase.** *Diabetologia* 1980, **18:**55-58.

145. Diabetic Complications Consortium: **Low-dose streptozotocin induction protocol,** http://www.diacomp.org/shared/document.aspx?id=19&docType=Protocol [Accessed July 30, 2017].

146. Willecke F, Scerbo D, Nagareddy P, Obunike JC, Barrett TJ, Abdillahi ML, Trent CM, Huggins LA, Fisher EA, Drosatos K, Goldberg IJ: **Lipolysis, and not hepatic lipogenesis, is the primary modulator of triglyceride levels in streptozotocin-induced diabetic mice.** *Arterioscler Thromb Vasc Biol* 2015, **35:**102-110.

147. Franko A, Huypens P, Neschen S, Irmler M, Rozman J, Rathkolb B, Neff F, Prehn C, Dubois G, Baumann M, Massinger R, Gradinger D, Przemeck GK, Repp B, Aichler M, Feuchtinger A, Schommers P, Stohr O, Sanchez-Lasheras C, Adamski J, Peter A, Prokisch H, Beckers J, Walch AK, Fuchs H, Wolf E, Schubert M, Wiesner RJ, Hrabe de Angelis M: **Bezafibrate improves insulin sensitivity and metabolic flexibility in STZ-induced diabetic mice.** *Diabetes* 2016, **65:**2540-2552.

148. Chaudhry ZZ, Morris DL, Moss DR, Sims EK, Chiong Y, Kono T, Evans-Molina C: **Streptozotocin is equally diabetogenic whether administered to fed or fasted mice.** *Lab Anim* 2013, **47:**257-265.

149. Yu X, Tesiram YA, Towner RA, Abbott A, Patterson E, Huang S, Garrett MW, Chandrasekaran S, Matsuzaki S, Szweda LI, Gordon BE, Kem DC: **Early myocardial dysfunction in streptozotocin-induced diabetic mice: a study using in vivo magnetic resonance imaging (MRI).** *Cardiovasc Diabetol* 2007, **6:**6.

150. Liu C, Lu XZ, Shen MZ, Xing CY, Ma J, Duan YY, Yuan LJ: **N-Acetyl Cysteine improves the diabetic cardiac function: possible role of fibrosis inhibition.** *BMC Cardiovasc Disord* 2015, **15:**84.

151. Moore A, Shindikar A, Fomison-Nurse I, Riu F, Munasinghe PE, Ram TP, Saxena P, Coffey S, Bunton RW, Galvin IF, Williams MJ, Emanueli C, Madeddu P, Katare R: **Rapid onset of cardiomyopathy in STZ-induced female diabetic mice involves the downregulation of pro-survival Pim-1.** *Cardiovasc Diabetol* 2014, **13:**68.

152. Wu J, Yan LJ: **Streptozotocin-induced type 1 diabetes in rodents as a model for studying mitochondrial mechanisms of diabetic beta cell glucotoxicity.** *Diabetes Metab Syndr Obes* 2015, **8:**181-188.

153. Deeds MC, Anderson JM, Armstrong AS, Gastineau DA, Hiddinga HJ, Jahangir A, Eberhardt NL, Kudva YC: **Single dose streptozotocin-induced diabetes: considerations for study design in islet transplantation models.** *Lab Anim* 2011, **45:**131-140.

154. Kahn BB, Flier JS: **Obesity and insulin resistance.** *J Clin Invest* 2000, **106:**473-481.

155. Gilbert ER, Fu Z, Liu D: **Development of a nongenetic mouse model of type 2 diabetes.** *Exp Diabetes Res* 2011, **2011:**416254.

156. Marciniak C, Marechal X, Montaigne D, Neviere R, Lancel S: **Cardiac contractile function and mitochondrial respiration in diabetes-related mouse models.** *Cardiovasc Diabetol* 2014, **13:**118.

157. Schreyer SA, Wilson DL, LeBoeuf RC: **C57BL/6 mice fed high fat diets as models for diabetes-accelerated atherosclerosis.** *Atherosclerosis* 1998, **136:**17-24.

158. Collins S, Martin TL, Surwit RS, Robidoux J: **Genetic vulnerability to diet-induced obesity in the C57BL/6J mouse: physiological and molecular characteristics.** *Physiol Behav* 2004, **81:**243-248.

159. Brainard RE, Watson LJ, Demartino AM, Brittian KR, Readnower RD, Boakye AA, Zhang D, Hoetker JD, Bhatnagar A, Baba SP, Jones SP: **High fat feeding in mice is insufficient to induce cardiac dysfunction and does not exacerbate heart failure.** *PLoS One* 2013, **8:**e83174.

160. Nguyen S, Shao D, Tomasi LC, Braun A, de Mattos ABM, Choi YS, Villet O, Roe N, Halterman CR, Tian R, Kolwicz SC, Jr.: **The effects of fatty acid composition on cardiac hypertrophy and function in mouse models of diet-induced obesity.** *J Nutr Biochem* 2017, **46:**137-142.

161. Carbone S, Mauro AG, Mezzaroma E, Kraskauskas D, Marchetti C, Buzzetti R, Van Tassell BW, Abbate A, Toldo S: **A high-sugar and high-fat diet impairs cardiac systolic and diastolic function in mice.** *Int J Cardiol* 2015, **198:**66-69.

162. Pulinilkunnil T, Kienesberger PC, Nagendran J, Sharma N, Young ME, Dyck JR: **Cardiac-specific adipose triglyceride lipase overexpression protects from cardiac steatosis and dilated cardiomyopathy following diet-induced obesity.** *Int J Obes (Lond)* 2014, **38:**205-215.

163. Cao L, Qin X, Peterson MR, Haller SE, Wilson KA, Hu N, Lin X, Nair S, Ren J, He G: **CARD9 knockout ameliorates myocardial dysfunction associated with high fat diet-induced obesity.** *J Mol Cell Cardiol* 2016, **92:**185-195.

164. Luo L: **Rho GTPases in neuronal morphogenesis.** *Nature reviews Neuroscience* 2000, **1:**173-180.

165. Wang Y, Zheng XR, Riddick N, Bryden M, Baur W, Zhang X, Surks HK: **ROCK isoform regulation of myosin phosphatase and contractility in vascular smooth muscle cells.** *Circulation research* 2009, **104:**531-540.

166. Loirand G, Guerin P, Pacaud P: **Rho kinases in cardiovascular physiology and pathophysiology.** *Circulation research* 2006, **98:**322-334.

167. Kaibuchi K, Kuroda S, Amano M: **Regulation of the cytoskeleton and cell adhesion by the Rho family GTPases in mammalian cells.** *Annu Rev Biochem* 1999, **68:**459-486.

168. Sah VP, Minamisawa S, Tam SP, Wu TH, Dorn GW, 2nd, Ross J, Jr., Chien KR, Brown JH: **Cardiac-specific overexpression of RhoA results in sinus and atrioventricular nodal dysfunction and contractile failure.** *J Clin Invest* 1999, **103:**1627-1634.

169. Lauriol J, Keith K, Jaffre F, Couvillon A, Saci A, Goonasekera SA, McCarthy JR, Kessinger CW, Wang J, Ke Q, Kang PM, Molkentin JD, Carpenter C, Kontaridis MI: **RhoA signaling in cardiomyocytes protects against stress-induced heart failure but facilitates cardiac fibrosis.** *Sci Signal* 2014, **7:**ra100.

170. Xiang SY, Vanhoutte D, Del Re DP, Purcell NH, Ling H, Banerjee I, Bossuyt J, Lang RA, Zheng Y, Matkovich SJ, Miyamoto S, Molkentin JD, Dorn GW, 2nd, Brown JH: **RhoA protects the mouse heart against ischemia/reperfusion injury.** *J Clin Invest* 2011, **121:**3269-3276.

171. Hamid SA, Bower HS, Baxter GF: **Rho kinase activation plays a major role as a mediator of irreversible injury in reperfused myocardium.** *Am J Physiol Heart Circ Physiol* 2007, **292:**H2598-2606.

172. Bao W, Hu E, Tao L, Boyce R, Mirabile R, Thudium DT, Ma XL, Willette RN, Yue TL: **Inhibition of Rho-kinase protects the heart against ischemia/reperfusion injury.** *Cardiovasc Res* 2004, **61:**548-558.

173. Hattori T, Shimokawa H, Higashi M, Hiroki J, Mukai Y, Tsutsui H, Kaibuchi K, Takeshita A: **Long-term inhibition of Rho-kinase suppresses left ventricular remodeling after myocardial infarction in mice.** *Circulation* 2004, **109:**2234-2239.

174. Higashi M, Shimokawa H, Hattori T, Hiroki J, Mukai Y, Morikawa K, Ichiki T, Takahashi S, Takeshita A: **Long-term inhibition of Rho-kinase suppresses angiotensin II-induced cardiovascular hypertrophy in rats in vivo: effect on endothelial NAD(P)H oxidase system.** *Circ Res* 2003, **93:**767-775.

175. Mallat Z, Gojova A, Sauzeau V, Brun V, Silvestre JS, Esposito B, Merval R, Groux H, Loirand G, Tedgui A: **Rho-associated protein kinase contributes to early atherosclerotic lesion formation in mice.** *Circ Res* 2003, **93:**884-888.

176. Lin G, Craig GP, Zhang L, Yuen VG, Allard M, McNeill JH, MacLeod KM: **Acute inhibition of Rho-kinase improves cardiac contractile function in streptozotocin-diabetic rats.** *Cardiovasc Res* 2007, **75:**51-58.

177. Sumi T, Matsumoto K, Nakamura T: **Specific activation of LIM kinase 2 via phosphorylation of threonine 505 by ROCK, a Rho-dependent protein kinase.** *The Journal of biological chemistry* 2001, **276:**670-676.

178. Soliman H, Gador A, Lu YH, Lin G, Bankar G, MacLeod KM: **Diabetes-induced increased oxidative stress in cardiomyocytes is sustained by a positive feedback loop involving Rho kinase and PKCbeta2.** *Am J Physiol Heart Circ Physiol* 2012, **303:**H989-H1000.

179. Lin G, Brownsey RW, Macleod KM: **Complex regulation of PKCbeta2 and PDK-1/AKT by ROCK2 in diabetic heart.** *PLoS One* 2014, **9:**e86520.

180. Soliman H, Nyamandi V, Garcia-Patino M, Varela JN, Bankar G, Lin G, Jia Z, MacLeod KM: **Partial deletion of ROCK2 protects mice from high-fat diet-induced cardiac insulin resistance and contractile dysfunction.** *Am J Physiol Heart Circ Physiol* 2015, **309:**H70-81.

181. Zhou H, Li YJ, Wang M, Zhang LH, Guo BY, Zhao ZS, Meng FL, Deng YG, Wang RY: **Involvement of RhoA/ROCK in myocardial fibrosis in a rat model of type 2 diabetes.** *Acta Pharmacol Sin* 2011, **32:**999-1008.

182. Thumkeo D, Keel J, Ishizaki T, Hirose M, Nonomura K, Oshima H, Oshima M, Taketo MM, Narumiya S: **Targeted disruption of the mouse rho-associated kinase 2 gene results in intrauterine growth retardation and fetal death.** *Mol Cell Biol* 2003, **23:**5043-5055.

183. Multiple Risk Factor Intervention Trial Research Group. **Multiple risk factor intervention trial. Risk factor changes and mortality results.** *JAMA* 1982, **248:**1465-1477.

184. Khaw KT, Wareham N, Bingham S, Luben R, Welch A, Day N: **Association of hemoglobin A1c with cardiovascular disease and mortality in adults: the European prospective investigation into cancer in Norfolk.** *Ann Intern Med* 2004, **141:**413-420.

185. Doshi SM, Friedman AN: **Diagnosis and management of type 2 diabetic kidney disease.** *Clin J Am Soc Nephrol* 2017, **12:**1366-1373.

186. Groop PH, Thomas MC, Moran JL, Waden J, Thorn LM, Makinen VP, Rosengard-Barlund M, Saraheimo M, Hietala K, Heikkila O, Forsblom C, FinnDiane Study G: **The**

presence and severity of chronic kidney disease predicts all-cause mortality in type 1 diabetes. *Diabetes* 2009, **58:**1651-1658.

187. Tseng KS, Lin C, Lin YS, Weng SF: **Risk of head and neck cancer in patients with diabetes mellitus: a retrospective cohort study in Taiwan.** *JAMA Otolaryngol Head Neck Surg* 2014, **140:**746-753.

188. Varma R: **From a population to patients: the Wisconsin epidemiologic study of diabetic retinopathy.** *Ophthalmology* 2008, **115:**1857-1858.

189. Rubler S, Dlugash J, Yuceoglu YZ, Kumral T, Branwood AW, Grishman A: **New type of cardiomyopathy associated with diabetic glomerulosclerosis.** *Am J Cardiol* 1972, **30:**595-602.

190. Nielsen LB, Bartels ED, Bollano E: **Overexpression of apolipoprotein B in the heart impedes cardiac triglyceride accumulation and development of cardiac dysfunction in diabetic mice.** *J Biol Chem* 2002, **277:**27014-27020.

191. Suarez J, Scott B, Dillmann WH: **Conditional increase in SERCA2a protein is able to reverse contractile dysfunction and abnormal calcium flux in established diabetic cardiomyopathy.** *Am J Physiol Regul Integr Comp Physiol* 2008, **295:**R1439-1445.

192. Duan J, Zhang HY, Adkins SD, Ren BH, Norby FL, Zhang X, Benoit JN, Epstein PN, Ren J: **Impaired cardiac function and IGF-I response in myocytes from calmodulin-diabetic mice: role of Akt and RhoA.** *Am J Physiol Endocrinol Metab* 2003, **284:**E366-376.

193. Ye G, Metreveli NS, Ren J, Epstein PN: **Metallothionein prevents diabetes-induced deficits in cardiomyocytes by inhibiting reactive oxygen species production.** *Diabetes* 2003, **52:**777-783.

194. Luo SY, Chen S, Qin YD, Chen ZW: **Urotensin-Receptor antagonist SB-710411 protects rat heart against ischemia-reperfusion injury via RhoA/ROCK pathway.** *PLoS One* 2016, **11:**e0146094.

195. Uehata M, Ishizaki T, Satoh H, Ono T, Kawahara T, Morishita T, Tamakawa H, Yamagami K, Inui J, Maekawa M, Narumiya S: **Calcium sensitization of smooth muscle mediated by a Rho-associated protein kinase in hypertension.** *Nature* 1997, **389:**990-994.

196. Mukai Y, Shimokawa H, Matoba T, Kandabashi T, Satoh S, Hiroki J, Kaibuchi K, Takeshita A: **Involvement of Rho-kinase in hypertensive vascular disease: a novel therapeutic target in hypertension.** *FASEB J* 2001, **15:**1062-1064.

197. Shimokawa H, Morishige K, Miyata K, Kandabashi T, Eto Y, Ikegaki I, Asano T, Kaibuchi K, Takeshita A: **Long-term inhibition of Rho-kinase induces a regression of arteriosclerotic coronary lesions in a porcine model in vivo.** *Cardiovasc Res* 2001, **51:**169-177.

198. Gabrielli L, Winter JL, Godoy I, McNab P, Padilla I, Cordova S, Rigotti P, Novoa U, Mora I, Garcia L, Ocaranza MP, Jalil JE: **Increased rho-kinase activity in hypertensive patients with left ventricular hypertrophy.** *Am J Hypertens* 2014, **27:**838-845.

199. Satoh S, Ueda Y, Koyanagi M, Kadokami T, Sugano M, Yoshikawa Y, Makino N: **Chronic inhibition of Rho kinase blunts the process of left ventricular hypertrophy leading to cardiac contractile dysfunction in hypertension-induced heart failure.** *J Mol Cell Cardiol* 2003, **35:**59-70.

200. Zhou Z, Meng Y, Asrar S, Todorovski Z, Jia Z: **A critical role of Rho-kinase ROCK2 in the regulation of spine and synaptic function.** *Neuropharmacology* 2009, **56:**81-89.

201. Klimas J, Kmecova J, Jankyova S, Yaghi D, Priesolova E, Kyselova Z, Musil P, Ochodnicky P, Krenek P, Kyselovic J, Matyas S: **Pycnogenol improves left ventricular function in streptozotocin-induced diabetic cardiomyopathy in rats.** *Phytotherapy research : PTR* 2010, **24:**969-974.

202. Emanueli C, Monopoli A, Kraenkel N, Meloni M, Gadau S, Campesi I, Ongini E, Madeddu P: **Nitropravastatin stimulates reparative neovascularisation and improves recovery from limb Ischaemia in type-1 diabetic mice.** *British journal of pharmacology* 2007, **150:**873-882.

203. Ram R, Mickelsen DM, Theodoropoulos C, Blaxall BC: **New approaches in small animal echocardiography: imaging the sounds of silence.** *American journal of physiology Heart and circulatory physiology* 2011, **301:**H1765-1780.

204. Li D, Wu J, Bai Y, Zhao X, Liu L: **Isolation and culture of adult mouse cardiomyocytes for cell signaling and in vitro cardiac hypertrophy.** *J Vis Exp* 2014, DOI: 10.3791/51357 [Epub ahead of print].

205. McCauley MD, Wehrens XH: **Ryanodine receptor phosphorylation, calcium/calmodulin-dependent protein kinase II, and life-threatening ventricular arrhythmias.** *Trends Cardiovasc Med* 2011, **21:**48-51.

206. Choi KM, Zhong Y, Hoit BD, Grupp IL, Hahn H, Dilly KW, Guatimosim S, Lederer WJ, Matlib MA: **Defective intracellular Ca(2+) signaling contributes to cardiomyopathy in Type 1 diabetic rats.** *Am J Physiol Heart Circ Physiol* 2002, **283:**H1398-1408.

207. Erickson JR, Pereira L, Wang L, Han G, Ferguson A, Dao K, Copeland RJ, Despa F, Hart GW, Ripplinger CM, Bers DM: **Diabetic hyperglycaemia activates CaMKII and arrhythmias by O-linked glycosylation.** *Nature* 2013, **502:**372-376.

208. van Oort RJ, McCauley MD, Dixit SS, Pereira L, Yang Y, Respress JL, Wang Q, De Almeida AC, Skapura DG, Anderson ME, Bers DM, Wehrens XH: **Ryanodine receptor phosphorylation by calcium/calmodulin-dependent protein kinase II promotes life-threatening ventricular arrhythmias in mice with heart failure.** *Circulation* 2010, **122:**2669-2679.

209. Eranti A, Kerola T, Aro AL, Tikkanen JT, Rissanen HA, Anttonen O, Junttila MJ, Knekt P, Huikuri HV: **Diabetes, glucose tolerance, and the risk of sudden cardiac death.** *BMC Cardiovasc Disord* 2016, **16:**51.

210. Lawrence IG, Weston PJ, Bennett MA, McNally PG, Burden AC, Thurston H: **Is impaired baroreflex sensitivity a predictor or cause of sudden death in insulin-dependent diabetes mellitus?** *Diabet Med* 1997, **14:**82-85.

211. Movahed MR, Hashemzadeh M, Jamal M: **Increased prevalence of ventricular fibrillation in patients with type 2 diabetes mellitus.** *Heart Vessels* 2007, **22:**251-253.

212. Fox CS, Coady S, Sorlie PD, Levy D, Meigs JB, D'Agostino RB, Sr., Wilson PW, Savage PJ: **Trends in cardiovascular complications of diabetes.** *JAMA* 2004, **292:**2495-2499.

213. Janszky I, Romundstad P, Laugsand LE, Vatten LJ, Mukamal KJ, Morkedal B: **Weight and weight change and risk of acute myocardial infarction and heart failure - the HUNT Study.** *Journal of internal medicine* 2016, DOI: 10.1111/joim.12494 [Epub ahead of print].

214. Kenchaiah S, Evans JC, Levy D, Wilson PW, Benjamin EJ, Larson MG, Kannel WB, Vasan RS: **Obesity and the risk of heart failure.** *The New England journal of medicine* 2002, **347:**305-313.

215. Kannel WB, Hjortland M, Castelli WP: **Role of diabetes in congestive heart failure: the Framingham study.** *The American journal of cardiology* 1974, **34:**29-34.

216. Fisher BM, Gillen G, Lindop GB, Dargie HJ, Frier BM: **Cardiac function and coronary arteriography in asymptomatic type 1 (insulin-dependent) diabetic patients: evidence for a specific diabetic heart disease.** *Diabetologia* 1986, **29:**706-712.

217. Krishnan A, Samtani R, Dhanantwari P, Lee E, Yamada S, Shiota K, Donofrio MT, Leatherbury L, Lo CW: **A detailed comparison of mouse and human cardiac development.** *Pediatric research* 2014, **76:**500-507.

218. Rider OJ, Francis JM, Ali MK, Petersen SE, Robinson M, Robson MD, Byrne JP, Clarke K, Neubauer S: **Beneficial cardiovascular effects of bariatric surgical and dietary weight loss in obesity.** *Journal of the American College of Cardiology* 2009, **54:**718-726.

219. Sankaralingam S, Abo Alrob O, Zhang L, Jaswal JS, Wagg CS, Fukushima A, Padwal RS, Johnstone DE, Sharma AM, Lopaschuk GD: **Lowering body weight in obese mice with diastolic heart failure improves cardiac insulin sensitivity and function: implications for the obesity paradox.** *Diabetes* 2015, **64:**1643-1657.

220. Zeng H, Vaka VR, He X, Booz GW, Chen JX: **High-fat diet induces cardiac remodelling and dysfunction: assessment of the role played by SIRT3 loss.** *Journal of cellular and molecular medicine* 2015, **19:**1847-1856.

221. Palmer AJ, Chung MY, List EO, Walker J, Okada S, Kopchick JJ, Berryman DE: **Age-related changes in body composition of bovine growth hormone transgenic mice.** *Endocrinology* 2009, **150:**1353-1360.

222. Montessuit C, Lerch R: **Regulation and dysregulation of glucose transport in cardiomyocytes.** *Biochimica et biophysica acta* 2013, **1833:**848-856.

223. Douard V, Ferraris RP: **Regulation of the fructose transporter GLUT5 in health and disease.** *American journal of physiology Endocrinology and metabolism* 2008, **295:**E227-237.

224. Peyot ML, Pepin E, Lamontagne J, Latour MG, Zarrouki B, Lussier R, Pineda M, Jetton TL, Madiraju SR, Joly E, Prentki M: **Beta-cell failure in diet-induced obese mice stratified according to body weight gain: secretory dysfunction and altered islet lipid metabolism without steatosis or reduced beta-cell mass.** *Diabetes* 2010, **59:**2178-2187.

225. Koonen DP, Jacobs RL, Febbraio M, Young ME, Soltys CL, Ong H, Vance DE, Dyck JR: **Increased hepatic CD36 expression contributes to dyslipidemia associated with diet-induced obesity.** *Diabetes* 2007, **56:**2863-2871.

226. Yang ZH, Miyahara H, Takeo J, Katayama M: **Diet high in fat and sucrose induces rapid onset of obesity-related metabolic syndrome partly through rapid response of genes involved in lipogenesis, insulin signalling and inflammation in mice.** *Diabetology & metabolic syndrome* 2012, **4:**32.

227. Tran TT, Poirier H, Clement L, Nassir F, Pelsers MM, Petit V, Degrace P, Monnot MC, Glatz JF, Abumrad NA, Besnard P, Niot I: **Luminal lipid regulates CD36 levels and downstream signaling to stimulate chylomicron synthesis.** *The Journal of biological chemistry* 2011, **286:**25201-25210.

228. Fang CX, Dong F, Thomas DP, Ma H, He L, Ren J: **Hypertrophic cardiomyopathy in high-fat diet-induced obesity: role of suppression of forkhead transcription factor**

and atrophy gene transcription. *American journal of physiology Heart and circulatory physiology* 2008, **295:**H1206-H1215.

229. Abel ED, O'Shea KM, Ramasamy R: **Insulin resistance: metabolic mechanisms and consequences in the heart.** *Arteriosclerosis, thrombosis, and vascular biology* 2012, **32:**2068-2076.

230. Folmes CD, Lopaschuk GD: **Role of malonyl-CoA in heart disease and the hypothalamic control of obesity.** *Cardiovasc Res* 2007, **73:**278-287.

231. Liu L, Shi X, Bharadwaj KG, Ikeda S, Yamashita H, Yagyu H, Schaffer JE, Yu YH, Goldberg IJ: **DGAT1 expression increases heart triglyceride content but ameliorates lipotoxicity.** *The Journal of biological chemistry* 2009, **284:**36312-36323.

232. Mirtschink P, Krishnan J, Grimm F, Sarre A, Horl M, Kayikci M, Fankhauser N, Christinat Y, Cortijo C, Feehan O, Vukolic A, Sossalla S, Stehr SN, Ule J, Zamboni N, Pedrazzini T, Krek W: **HIF-driven SF3B1 induces KHK-C to enforce fructolysis and heart disease.** *Nature* 2015, **522:**444-449.

233. Delbridge LM, Benson VL, Ritchie RH, Mellor KM: **Diabetic cardiomyopathy: The case for a role of fructose in disease etiology.** *Diabetes* 2016, **65:**3521-3528.

234. Lemos DR, Babaeijandaghi F, Low M, Chang CK, Lee ST, Fiore D, Zhang RH, Natarajan A, Nedospasov SA, Rossi FM: **Nilotinib reduces muscle fibrosis in chronic muscle injury by promoting TNF-mediated apoptosis of fibro/adipogenic progenitors.** *Nature medicine* 2015, **21:**786-794.

235. Sverdlov AL, Elezaby A, Behring JB, Bachschmid MM, Luptak I, Tu VH, Siwik DA, Miller EJ, Liesa M, Shirihai OS, Pimentel DR, Cohen RA, Colucci WS: **High fat, high sucrose diet causes cardiac mitochondrial dysfunction due in part to oxidative post-**

translational modification of mitochondrial complex II. *J Mol Cell Cardiol* 2015, **78:**165-173.

236. Paik SG, Fleischer N, Shin SI: **Insulin-dependent diabetes mellitus induced by subdiabetogenic doses of streptozotocin: obligatory role of cell-mediated autoimmune processes.** *Proc Natl Acad Sci U S A* 1980, **77:**6129-6133.

237. McEvoy RC, Andersson J, Sandler S, Hellerstrom C: **Multiple low-dose streptozotocin-induced diabetes in the mouse. Evidence for stimulation of a cytotoxic cellular immune response against an insulin-producing beta cell line.** *J Clin Invest* 1984, **74:**715-722.

238. Motyl K, McCabe LR: **Streptozotocin, type I diabetes severity and bone.** *Biol Proced Online* 2009, **11:**296-315.

239. Prakoso D, De Blasio MJ, Qin C, Rosli S, Kiriazis H, Qian H, Du XJ, Weeks KL, Gregorevic P, McMullen JR, Ritchie RH: **Phosphoinositide 3-kinase (p110alpha) gene delivery limits diabetes-induced cardiac NADPH oxidase and cardiomyopathy in a mouse model with established diastolic dysfunction.** *Clin Sci (Lond)* 2017, **131:**1345-1360.

240. Palm F, Ortsater H, Hansell P, Liss P, Carlsson PO: **Differentiating between effects of streptozotocin per se and subsequent hyperglycemia on renal function and metabolism in the streptozotocin-diabetic rat model.** *Diabetes Metab Res Rev* 2004, **20:**452-459.

241. Schacht RG, Feiner HD, Gallo GR, Lieberman A, Baldwin DS: **Nephrotoxicity of nitrosoureas.** *Cancer* 1981, **48:**1328-1334.

242. Schein PS, Loftus S: **Streptozotocin: depression of mouse liver pyridine nucleotides.** *Cancer Res* 1968, **28:**1501-1506.

243. Reffay M, Parrini MC, Cochet-Escartin O, Ladoux B, Buguin A, Coscoy S, Amblard F, Camonis J, Silberzan P: **Interplay of RhoA and mechanical forces in collective cell migration driven by leader cells.** *Nat Cell Biol* 2014, **16:**217-223.

244. David M, Petit D, Bertoglio J: **Cell cycle regulation of Rho signaling pathways.** *Cell Cycle* 2012, **11:**3003-3010.

245. Bhadriraju K, Yang M, Alom Ruiz S, Pirone D, Tan J, Chen CS: **Activation of ROCK by RhoA is regulated by cell adhesion, shape, and cytoskeletal tension.** *Exp Cell Res* 2007, **313:**3616-3623.

246. Marinissen MJ, Chiariello M, Gutkind JS: **Regulation of gene expression by the small GTPase Rho through the ERK6 (p38 gamma) MAP kinase pathway.** *Genes Dev* 2001, **15:**535-553.

247. Chitaley K, Weber D, Webb RC: **RhoA/Rho-kinase, vascular changes, and hypertension.** *Curr Hypertens Rep* 2001, **3:**139-144.

248. Mori-Kawabe M, Tsushima H, Fujimoto S, Tada T, Ito J: **Role of Rho/Rho-kinase and NO/cGMP signaling pathways in vascular function prior to atherosclerosis.** *J Atheroscler Thromb* 2009, **16:**722-732.

249. Kam MK, Lee KY, Tam PK, Lui VC: **Generation of NSE-MerCreMer transgenic mice with tamoxifen inducible Cre activity in neurons.** *PloS one* 2012, **7:**e35799.

250. Sohal DS, Nghiem M, Crackower MA, Witt SA, Kimball TR, Tymitz KM, Penninger JM, Molkentin JD: **Temporally regulated and tissue-specific gene manipulations in**

the adult and embryonic heart using a tamoxifen-inducible Cre protein. *Circ Res* 2001, **89:**20-25.

251. Parker TG, Packer SE, Schneider MD: **Peptide growth factors can provoke "fetal" contractile protein gene expression in rat cardiac myocytes.** *J Clin Invest* 1990, **85:**507-514.

252. Zhou H, Zhang KX, Li YJ, Guo BY, Wang M, Wang M: **Fasudil hydrochloride hydrate, a Rho-kinase inhibitor, suppresses high glucose-induced proliferation and collagen synthesis in rat cardiac fibroblasts.** *Clin Exp Pharmacol Physiol* 2011, **38:**387-394.

253. Conrad CH, Brooks WW, Hayes JA, Sen S, Robinson KG, Bing OH: **Myocardial fibrosis and stiffness with hypertrophy and heart failure in the spontaneously hypertensive rat.** *Circulation* 1995, **91:**161-170.

254. Diez J, Querejeta R, Lopez B, Gonzalez A, Larman M, Martinez Ubago JL: **Losartan-dependent regression of myocardial fibrosis is associated with reduction of left ventricular chamber stiffness in hypertensive patients.** *Circulation* 2002, **105:**2512-2517.

255. Li J, Zhu H, Shen E, Wan L, Arnold JM, Peng T: **Deficiency of rac1 blocks NADPH oxidase activation, inhibits endoplasmic reticulum stress, and reduces myocardial remodeling in a mouse model of type 1 diabetes.** *Diabetes* 2010, **59:**2033-2042.

256. Zhang Y, Wang JH, Zhang YY, Wang YZ, Wang J, Zhao Y, Jin XX, Xue GL, Li PH, Sun YL, Huang QH, Song XT, Zhang ZR, Gao X, Yang BF, Du ZM, Pan ZW: **Deletion of interleukin-6 alleviated interstitial fibrosis in streptozotocin-induced diabetic**

cardiomyopathy of mice through affecting TGFbeta1 and miR-29 pathways. *Sci Rep* 2016, **6:**23010.

257. Lijnen PJ, Petrov VV, Fagard RH: **Induction of cardiac fibrosis by transforming growth factor-beta(1).** *Mol Genet Metab* 2000, **71:**418-435.

258. Shen N, Li X, Zhou T, Bilal MU, Du N, Hu Y, Qin W, Xie Y, Wang H, Wu J, Ju J, Fang Z, Wang L, Zhang Y: **Shensong Yangxin Capsule prevents diabetic myocardial fibrosis by inhibiting TGF-beta1/Smad signaling.** *J Ethnopharmacol* 2014, **157:**161-170.

259. Zhang S, Fei T, Zhang L, Zhang R, Chen F, Ning Y, Han Y, Feng XH, Meng A, Chen YG: **Smad7 antagonizes transforming growth factor beta signaling in the nucleus by interfering with functional Smad-DNA complex formation.** *Mol Cell Biol* 2007, **27:**4488-4499.

260. Chen HY, Huang XR, Wang W, Li JH, Heuchel RL, Chung AC, Lan HY: **The protective role of Smad7 in diabetic kidney disease: mechanism and therapeutic potential.** *Diabetes* 2011, **60:**590-601.

261. Connelly KA, Kelly DJ, Zhang Y, Prior DL, Advani A, Cox AJ, Thai K, Krum H, Gilbert RE: **Inhibition of protein kinase C-beta by ruboxistaurin preserves cardiac function and reduces extracellular matrix production in diabetic cardiomyopathy.** *Circ Heart Fail* 2009, **2:**129-137.

262. Bjornstad JL, Skrbic B, Marstein HS, Hasic A, Sjaastad I, Louch WE, Florholmen G, Christensen G, Tonnessen T: **Inhibition of SMAD2 phosphorylation preserves cardiac function during pressure overload.** *Cardiovasc Res* 2012, **93:**100-110.

263. Schneiders D, Heger J, Best P, Michael Piper H, Taimor G: **SMAD proteins are involved in apoptosis induction in ventricular cardiomyocytes.** *Cardiovasc Res* 2005, **67:**87-96.

264. Saltzman A, Munro R, Searfoss G, Franks C, Jaye M, Ivashchenko Y: **Transforming growth factor-beta-mediated apoptosis in the Ramos B-lymphoma cell line is accompanied by caspase activation and Bcl-XL downregulation.** *Exp Cell Res* 1998, **242:**244-254.

265. Numaga-Tomita T, Kitajima N, Kuroda T, Nishimura A, Miyano K, Yasuda S, Kuwahara K, Sato Y, Ide T, Birnbaumer L, Sumimoto H, Mori Y, Nishida M: **TRPC3-GEF-H1 axis mediates pressure overload-induced cardiac fibrosis.** *Sci Rep* 2016, **6:**39383.

266. Chen S, Crawford M, Day RM, Briones VR, Leader JE, Jose PA, Lechleider RJ: **RhoA modulates Smad signaling during transforming growth factor-beta-induced smooth muscle differentiation.** *J Biol Chem* 2006, **281:**1765-1770.

267. Yang X, Li Q, Lin X, Ma Y, Yue X, Tao Z, Wang F, McKeehan WL, Wei L, Schwartz RJ, Chang J: **Mechanism of fibrotic cardiomyopathy in mice expressing truncated Rho-associated coiled-coil protein kinase 1.** *FASEB J* 2012, **26:**2105-2116.

268. Zhang YM, Bo J, Taffet GE, Chang J, Shi J, Reddy AK, Michael LH, Schneider MD, Entman ML, Schwartz RJ, Wei L: **Targeted deletion of ROCK1 protects the heart against pressure overload by inhibiting reactive fibrosis.** *FASEB J* 2006, **20:**916-925.

269. Shantaram V: **Pathogenesis of atherosclerosis in diabetes and hypertension.** *Clin Exp Hypertens* 1999, **21:**69-77.